UNIVERSIDADE ESTADUAL DE CAMPINAS
INSTITUTO DE BIOLOGIA

THALITA CAMÊLO DA SILVA FERREIRA

RELEVANCE OF MULTI-SPECIES PHENOTYPIC ASSAYS IN *LEISHMANIA* EARLY DRUG DISCOVERY

RELEVÂNCIA DE ENSAIOS FENOTÍPICOS COM DIVERSAS ESPÉCIES DE *LEISHMANIA* NA DESCOBERTA INICIAL DE FÁRMACOS

CAMPINAS
2019

THALITA CAMÊLO DA SILVA FERREIRA

RELEVANCE OF MULTI-SPECIES PHENOTYPIC ASSAYS IN *LEISHMANIA* EARLY DRUG DISCOVERY

RELEVÂNCIA DE ENSAIOS FENOTÍPICOS COM DIVERSAS ESPÉCIES DE *LEISHMANIA* NA DESCOBERTA INICIAL DE FÁRMACOS

Thesis presented to the Biology Institute of the State University of Campinas in partial fulfillment of the requirements for the degree of Doctor in Genetics and Molecular Biology in the area of Microbiology

Tese apresentada ao Instituto de Biologia da Universidade Estadual de Campinas como parte dos requisitos exigidos para a obtenção do título de Doutora em Genética e Biologia Molecular, na área de Microbiologia.

Supervisor: Dr. Lucio Holanda Gondim de Freitas Junior

ESTE EXEMPLAR CORRESPONDE À VERSÃO FINAL DA TESE, DEFENDIDA PELA ALUNA THALITA CAMÊLO DA SILVA FERREIRA E ORIENTADA PELO DR. LUCIO HOLANDA GONDIM DE FREITAS JUNIOR

CAMPINAS

2019

Agência (s) de fomento e n°(s) de processo(s): CNPq, 870370/1997-9; FAPESP, 2015/10436-6

Ficha catalográfica
Universidade Estadual de Campinas
Biblioteca do Instituto de Biologia
Mara Janaina de Oliveira - CRB 8/6972

F413r

Ferreira, Thalita Camêlo da Silva, 1992-
Relevance of multi-species phenotypic assays in *Leishmania* early drug discovery / Thalita Camêlo da Silva Ferreira. – Campinas, SP : [s.n.], 2019.

Orientador: Lucio Holanda Gondim de Freitas Junior.
Tese (doutorado) – Universidade Estadual de Campinas, Instituto de Biologia.

1. *Leishmania*. 2. Leishmaniose. 3. Descoberta de drogas. 4. Ensaios de triagem em larga escala. I. Freitas-Junior, Lucio Holanda. II. Universidade Estadual de Campinas. Instituto de Biologia. III. Título.

-Informações para Biblioteca Digital

Título em outro idioma: Relevância de ensaios fenotípicos com diversas espécies de *Leishmania* na descoberta inicial de fármacos **Palavras-chave em inglês:**
Leishmania
Leishmaniasis
Drug discovery
High-throughput screening assays
Área de concentração: Microbiologia
Titulação: Doutora em Genética e Biologia Molecular **Banca examinadora:**
Lucio Holanda Gondim de Freitas Junior [Orientador]
Elizabeth Bilsland
André Gustavo Tempone Cardoso
Jadel Muller Kratz
Rafael Lemos Miguez Couñago
Data de defesa: 27-02-2019
Programa de Pós-Graduação: Genética e Biologia Molecular

Identificação e informações acadêmicas do(a) aluno(a)
-ORCID do autor: https://orcid.org/0000-0001-8282-5708

-Currículo Lattes do autor: http://lattes.cnpq.br/9465460141211530

EXAMINATION COMMITTEE

Dr. Lucio Holanda Gondim de Freitas Junior (supervisor)
Profa. Dra. Elizabeth Bilsland
Prof. Dr. André Gustavo Tempone Cardoso
Prof. Dr. Jadel Muller Kratz
Dr. Rafael Lemos Miguez Couñago

The members of the Examination Committee signed the Defense Act, which is in the student's academic life record.

Os membros da Comissão Examinadora acima assinaram a Ata de Defesa, que se encontra no processo de vida acadêmica do aluno.

ACKNOWLEDGMENTS

First and foremost, I praise God for giving me the opportunity, knowledge, ability, and strength to undertake this research study and to persevere and complete it.

Dedicated to my eternal cheerleader, my mom: because I owe all to you. Many Thanks!

I would like to express my sincere gratitude to my supervisors, Lucio Freitas-Junior and Carolina Borsoi, for accepting me as a doctoral student and for all their support. This accomplishment would not have been possible without them. Thank you.

I have great pleasure in acknowledging my gratitude to the past and present members of our lab: Adalberto Araújo, Bruno Pascoalino, Caio Haddad, Claudia Bertolacini, Denise Pilger, Giovana Cintra, Luisa Naves, Nicolli Bellotti, Rafaela Bonotto, Vanessa Fontana and Valber Florêncio. Their support, encouragement and credible ideas have been great contributors in the completion of this work. It was great sharing laboratory with all of you! With a special mention to my leishmaniac colleague, Laura Alcântara, thanks for your patience, insightful discussions, and your always solicitous support.

I want to express my deep thanks to professors Danilo Ciccone and Mauro Cortez for kindly allowing me to use their facilities and teaching me so much during this period.

This thesis appears in its current form due to the support and assistance of several institutions. I would therefore like to offer my sincere thanks to all of them This project was partially carried out in the Brazilian Center for Research in Energy and Materials (CNPEM). Partial results were also obtained in the following organizations: (i) Butantan Institute; (ii) Immunobiology of the *Leishmania*-macrophage Interaction lab (Lab head: Prof. Mauro Cortez), in the Institute of Biomedical Sciences (ICB) of the University of São Paulo (USP); and (iii) *Leishmania* Infection Biology Studies lab _ LEBIL (Lab head: Prof. Danilo Ciccone), in the Institute of Biology of the University of Campinas (UNICAMP). The CEFAP-USP (Centro de Facilidades de Apoio à Pesquisa) and FMRP-USP (Faculdade de Medicina de Ribeirão Preto) provided service to the use of High Content Image Screening equipment. I would like to thank FAPESP (#15/10436-6) and CNPq (#870370/1997-9) for awarding me a doctoral fellowship. I also wish to express gratitude to the Drugs for Neglected Diseases initiative (DND*i*) and the Medicines for Malaria Venture (MMV) for partially funding this research project. I would still like to thank the Graduate Program in Genetics and Molecular Biology for all the assistance.

I am grateful to my family and friends for their prayers throughout my years of study. I warmly thank my father and my friend Danilo Ferreira for their material and moral support. Emerson, Thais, Ingrid Ester, and Milena Rosa, my beloved siblings, thank you for your love! My little nephew, Kauã, who always brings so much joy and happiness to my life, thank you!

Finally, I must express my very profound gratitude to my friend, Luiz Gustavo dos Santos, for providing me with unfailing support and continuous encouragement throughout the writing process of this thesis.

ABSTRACT

The leishmaniasis are a group of poverty-associated diseases caused by the protozoan *Leishmania spp*. The complexity of this kinetoplastid parasite is highlighted by biological, ecological, and epidemiological aspects. It is endemic in more than 98 countries affecting around 12 million people. Approximately 20 species can be transmitted to humans by 78 species of the phlebotomine sandfly vector. Infected people can develop one of the several pathologies from which the most common are: cutaneous lesions, the disfiguring mucocutaneous disorder, and the life-threatening visceral disease. The final outcome is multifactorial, depending on intricate host-parasite interactions and environmental factors. The few chemotherapeutic options available are mostly unsatisfactory due to low efficacy, poor safety, emergence of parasite resistance, and other factors related to treatment (such as administration route, length of treatment or high costs) that are not suitable for the socioeconomic reality of affected populations. The current scenario demands research focused on the identification of novel effective therapeutics. Modern technologies enable the screening of millions of compounds, but a more predictive *in vitro* assays is still lacking. It is a common practice for a research group to target a single species, usually *L. dovovani*, the causative agent of visceral disease. Addressing a representative sample of viscerotropic and dermotropic species/strains of *Leishmania* can be useful to prioritize compounds based on their spectrum of activity. This work focused on the discovery of starting points for the development of new antileishmanials using an image-based methodology. Careful standardization was carried out aiming to achieve robustness and reproducibility, based on: (i) the biological model, determining the best condition for parasite and host cell culture, infection and drug exposure, and (ii) the image analysis algorithm. The multi-species high content assay was successfully established and validated to assess compound activity against some of the most clinically relevant dermotropic (*L. amazonensis* and *L. braziliensis*) and viscerotropic agents (*L. donovani and L. infantum*). This semi-automated assay is based on THP-1 macrophages infected with stationary phase promastigotes and can be virtually adapted to any *in vitro* infective species, providing the basis for the discovery of broad-spectrum antileishmanial molecules. A species-specific profile was observed in the general activity of libraries screenings, and a reduced number of compounds were active for all species. The simultaneous screening of the Pathogen Box library against four *Leishmania* species along with literature data analysis resulted in the identification of 12 pan-antileishmanial compounds. Although these molecules have been reported as anti-kinetoplastid agents, their activity against different *Leishmania* species had not been explored yet. The results obtained from this study demonstrate the potential value of including a panel of species in early steps of the drug discovery process, which can facilitate the prospection, validation and progression of more promising compounds. The species panel, together with other reported secondary assays, is suggested as part of a cell-based assay pipeline for *Leishmania spp*. aiming to empower the prioritization of compounds based on crucial aspects besides the physico-chemical and toxicity filters traditionally applied.

RESUMO

As leishmanioses são um grupo de doenças associadas à pobreza causadas por protozoários do gênero *Leishmania*. A complexidade desse kinetoplastídeo é evidenciada por aspectos biológicos, ecológicos e epidemiológicos. Essas doenças são endêmicas em mais de 98 países e acometem em torno de 12 milhões de pessoas. Aproximadamente 20 espécies de *Leishmania* infectam humanos e são transmitidas por 78 espécies de flebotomíneos. Uma vez infectados, os pacientes podem desenvolver diversas patologias dentre as quais as mais comuns são: leishmaniose cutânea, leishmaniose mucocutânea e leishmaniose visceral. Múltiplos determinantes estão envolvidos na manifestação clínica, incluindo complexas interações entre o parasita e o hospedeiro, além de fatores ambientais. As poucas farmacoterapias disponíveis são, em grande parte, insatisfatórias devido a baixa eficácia, pouca segurança, surgimento de resistência e outros aspectos relacionados ao tratamento (rota de administração, duração e custo elevado) que são incompatíveis com a realidade socioeconômica da população afetada. A atual conjuntura requer pesquisa focada na identificação de novas moléculas antileishmaniais. Devido aos avanços tecnológicos, atualmente é possível testar milhões de compostos de maneira contínua, entretanto, ainda é necessário o desenvolvimento de ensaios mais preditivos. É comum que grupos de pesquisa limitem os testes *in vitro* a uma única espécie, geralmente *L. donovani*, agente etiológico da doença visceral. Estabelecer ensaios com uma amostra representativa de espécies vicerotrópicas e dermotrópicas pode ser uma abordagem útil na priorização de compostos baseando-se no espectro de atividade. Este estudo objetivou a identificação de agentes antileishmaniais usando uma metodologia baseada em imagens. Uma padronização cuidadosa foi realizada para alcançar robustez e reprodutibilidade, focando em dois aspectos-chave: (i) o modelo biológico, determinando as condições para cultura da célula hospedeira e do parasita, parâmetros de infecção e tempo de exposição aos compostos; (ii) método de análise das imagens. O ensaio fenotípico foi estabelecido e validado para avaliar a atividade de compostos contra algumas das espécies dermotrópicas (*L. amazonensis* e *L. braziliensis*) e vicerotrópicas (*L. donovani* e *L. infantum*) mais relevantes clinicamente. Esse protocolo é semi-automatizado, baseia-se na infecção de células THP-1 com promastigotas em fase estacionária e tem potencial para ser adaptado a qualquer espécie infectiva *in vitro*, representando a base para descoberta de moléculas com amplo espectro. Um perfil espécie-específico foi observado na triagem de bibliotecas e uma quantidade reduzida de compostos foi ativa para todas as espécies. O teste da biblioteca Pathogen Box contra quatro espécies, juntamente com a análise da literatura, resultou na identificação de 12 compostos pan-antileishmaniais. Embora esses compostos terem atividade reportada contra kinetoplastídeos, o amplo espectro de ação contra diversas espécies de *Leishmania* não havia sido explorado. Os resultados obtidos nesse estudo demonstram o potencial da inserção de um conjunto de espécies nas etapas iniciais do processo de descoberta de novos fármacos, facilitando a prospecção, validação e progressão de compostos mais promissores. O painel de espécies, juntamente com outros ensaios secundários, é sugerido como integrante de um *pipeline* de ensaios celulares para *Leishmania spp.* objetivando a priorização de compostos baseada em aspectos cruciais além dos filtros tradicionalmente aplicados de propriedades físico-químicas e de toxicidade.

LIST OF FIGURES

Figure 1.1 Life cycle of *Leishmania* spp. 1.. 17

Figure 1.2 *Leishmania* species and more often related clinical manifestation. 20

Figure 1.3 Drug discovery pipeline. 24

Figure 1.4 Advantages and limitations of assays with the different stages of *Leishmania spp.* 26

Figure 1.5 Differentiation of THP-1 cells. 31

Figure 1.6 Drug discovery approaches. 33

Figure 3.1 Intracellular amastigotes assay protocol. 41

Figure 3.2 Z'-factor determination. 44

Figure 4.1 Harmony software image analysis building-blocks. 48

Figure 4.2 Harmony software sensitivity. 50

Figure 4.3 DRCs of reference compounds assessed by Operetta and IN Cell Analyzer. 51

Figure 4.4 Standardization of RAW 264.7 and J774A.1 cell lines density in 384-well plates. 53

Figure 4.5 Evaluation of THP-1 cells fagocytic capacity after PMA differentiation. 54

Figure 4.6 Infection performed at 34°C is better for CL species. 56

Figure 4.7 Infection performed at 34°C increases CL species infectivity. 57

Figure 4.8 THP-1 cells incubated at 34 °are viable. 58

Figure 4.9 Evaluation of growth and infectivity of promastigotes cultured in different media.. 59

Figure 4.10 Infection parameters standardization. 60

Figure 4.11 *L. braziliensis* infection ratio dynamic over time. 61

Figure 4.12 Representative images panel of THP-1 cells infected with Leishmania spp. 62

Figure 4.13 Determination of the drug exposure window. 63

Figure 4.14 Growth curve of promastigotes at 34° C. 65

Figure 4.15 *L. amazonensis* communal parasitophorous vacuoles in infected THP-1 cells. 66

Figure 4.16 Representative images of infected THP-1 and BMDM cells. 67

Figure 4.17 Infection dynamic of *L. amazonensis* and *L. braziliensis* in THP-1 and BMDM cells. 68

Figure 4.18 Validation of potency determination. 69

Figure 4.19 Determination of Minimum Significant Difference (MSD). 70

Figure 4.20 Plate maps showing controls and samples positioning. 71

Figure 4.21 Single point screening validation for *L. amazonensis* and *L. brazililensis*. 72

Figure 4.22 General scheme of *Leishmania* high content assay.. 73

Figure 4.23 Dose-response curves of reference compounds for *Leishmania* species. 75

Figure 4.24 Therapeutic profile of LOPAC selected compounds. 77

Figure 4.25 Differential activity of LOPAC compounds for *Leishmania* species. 80

Figure 4.26 Summary of LOPAC screening against *Leishmania spp.* species. 81

Figure 4.27 Profile of PBox screening. 84

Figure 4.28 Differential activity of the PBox compounds for *Leishmania* species.....85

Figure 4.29 Venn Diagram comparing the selected compounds for each specie. 87

Figure 4.30 Cell-based assay cascade for *Leishmania spp*. in early drug discovery.....90

Figure 4.31 Molecular structure of compounds with broad-spectrum activity (1-16). 92

Figure 4.32 Molecular structure of compounds with broad-spectrum activity (17-32). 93

Figure 4.33 Heatmap based on chemical structure similarity determined by Tanimoto coefficient. 94

LIST OF TABLES

Table 1.1Current antileishmanial chemotherapy.....22

Table 1.2 Optimal Target product profile of new chemical entities for leishmaniasis 25

Table 1.3 HCS assays reported for *Leishmania spp.*: general biological parameters 29

Table 1.4 HCS assays reported for *Leishmania spp.*: imaging and analysis.....30

Table 3.1 Parameters of Harmorny software.....42

Table 3.2 Parameters of Investigator software.....42

Table 3.3 EC_{50} and pEC_{50} values 43

Table 4.1 Comparation between Operetta and IN Cell Analyzer analysis.....50

Table 4.2 pEC_{50} values determined by Operetta and IN Cell Analyzer analysis 51

Table 4.3 pEC_{50} values at 72-, 96-, and 144-h of continuous reference compounds exposure.....64

Table 4.4 LOPAC screening for *L. amazonensis* and *L. braziliensis*.....71

Table 4.5 pEC 50 values of reference compounds for *Leishmania* species. 75

Table 4.6 LOPAC primary screening quantitative data 76

Table 4.7 Compounds related with neurotransmission reported as active against *Leishmania spp*.....77

Table 4.8 LOPA C compounds maximum activity and pEC50 values 82

Table 4.9 Pathogen Box primary screening quantitative data.....83

Table 4.10 PBox most active compounds list 86

Table 4.11 Compounds within PBox supporting information with $pEC_{50} > 4.7$.....87

Table 4.12 Activity of the 16 most potent PBox compounds reported by (Duffy et al. 2017) 88

Table 4.13 Activity of the 7 most potent PBox compounds reported by (Berry et al. 2018).....89

Table 4.14 List of compounds with broad-spectrum activity.....91

Table 4.15 Pan-antileishmanial compounds.....95

TABLE OF CONTENTS

1 Introduction 13
1.1 General aspects of leishmaniasis 13
1.2 The complex biology of *Leishmania spp.* parasite 15
1.3 Current antileishmanial chemotherapy 21
1.4 The challenging *Leishmania* drug discovery pipeline 23
1.5 Cutaneous leishmaniasis: neglected within neglected tropical diseases 34
2 Objectives 36
3 Material and methods 37
3.1 Cell lines and parasite lineages 37
3.2 Animals 37
3.3 Reference compounds 38
3.4 LOPAC library 38
3.5 Pathogen Box library 38
3.6 *Leishmania spp.* culture 38
3.7 Raw 264.7 and J774A.1 cell lines culture 39
3.8 Culture of L929 cells and recovery of supernatant 39
3.9 BMDM isolation 39
3.10 THP-1 culture and differentiation 40
3.11 Intracellular amastigotes assay 40
3.12 High content image acquisition and data analysis 41
3.13 Resazurin assay 44
3.14 Determination of the drug exposure window 44
3.15 EdU incorporation test 45
3.16 Tanimoto structural similarity index 45
4 Results and Discussion 46
4.1 Image analysis protocol 46
4.2 Establishment of the intracellular *Leishmania spp*. assay for dermotropic species 52
4.3 HCS assay validation for dermotropic species 68
4.4 The multi-species high content assay 73

4.5 Library of Pharmaceutically Active Compounds (LOPAC) 75
4.6 Pathogen Box library 83
4.7 Pan-antileishmanial compounds 91
5 Final considerations 97
REFERENCES 100
APPENDIX 1 111
APPENDIX 2 112
ANNEX I 118
ANNEX II 119
ANNEX III 120
ANNEX IV 121

1 Introduction

1.1 General aspects of leishmaniasis

Leishmaniasis encompasses a complex group of diseases categorized by the clinical symptomatology, where three major forms stand out: cutaneous leishmaniasis (CL), mucocutaneous leishmaniasis (ML) and visceral leishmaniasis (VL). The etiological agent of leishmaniasis is the protozoan *Leishmania spp*, which is transmitted by the bite of an insect vector, the phlebotomine sandfly. The term "cutaneous leishmaniasis" refers to a specific localized form, therefore "tegumentary leishmaniasis" will be used as an overall term for all forms of leishmaniasis involving cutaneous/mucosal tissue.

According to WHO, human *Leishmania spp*. infection is endemic in more than 98 countries; mostly in South/Central America, Africa and the Middle East. However, these diseases have been expanding its geographic area, mainly as a result of the increase traveling to and from these regions, forced displacement resulted from international conflicts, and the deforestation/urbanization process (WHO 2018). Apart from that, climate changes due to global warming are prospected to enable a northwards expansion in Europe of areas with suitable climatic conditions for several vector species (*P. alexandri, P. neglectus, P. papatasi, P. perfiliewi, P. tobbi*) (Koch *et al.* 2017). In addition, even small fluctuations in temperature, rainfall and humidity can affect the cycle of *Leishmania spp.* in sandflies and reservoir hosts, allowing transmission of the parasite in regions traditionally regarded as leishmaniasis-free (Chalghaf *et al.* 2018). All these factors have contributed to the increasing number of cases observed during the last 25 years throughout the world. The estimated world prevalence of all forms of the disease is 12 million, with 2 million new cases annually (1.5 million tegumentary pathologies and 0.5 million VL cases). The visceral disease kills about 50,000 people each year. It is noteworthy to mention these numbers are probably underestimated due to the under-reporting of cases and limitations inherent to the countries' surveillance systems (WHO 2018).

Leishmaniasis are associated with elevated incidence rate and wide geographic distribution in the Central and South Americas, which contributes to variations in transmission cycles, reservoir hosts, sandfly vectors, clinical manifestations, response to therapy, and parasite diversity, with multiple *Leishmania* species circulating in the region. In 2016, 17 endemic American countries reported 48,915 CL/ML cases and seven countries registered 3,354 VL cases. Highlighting that in this period VL fatality rate has reached 7.9% and the percentage of CL in children under 10 years old has also reached 15.5%. Brazil is the country with the highest numbers of registered cases, with12,690 CL/ML cases and 3,200 VL cases

reported in 2016, representing 26% and 95% of the total reported cases in the continent, respectively (PAHO 2018).

In most geographic areas, leishmaniasis are considered zoonotic diseases, because infected people are not involved in the natural transmission cycle. Thus, others mammalian species, along with the sandfly vectors, maintain the cycle. But in some parts of the world, no animal reservoir has been identified, thereby transmission is thought to occur from human to sandfly to human. This type of transmission is called anthroponotic, and it is typical of the *L. donovani* and *L. tropica* infection in the Indian subcontinent (Bern *et al.* 2008).

The accurate diagnosis of human leishmaniasis is challenging. The pathological aspects are diverse and depend on the infecting *Leishmania* species and the host immune response. The definitive diagnosis is based on clinical inspection, followed by isolation, visualization, and culturing of the parasite from infected organs tissues, such as skin lesions, bone marrow, lymph node or spleen. The direct visualization of parasites is the reference standard for diagnosis, but requires trained technicians, involves invasive sampling, and has variable sensitivity (WHO 2012). Less invasive diagnostic methods include serologic detection of antibodies to recombinant K39 antigen, and amplification of *Leishmania* DNA by polymerase chain reaction (PCR) assays. On the other hand, such approaches present relatively high costs and cannot discriminate between active disease from past or asymptomatic infections (Galluzzi *et al.* 2018; Sundar and Singh 2018). Additionally, the rK39 rapid immunochromatographic test (ICT) provided high sensitivity and specificity in the Indian sub-continent and Brazil, but showed to be less sensitive and specific in sub-Saharan Africa, revealing a variability in sensitivity (Bezuneh *et al.* 2014).

Since there is no registered vaccine that prevents human leishmaniasis, epidemiological management relies on vectors and reservoirs control strategies. Approaches directed to the canine reservoirs (culling, vaccination, repellent impregnated dog collars) or to the vector (insecticide spraying, insecticide treated bed nets) are often impractical or even unrealistic in large urban centers. Besides, the effectiveness of such strategies is open for debate (Romero and Boelaert 2010). Thus, the main strategy for disease control is treatment of patients, primarily in anthroponotic transmission scenarios, which emphasizes the importance of early detection and treatment for public health purposes (Burza *et al.* 2018). However, leishmaniasis treatment lean on drugs that present major drawbacks, such as high toxicity, contraindications and complex administration regimens (discussed ahead, in section 1.3.)

1.2 The complex biology of *Leishmania spp.* parasite

Despite intensive research, several aspects of *Leishmania spp.* infection remain insufficiently understood. This is in part due to the disease several complexity levels, from the parasite's perplexing life cycle to the broad spectrum of clinical outcomes.

The complexity begins by the taxonomy of *Leishmania* organisms. Considerable genetic intraspecies variability complicates classification, and no single categorization is generally accepted. According with Akhoundi *et al.*, they are classified as follow: kingdom *Protista*, phylum *Euglenozoa*, class *Kinetoplastea*, subclass *Metakinetoplastina*, order *Trypanosomatida*, family *Trypanosomatidae*, subfamily *Leishmaniinae*, and genus *Leishmania*. Kinetoplastids are flagellated protists whose mitochondrial genome is organized into a complex and concatenated network of DNA maxi and minicircles, named kinetoplast (and thus their mitochondrial DNA is known as kDNA). According to the development of the parasite in the gut of sandfly (suprapylarian and peripylarian region), the genus *Leishmania* is still subdivided in two subgenera (*Leishmania* and *Viannia*, respectively). Other subgenera or complexes have been described (*Sauroleishmani*a, *L. enriettii* complex, and *Paraleishmania*), but they are not relevant to human diseases. There are 53 different species of *Leishmania* from which about 20 have been described as pathogenic for humans. Furthermore, they are categorized based on geographic occurrence: Old World, for *Leishmania* species found in Africa, Asia, Middle East, Mediterranean countries, and India; and New World, for species found in Central and South America (Akhoundi *et al.* 2016).

Leishmania has a digenetic life cycle, infecting an invertebrate (phlebotominae sandflies) and a vertebrate (mammals, including humans) hosts. In addition, it presents two very distinct stages: promastigotes (extracellular and flagellated forms found in the insect gut) and amastigotes (intracellular and round forms that multiply within phagocytic immune cells). An illustration summarizing the life cycle can be seen in Figure 1.1**.** Mammals are infected by the bite of female sandflies that regurgitate infective promastigotes during a blood meal (Sacks and Kamhawi 2001). Upon entering the host, promastigotes are phagocyted by phagocytic cells. Neutrophils are the first cells to infiltrate the site of parasite inoculation, where they engulf the parasites. *Leishmania spp.* have a variety of mechanisms to escape neutrophil killing, some species even resist to the microbicity associated with neutrophil extracellular trap (NET) formation (revised in Hurrell *et al.* 2016). Concomitantly, promastigotes are phagocytosed by macrophages, where they differentiate into amastigotes inside phagolysosomal compartments. The parasites may enter directly into the macrophages through receptor recognition, or may be transferred silently *via* engulfment of infected neutrophils, known as “Trojan horses”

(Gonçalves-de-Albuquerque *et al.* 2017; Peters *et al.* 2008; Ridley 1980). After successive multiplication, that may occur in tight individual vacuoles (most *Leishmania spp*.) or in large communal parasitophorous vacuoles (*L. mexicana* complex) (Moradin and Descoteaux 2012), amastigotes are released from macrophages and re-infect new cells, such as macrophages, dendritic cells, and fibroblasts. Despite the ability of *Leishmania* parasites to infect a variety of host cell types, it seems that only macrophages support replication (Bogdan *et al.* 2000). The intracellular amastigote is, therefore, the disease-causing stage of *Leishmania*. The mechanisms involved in extracellular amastigotes release is not completely elucidated, and it may occur through host cell rupture and release of free amastigotes or enclosed within host cell membranes, such as inside apoptotic blebs, without exposure to extracellular milieu (Real *et al.* 2014; Rittig and Bogdan 2000; Ridley 1980). Occasionally, upon feeding on a *Leishmania*-infected mammal, sandflies ingest parasites and infected cells. In the invertebrate host, the *Leishmania* life cycle is restricted to the digestive tract and involves several morphological forms. Primarily, the ingested amastigotes transform into procyclic promastigotes, a weakly motile, replicative form that multiplies confined by the peritrophic matrix (PM). Then parasites differentiate into nectomonad form, elongate and strongly motile promastigotes. Nectomonads escape the PM and attach to the microvilli in the midgut before moving to the thoracic midgut and stomodeal valve. Once they reach the stomodeal valve, the nectomonad promastigotes transform into leptomonad promastigotes, replicative shorter forms. These are responsible for the secretion of promastigote secretory gel (PSG), triggering the metacyclogenesis process (Sacks and Kamhawi 2001). New insights in the *Leishmania* life cycle are constantly reported. Until now, metacyclic promastigotes (mammalian-infective stages) have been considered a terminally differentiated stage inside the vector. However, a remarkable work by Serafim *et al.* recently showed that a second uninfected blood meal by infected sandflies triggers dedifferentiation of some metacyclic promastigotes to a leptomonad-like stage, the retroleptomonad promastigote. This highly multiplicative form rapidly differentiate to more metacyclic promastigotes enhancing the sandfly's infectiousness (Serafim *et al.* 2018). Ultimately, *Leishmania* are delivered to the skin of a new vertebrate host during sandfly next blood feeding, thus keeping the cycle.

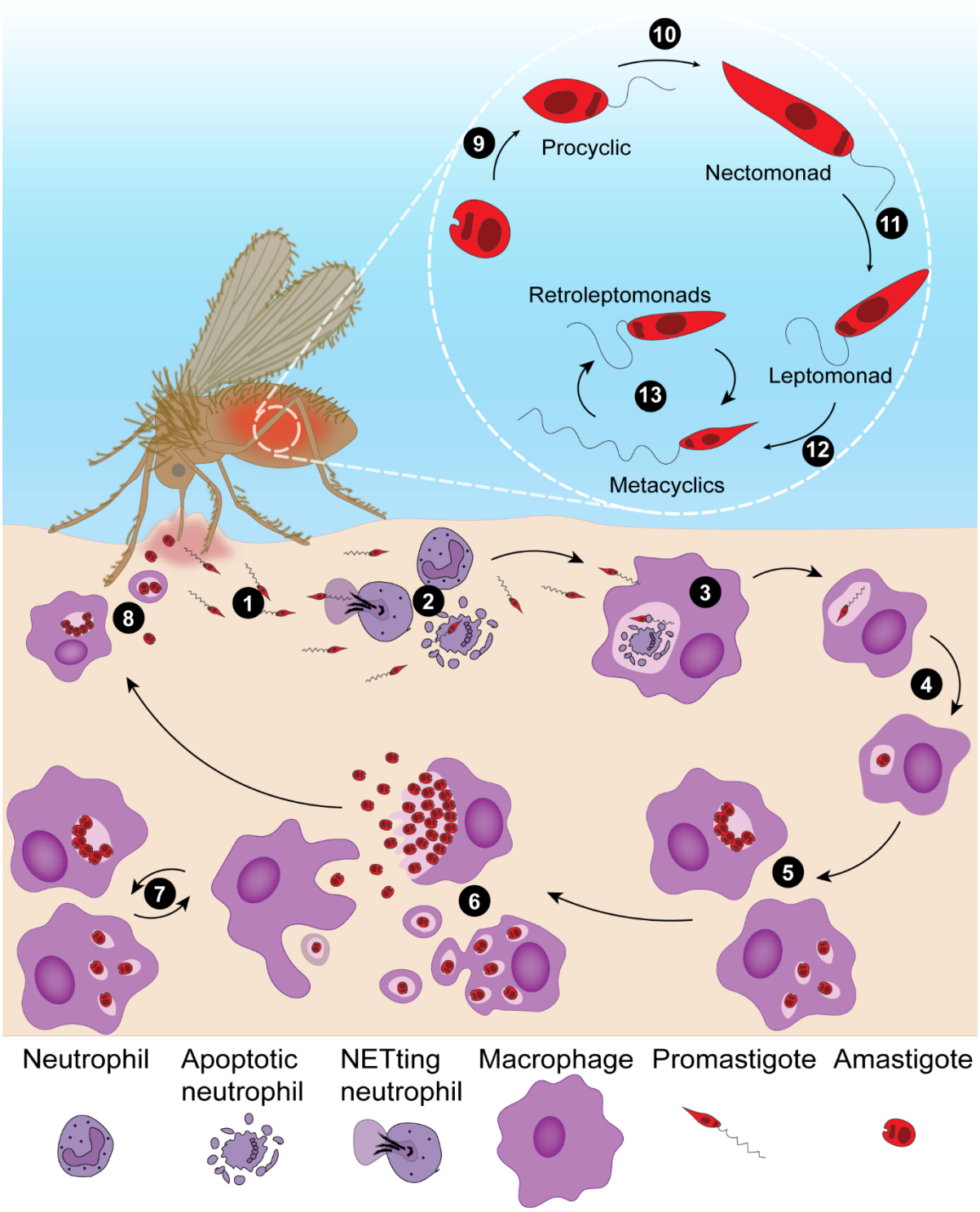

Figure 1.1 Life cycle of *Leishmania spp.* 1. Host infection by metacyclic promastigotes injection during a blood meal of sandflies **2.** Neutrophils recruitment **3.** Macrophages infection **4.** Differentiation to amastigote stage **5.** Multiplication in individual vacuoles (most *Leishmania spp*.) or in large communal parasitophorous vacuoles (*L. mexicana* complex) **6.** Release of free amastigotes or enclosed within host cell membranes **7.** Infection of new cells **8.** Ingestion of parasites and infected cells by sandflies **9.** Amastigotes differentiation in procyclic promastigotes inside sandfly digestive tract **10.** Differentiation to nectomonad promastigotes **11.** Differentiation to leptomonad promastigotes **12.** Differentiation to metacyclic promastigotes **13.** Cyclic differentiation between metacyclic and retroleptomonad promastigotes.

Once infected, the majority of humans remain asymptomatic. The progression into one of the different pathologies is determined by host parameters, such as genetic characteristics and immunological status (Blackwell *et al.* 2009; Sakthianandeswaren *et al.* 2009; Jeronimo *et al.* 2007), and parasite features, including heterogenecity in the virulence of different species/strains (Naderer *et al.* 2004). The clinical spectrum of leishmaniasis ranges from skin lesions (Cutaneous leishmaniasis – CL) and mucocutaneous ulcers (Mucocutaneous Leishmaniasis – ML) to systemic multiorgan damage (Visceral leishmaniasis – VL). The parasite's thermotropism plays a role in the pathology of leishmaniasis, VL species are able to grow at temperatures of deep tissues and organs, whereas those causing CL/ML grow best at lower temperatures of superficial tissues, such as the skin (Callahan *et al.* 1996).

The most frequent clinical manifestation of *Leishmania spp.* infections is CL, characterized by lesions on the patient's skin. The lesions range from simple spontaneously healing to severely inflamed ulcers that heal in months or even years. Self-healing is achieved by a balanced immune response. CL can be further subdivided into localized, recidivans, and post–kala-azar dermal leishmaniasis (PKDL). Again, host-parasite interactions determine the course of the disease.

In the localized cutaneous leishmaniasis there is a single or few ulcers, usually present in exposed areas of the body and can self-heal without treatment. Several species can cause these localized lesions: *L. major, L. mexicana, L. tropica, L. aethiopica,* among others. Leishmaniasis recidivans, caused by *L. tropica*, is a relapsing form of cutaneous leishmaniasis that occur at the border of old CL scars. PKDL is distinguished by appearance of lesions that affect the entire extension of patient's body after the clinical cure of visceral leishmaniasis caused by *L. donovani*. CL is not a life-threatening condition and severe complications are rare, yet its consequences may be socially and psychologically serious, because of disfiguring lesions and scars (Hartley *et al.* 2014).

Some infections can evolve to more severe forms known as mucocutaneous leishmaniasis (ML) and disseminated leishmaniasis (DL). This development is caused by hematogenous or lymphatic dissemination of amastigotes to secondary sites and the formation of metastatic lesions. The underlying mechanism of metastatic leishmaniasis development remains largely unknown. Interestingly, despite such lesions often present very low parasite numbers, there is wide tissue destruction caused by exaggerated inflammatory response (revised in Rossi and Fasel 2018). The disseminated manifestation, commonly associated with *L. amazonensis* and *L. braziliensis*, is characterized by nodules located on the head, arms and legs, and the number of lesions can reach hundreds. In such cases, patients are often

unresponsive to treatments. The mucocutaneous outcome is caused predominantly by *L. braziliensis*, but may also be caused by others species, such as *L. amazonensis* and *L. guyanensis*. This disease mainly affects the nasal mucosa, but the palate, pharyns, and larynx can also be affected. In some cases, mucosal involvement may lead to destruction of the face structure, causing respiratory failure associated with death (Marra *et al.* 2014). In addition, presence of *Leishmania* RNA virus 1 (LRV1) in the cytoplasm of the parasite has recently been shown to influence the severity of mucosal lesions and the overall course of the disease, being associated with failure of first-line treatment in patients infected with *L. guynensis* and *L. braziliensis* containing LRV1 (Adaui *et al.* 2016; Bourreau *et al.* 2016; Brettmann *et al.* 2016).

The most extreme form of the disease is the VL, caused by *L. donovani* and *L. infantum* (synonym, *L. chagasi)*, being potentially lethal if not treated. Commonly referred as kala-azar in the Indian subcontinent, it is characterized by systemic and chronic infection, affecting mainly organs such as spleen, liver and bone marrow. Symptoms include anemia, progressive cachexia, intermittent fever, hepatomegaly and splenomegaly (Piscopo and Azzopardi 2007).

There are still some rare manifestations, such as the diffuse cutaneous leishmaniasis (DCL) seen in anergic individuals. DCL is characterized for numerous non-ulcerated nodules with an abundant intracellular amastigote load, resulted from strong humoral immune response and weak T cell activation. This chronic disease caused predominantly by *L. amazonensis* does not heal spontaneously and is associated with incomplete response to treatment, resulting in frequent relapses (Scott and Novais 2016).

Consistently, there is a causal relationship between species and clinical outcomes (see Figure 1.2), but this is not always the case. Dermotropic species, for instance *L. braziliensis* and *L. amazonensis*, have been described to cause visceral disease in individuals co-infected with Human Immunodeficiency Virus (HIV); conversely, viscerotropic species like *L. infantum* have been reported in cutaneous lesions (Lindoso *et al.* 2016).

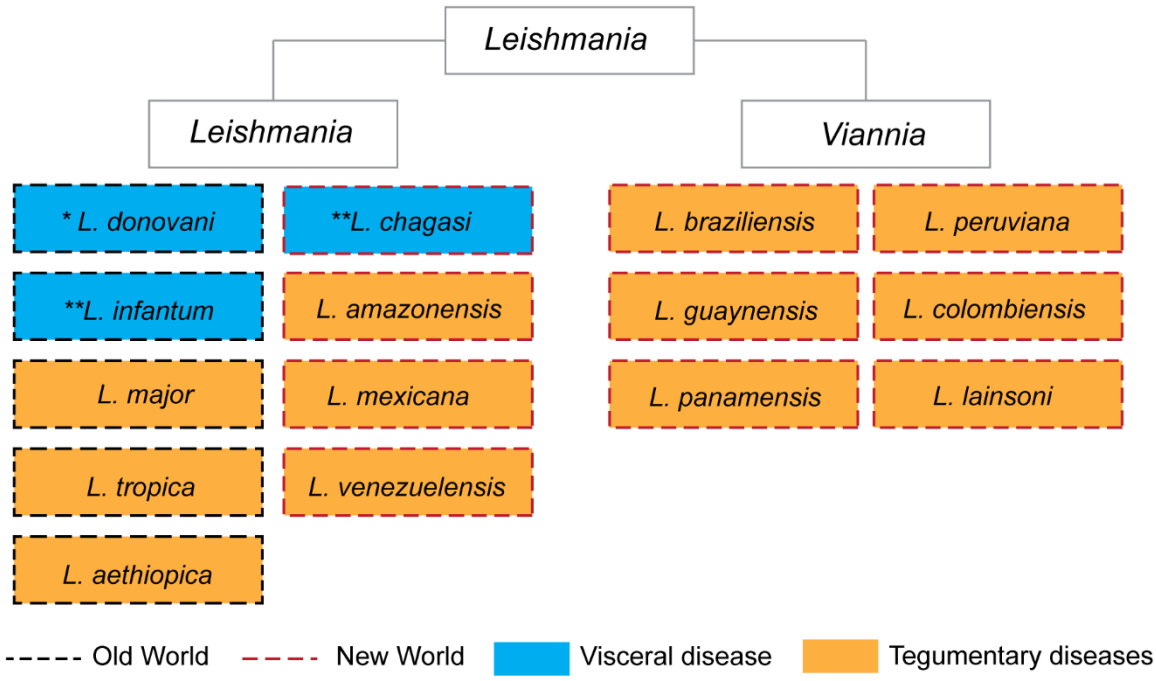

Figure 1.2 *Leishmania* species and more often related clinical manifestation. The genus *Leishmania* has two subgenera: *Leishmania* and *Viannia*. The most frequent species in the Old and New World are displayed. ***L. donovani* is the causative agent of post–kala-azar dermal leishmaniasis (PKDL). ** In South Americas, *L. infantum* is known as *L. chagasi*. Adapted from (Akhoundi et al. 2016).

The vectors and reservoirs add a further layer of complexity, their variety reflects a long association that equipped the parasite with unique metabolic features to maintain its transmission and pathogenicity. Among over 800 species of sandflies, 78 are proven vectors of human leishmaniasis; these include 31 *Phlebotomus* species (Old World) and 47 *Lutzomyia* species (New World) (Akhoundi *et al.* 2016). Besides, there are so many hosts of *Leishmania* parasites, showing regional and temporal variations, that only local studies involving ecological and parasitological analysis can determine whether an animal is playing a role as reservoir in a given region. In addition to humans, a wide range of wild and domestic mammals have been recorded as hosts and/or reservoirs of *Leishmania spp* (domestic dogs, sloths, opossums and rodents, among others). Notwithstanding, the classification into visceral and cutaneous forms, based on tissue tropism of *Leishmania spp.* in humans, cannot be applied to the infection in other mammals (Roque and Jansen 2014). For instance, dogs infected with *L. infantum* present mixed forms in almost every case, where parasite isolation is common even from intact skin (Miró and López-Vélez 2018).

In nature, the competent vectors often display specific relationships with parasites, transmitting only a single or limited number of *Leishmania* species. However, some sandflies are considered permissive (or non-specific) vectors, because it is possible to experimentally infect them with several *Leishmania spp*. The association between vector-parasite generate

region-specific epidemiological characteristics (Sacks and Kamhawi 2001). In spite of such strong association, *Leishmania spp.* show an impressive plasticity to adapt to new vector species under environmental condition changes. In the Andean valleys of Chaparral, *Lutzomyia longiflocosa* was found to be the vector in *L. guyanensis* transmission, very different from the previous known vector *Nyssomyia umbratilis* (Ferro *et al.* 2011, 2015).

1.3 Current antileishmanial chemotherapy

It has been more than 100 years since Gaspar Vianna tested emetic tartar to treat cutaneous leishmaniasis (Vianna 1912). Later on, in 1920, Upendranath Brahmachari produced the first organic antimonial to achieve wide acceptance as a treatment for human leishmaniasis, which saved thousands of lives in India (Brahmachari 1989). Since then, less toxic pentavalent antimonials (sodium stibogluconate and meglumine antimoniate) were produced, but they still require long course parenteral treatment and careful health monitoring (Chulay *et al.* 1988). Injectable pentavalent antimonials were the single regimen available to treat VL for more than 50 years, and up to now remain a pillar of therapy for leishmaniasis, except in the Indian subcontinent, where they have been abandoned due to widespread resistance (Kuhlmann and Fleckenstein 2017).

New drugs have been introduced in the therapeutics of leishmaniasis over time. The first use of Pentamidine for VL treatment was reported in India in 1949 and in Spain in 1950 (Hazarika 1949; Martinez Garcia *et al.*1950). *In vitro* activity of amphotericin B was for the first time reported in 1960 and the first successful treatment of patients with VL was reported in 1963 in Brazil (Furtado *et al.* 1960; Prata 1963). In early 1990's, the advent of the first lipid-carrier formulation decreased acute and chronic toxic effects of deoxycholate formulation of amphotericin B (Gulati *et al.* 1998; Meunier *et al.* 1991). Miltefosine was identified and evaluated independently in the early 1980s as a potential anti-cancer drug in Germany and as a leishmanicidal drug in the UK; and in 2002, it was approved in India as the first oral treatment of VL (Croft and Engel 2006). Paramomycin was shown to be efficacious for the treatment of CL in 1966 and for VL in 1990 in Kenya (Chunge *et al.* 1990; Moskalenko and Pershin 1996).

Against the progress achieved by the introduction of new therapeutic options, all current drugs present important drawbacks, such as: low efficacy, high toxicity, length of treatment or high cost (revised in Uliana *et al.* 2018). For example, miltefosine, the only available oral drug, is teratogenic and causes severe gastrointestinal side effects; already liposomal amphotericin B has intravenous administration, requires unbroken cold chain for distribution and is highly costly. Table 1.1 summarizes the limitations of current treatment.

Table 1.1Current antileishmanial chemotherapy

Drugs	Usual Regimen	Administration	Efficacy	Resistance	Toxicity	Advantages	Limitations
Sodium stibogluconate and meglumine antimoniate (Pentostam® and Glucantime®)	20 mg/kg/day for 30 days	Intravenous, Intramuscular or Intralymphatic	Varies between 35-95% based on area	Common more than 65% in Bihar, India	Severe cardiotoxicity, nephrotoxicity, pancreatitis and hepatotoxicity	Availability	Confirmed resistance in Bihar, India Compliance issues (lengthy treatment and painful administration)
Amphotericin B deoxycholate (Fungizone®)	1 mg/kg/day for 30 days	Intravenous	> 90%	Laboratory strains	Severe nephrotoxicity, thrombophlebitis and hypokalaemia	Primary resistance not documented	Heat instability Hospitalization for slow intravenous infusion
Liposomal Amphotericin (Ambisome®)	3-5 mg/kg/day for 20 days	Intravenous	> 96%	Not documented	Mild nephrotoxicity, chills and fever during infusion	Low toxicity, resistance not documented	Heat instability High cost
Miltefosine (Impavido™)	2-2.5 mg/kg/day for 28 days	Oral	> 94%	Laboratory strains	Hepatotoxicity, nephrotoxicity and teratogenicity	Oral treatment	Long half-life encourages emerging resistance Cannot be administered to pregnant patients
Paromomycin (Humatin®)	15 mg/kg/day for 21 days	Intramuscular Topical	> 94% in Asia and 46-85% in Africa	Laboratory strains	Ototoxicity, nephrotoxicity and hepatotoxicity	Low cost	Efficacy varies between different strains of *Leishmania* Potential for resistance
Pentamidine (Pentacarinat®)	3 mg/kg/day for 4 days	Intramuscular	Varies between 36-96% based on area	Not documented	Severe hyperglycaemia, Mayocarditis hypotension and tachycardia	Short dosage regimen	Efficacy varies based of geographical location of the disease

Adapted from (Zulfiqar *et al.* 2017).

Furthermore, factors associated with low adherence of patients and treatment schemes not well clinically validated promote disease relapse and emergence of drug resistance, contributing to the therapeutic failure. The inconsistent methodologies used in clinical trials to assess regimens options especially hampers the progress of CL treatment standardization (Olliaro *et al.* 2018).

In order to increase treatment efficacy, drug combination has been explored in leishmaniasis clinical trials. Improvement in tolerability are expected, as the two drugs can be administered below their individual dose limits, possibly reducing their side effects. Furthermore, this approach has demonstrated potential results to prevent and/or delay the emergence of pathogen resistance (Alirol *et al.* 2013; MacLean *et al.* 2010). Visceral leishmaniasis' clinical studies using amphotericin B in combination with miltefosine or paromomycin have shown promising results: both combinations were well tolerated and safe, with cure ratios that exceeded 94% (Rahman *et al.* 2017). The use of pentavalent antimonial combined with pentoxifylline has also been proved effective against cutaneous and mucocutaneous leishmaniasis (Brito *et al.* 2017; Machado *et al.* 2007). Topical formulations combined with systemic drug may also represent an interesting option to severe forms of CL, as in such cases only topical or local treatment are not recommended (Uliana *et al.* 2018).

Given the epidemiologic impact of leishmaniasis as well as the lack of appropriate treatment options, the development of safer, more effective and affordable new drug candidates and/or the improvement of existing therapies remains a priority.

1.4 The challenging *Leishmania* drug discovery pipeline

Drug discovery and development is a long and complex process (see Figure 1.3). At the outset, basic research relies on two approaches: (i) the identification, validation and characterization of drug targets; and (ii) establishment of appropriate cell-based models. Then screening technologies allow test of libraries with novel pharmacophores to identify hits in both target-based and cell-based assays. Partnership between university and industry, and financial support are essential to maximize the number of tested samples. Such support from public-private partnerships and interaction with the pharma/biotech sector is also important to bring expertise in lead optimization and preclinical studies (toxicology, pharmacokinetics and pharmacodynamics). Eventually, a compound is targeted to clinical trials in humans and, once showing a satisfactory profile, it is defined as a drug candidate. Multidisciplinary centers and integrated network are fundamental to trial design standardization and systematic reporting, making feasible the comparison of efficacy among studies with different drugs and regions.

The last steps of the development process include registration and manufacturing of the medicine. In this case, governmental policies are the responsible for an adequate drug legislation, and a functioning drug regulatory authority with adequate resources and infrastructure to enforce the legislation and regulations (revised in Alcântara *et al.* 2018).

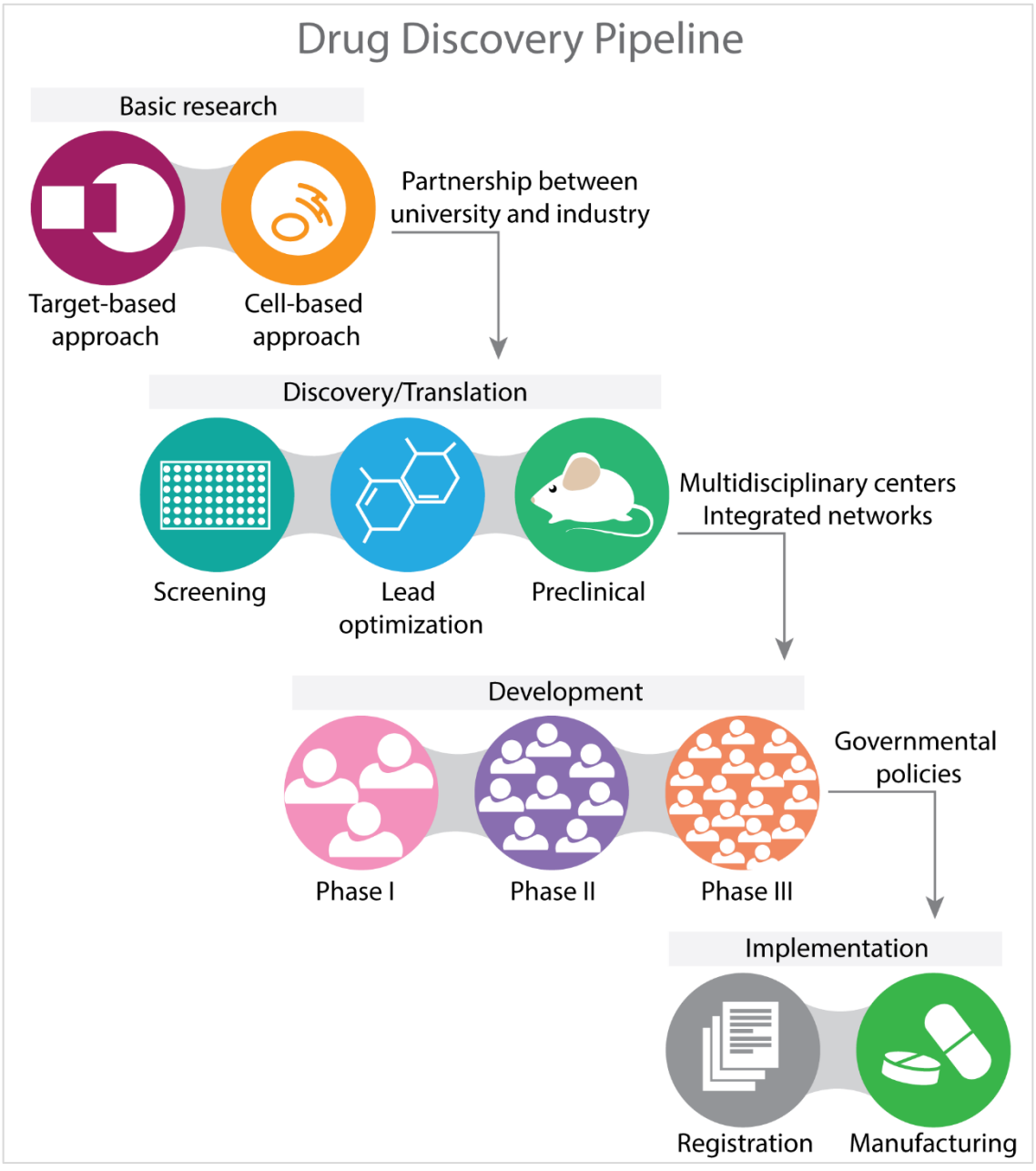

Figure 1.3 Drug discovery pipeline. The process often starts with basic research in order to (i) identify and validate molecular/biochemical targets (target-based assays) or (ii) develop and validate phenotypic assays (cell-based assays), which will be used to screen compounds. Medicinal chemistry experts will then optimize selected compounds. Next steps consist in testing candidates in animal models and assessing their performances by determining pharmacokinetics and pharmacodynamics properties. Finally, a compound is targeted to clinical trials in humans and, once showing a satisfactory profile, it is defined as a drug candidate. The last steps of the pipeline include registration and manufacturing of the medicine. The arrows show institutions that helps to integrate the whole process.

Target product profile (TPP) is defined as a planning tool for promising therapeutic candidates. Basically, TPP takes into account factors, such as compounds' clinical efficacy, delivery mode, safety and tolerability, contraindications, dosage form, stability, treatment duration, and cost (NIH 2018; Bandyopadhyay 2017). When applied properly, it can play a central role in drug discovery pipeline, driving both compounds progression and prioritization (Field *et al.* 2017; Wyatt *et al.* 2011). Table 1.2 display the optimal TPP established by DND*i* for leishmaniasis. Overall, drug candidates should present broad-spectrum activity, in terms of distinct species and geographic regions.

Table 1.2 Optimal Target product profile of new chemical entities for leishmaniasis

	Visceral Leishmaniasis	Cutaneous Leishmaniasis
Species	All species	All species
Distribution	All areas	All areas
Clinical Efficacy	> 95%	>95%, minimal scar and no relapse
Safety and Tolerability	Should not require monitoring	Should not require monitoring
Contraindications	None	None
Interactions	None – Compatible for combination	None – Compatible for combination
Formulation	Oral /intramuscular depot	Topical / oral
Treatment Regimen	1/day for 10 days po/ 3 shots over 10 days	Topical: 14 days; Oral: < 7 days
Stability	3 yrs in zone 4	No cold chain, at least 3 years at 37ºC
Cost	< $10 / course	US$5

Data available at www.dndi.org, Nov, 2018

Recently, *in vitro* cell-based assays have become the main screening strategy in drug discovery for *Leishmania spp*. Enzymatic-based approaches are less applied mainly because not many targets have been genetically or chemically validated (Jones *et al.* 2018). Additionally, there is a lack of knowledge about the exact mode of action for standard antileishmanial drugs, which potency seems to reflect the inhibition of multiple targets or pathways (Castillo *et al.* 2010). Although target identification is not necessarily required for clinical development, it does represent a key knowledge that can support optimization and development of back-up series, as well as the assessment of possible off-target effects and emergence of drug resistance. Notwithstanding, in the past few years, two promising antileishmanial compounds with known targets have emerged, both primarily identified by cell-based assays. Khare *et al.* identified the triazolopyrimidine molecule GNF6702 as having potent activity against *Leishmania*. It acts by inhibiting the cell's proteasomal protein-degradation machinery (Khare *et al.* 2016). Secondly, Willie and collaborators reported a potential drug candidate (DDD853651/GSK3186899) that inhibits the parasite protein kinase enzyme CRK12.

This drug showed *in vitro* potency and *in vivo* efficacy with appropriate pharmacokinetic, physicochemical and safety properties, being approved to human clinical trials (Wyllie *et al.* 2018).

The cell-based models evaluate compound activity based on inhibition of parasite multiplication and viability. There are several screening assays available against *Leishmania spp.* based on the parasite different stages: promastigotes, axenic amastigotes or intracellular amastigotes. As can been seen in Figure 1.4, the use of each stage has advantages and disadvantages (revised in Zulfiqar *et al.* 2017).

Insect stage	Mammalian stage	Mammalian stage
		
Promastigotes	Axenic amastigotes	Intracellular Amastigotes
Assays		
- Colorimetry - Fuorescence - Chemiluminescence - Radionucleotide uptake	- Colorimetry - Fuorescence - Chemiluminescence - Radionucleotide uptake	- Direct counting - Chemiluminescence - Fuorescence - High-content imaging
Advantages		
- Quicker results - Higher throughput - Reproducibility	- Quicker results - Higher throughput - Reproducibility - Relevant stage of parasite	- Relevant stage - Phagolysosome (acidic milieu)
Limitations		
- Non-relevant stage - Lack of correlation with intracellular assays	- Lack of correlation with intracellular assays	- Lower throughput - Lower reproducibility - Lower hit rates

Figure 1.4 Advantages and limitations of assays with the different stages of *Leishmania spp.*

Screenings with axenic forms of *Leishmania* present several advantages; (i) easily yield sufficient number of parasites to test many compounds; (ii) faster read-outs; (iii) higher throughput; and (iv) reproducibility. These features are particularly attractive for initial screening of large sample libraries. However, *Leishmania* promastigotes and amastigotes survive and proliferate in very different environments. The parasites optimize their metabolism in order to utilize the available resources, which explains the observed stage-specific differences to drugs (Subramanian and Sarkar 2017). Siqueira-Neto *et al.* showed that 50% of the hits detected against the intracellular amastigote are not detected in the promastigote

screening (Siqueira-Neto *et al.* 2012). Still, although axenic amastigote screenings are performed using the clinically relevant stage of the parasite, the capacity of drug penetration in the host cell is not evaluated, neither is the activity in the phagolysosomal environment (acidic milieu). There is a high false-positive rate for the axenic amastigote assay, showing a lack of correlation with intracellular amastigote assays (De Rycker *et al.* 2013). In addition, the establishment of axenic amastigote cultures is not successful achieved for all *Leishmania* species (Gomes-Alves *et al.* 2018). Lastly, axenic assays do not allow identification of compounds when host cell metabolism is required for activity, or when antileishmanial capacity is promoted by modulation of the infected macrophages.

Despite all drawbacks, axenic amastigote assays can be used to identify antileishmanial candidates, since associated with intracellular assays for further characterization of compounds activity. A successful example is the recent screening of 3 million compounds against *L. donovani* axenic amastigotes (Khare *et al.* 2016). The library was also concomitantly screened against *Trypanosoma cruzi* intracellular amastigotes and *Trypanosoma brucei* bloodstream trypomastigotes. An azabenzoxazole compound, GNF5343, was identified as a hit in the primary screening for *L. donovani* and *T. brucei*, but not for *T cruzi*. Interestingly, the compound demonstrated anti-*T. cruzi* activity in secondary assays, which further demonstrates the difficulty to primary identification of compounds in intracellular models. The initial EC_{50} value of GNF5343 against *L. donovani* intracellular amastigotes was 7.3 µM. Its chemical optimization, focused on improving bioavailability and potency on inhibition of *L. donovani* growth within macrophages, led to the discovery of a more potent analog: GNF6702 (EC_{50} of 18 nM). The GNF6702 was able to clear parasites from mice in all three models of infection. Further studies identified GNF6702 as a selective inhibitor of the kinetoplastid proteasome (Khare *et al.* 2016).

The intracellular amastigote assay of *Leishmania spp.* is recognized as the more representative model for drug discovery. Because beyond the activity against the amastigote stage, the ability of crossing multiples membranes and stability in the parasitopharous vacuole acid milieu (pH 5.5) is evaluated. The main drawback is the low rate of active compounds, for reasons that are not well understood, but may be partially explained by slow replication of intracellular amastigotes (Tegazzini *et al.* 2016). The reported *in vitro* intracellular models involve primary isolated macrophages as host cells (mouse peritoneal macrophages, mouse bone-marrow-derived macrophages or human blood monocyte-derived macrophages), murine cell lines (Raw 264.7 and J774A.1) or human-monocyte transformed macrophages cell lines (THP-1, U937, and HL-60). The activity of tested drugs is measured by microscopic counting

of infected cells and number of amastigotes per macrophage or by colorimetric/fluorimetric methods (Croft *et al.* 2006). Thus, there are several cell-based assays, making it complicated to compare screening data between different laboratories using distinct screening methods. A common denominator for comparison of different protocols would be the level of activity of reference drugs, which should, theoretically, perform similarly. However, the *in vitro* activity of antileishmanial drugs has been reported as host-cell dependent (Seifert *et al.* 2010), and variation in *Leishmania* species sensitivity is extensively described (Morais-Teixeira *et al.* 2011; Escobar *et al.* 2002; Yardley and Croft 2000).

In the intracellular amastigote assays context, High Content Screening (HCS) has been highlighted. The HCS methodology is based on automated imaging followed by analysis and data extraction by a software (Lansing *et al.* 2007). This setup enables qualitative and quantitative systematic evaluations of varied cellular phenomena (for example, absence or reduction of parasites in host cells), being used to measure compound activity. In this case, all potential targets are exposed to tested compounds, thereby increasing the probability of finding active compounds with different modes of action. Since the description of the first HCS assay for intracellular amastigote (Siqueira-Neto *et al.* 2010), several protocols have been stablished. The differences are based on the host cells type, parasite stage used to infect cells (promastigotes or amastigotes), periods of incubation and the fluorophores used for detection (Tables 1.3 and 1.4).

Among the limitations of HCS approaches, when compared to fast-reading assays (colorimetric/fluorescent/luminescent), are the need of data storing and management capacity, and the relatively low speed of HCS data acquisition and analysis, which has been constantly improved by HCS systems manufacturers. Considering its complex cellular models and higher sensitivity to micro-environmental variations (mechanical forces and thermic oscillation), cell-based assays also tend to present lower reproducibility when compared to target-based assays (Moraes and Franco 2016).

Despite the limitations, HCS of intracellular amastigote remain the benchmark for *Leishmania* drug discovery. This is mainly because HCS technologies also permits the early assessment of potential toxicity against the host cells, and morphological changes examination that can provide useful information to understand the mode of action of the compounds of interest. In addition, HCS association with High Throughput Screening (HTS), miniaturized and totally automated assay version, makes it possible to screen thousands of compounds in a single run (Zanella *et al.* 2010).

Table 1.3 HCS assays reported for *Leishmania spp*.: general biological parameters

Reference	Species	AMB pEC_{50}	Parasite culture medium	Parasite stage	Cell	MOI	Treatment period
(Gomes-Alves *et al.* 2018)	*L. infantum* (MHOM/MA/67/ITMAP-263)	7.4	RPMI 1640 10% FBS	Axenic amastigotes	BMDM, BALB/c	10	24 h
(Gomes-Alves *et al.* 2018)	*L. amazonensis* (MHOM/BR/LTB0016)	7.4	Schneider's 10% FBS	Stationary promastigotes	BMDM, BALB/c	10	24 h
(Eren *et al.* 2018)	*L. guyanensis* (MHOM/BR/75/M4147)	6.6	Schneider's 20% FBS	Stationary promastigotes	BMDM, C57BL/6	10	48 h
(Duffy *et al.* 2017)	*L. donovani* (MHOM/IN/80/ DD8)	6.5	M199 10% FBS	Stationary promastigotes	THP-1	5	96 h
(Tegazzini *et al.* 2016)	*L. donovani* (MHOM/SD/62/1S-CL2D, LdBOB) eGFP	7.2	Specifc media decribed in (Goyard *et al.* 2003)	Axenic amastigotes	THP-1	10	96 h
(Dagley *et al.* 2015)	*L. mexicana* (MNYC/BZ/62/M379)	6.3	RPMI 1640 10% FBS	Axenic amastigotes	THP-1	10	96 h
(Aulner *et al.* 2013)	*L. amazonensis* DsRed2 (MPRO/BR/1972/M1841, LV79)	6.8	-	Amastigotes freshly purified from lesions	BMDM, BALB/c	3	72h
(De Rycker *et al.* 2013)	*L. donovani* eGFP (MHOM/SD/62/1S-CL2D, LdBOB)	6.7	Specifc media decribed in (Goyard *et al.* 2003)	Axenic amastigotes	THP-1	5	72h
(De Muylder *et al.* 2011)	*L. donovani* (MHOM/SD/62/1S-cl2D)	7.1	RPMI 1640 10% FBS and 10% Brain Heart Tryptose	Stationary promastigotes	THP-1	15	72h
(Siqueira-Neto *et al.* 2010)	*L. donovani* (MHOM/ET/67/HU3)	6.5	M199 10% FBS	Stationary promastigotes	THP-1	50	96 h

pEC_{50} = -log EC_{50} (M)

Table 1.4 HCS assays reported for *Leishmania spp*.: imaging and analysis

Reference	Assay format	Staining	Mangnification/ Nº images per well	Image acquisition system/ analysis software	Number of tested compounds
(Gomes-Alves *et al.* 2018)	96-well	DAPI, CellMask Deep Red and antibody against *Leishmania* Alexa Fluor 568	20X/ 4 images	IN Cell Analyzer/ Investigator or CellProfiler	Only reference compounds
(Gomes-Alves *et al.* 2018)	96-well	DAPI, CellMask Deep Red and antibody against *Leishmania* Alexa Fluor 568	20X/ 4 images	IN Cell Analyzer/ Investigator or CellProfiler	Only reference compounds
(Eren *et al.* 2018)	96-well	DAPI and phalloidin-Alexa488	40x/ 49 images	MetaXpress and AcquityEpress	1,280
(Duffy *et al.* 2017)	384-well	SYBR green/ CellMask Deep Red	20X/ 4 images	Opera / Acapella	400
(Tegazzini *et al.* 2016)	384-well	DAPI/ eGFP	20x/ 4 images	Opera QEHS/ Acapella	176
(Dagley *et al.* 2015)	384-well	DAPI, CellTracker Green (CMFDA) and CellTracker Orange CMRA	20x/ 25 images	Cellomics ArrayScan VTI/Cellomics Colocalization V4 BioApplication	Only reference compounds
(Aulner *et al.* 2013)	384-well	Hoechst 33342 and LysoTracker DND-26	10x/ 15 images	Opera QEHS, Acapella	60
(De Rycker *et al.* 2013)	384-well	DAPI, HCS Cellmask Deep Red/eGFP	10x/ no reported	IN Cell Analyzer 1000 or 2000/ Investigator	15,659
(De Muylder *et al.* 2011)	96-well	DAPI	20x/ 8 images	INCell Analyzer 1000/ INCell Developer Toolbox 1.7	909
(Siqueira-Neto *et al.* 2010)	384-well	Draq5	20x/ 4 images	Opera/ Image Mining (IM) software in-house.	26,500

As can be observed in Table 1.3, the THP-1 macrophages have been widely applied in HCS assays. THP-1 is a human monocyte-like cell line, derived from the peripheral blood of a childhood case of acute monocytic leukemia (Tsuchiya *et al.* 1980). They need to be activated to induce differentiation into macrophage-like cells. Phorbol 12-myristate 13-acetate (PMA) and 1 α, 25-dihydroxyvitamin D3 (VD3) are two common activators for THP-1, after stimulation cells become adherent, acquire morphological features of macrophage-like cells, upregulate phagocytic receptors and stop proliferation (Schwende *et al.* 1996; Tsuchiya *et al.* 1982). Although PMA is not a substance endogenously produced in the host, PMA-stimulated differentiation generates cells more similar to macrophages derived from human peripheral blood mononuclear cell (PBMC) (Schwende *et al.* 1996). However, little is known about the PMA mechanism responsible for regulating this differentiation process, but there is evidences that the phosphoinositide-3-kinase/AKT (PI3K/AKT) signaling pathway is involved (Zeng et al. 2015). Surprisingly, THP-1 cells do not respond to macrophage colony-stimulating factor (M-CSF), a potent a hematopoietic growth factor that regulates functional activation of monocytes, but rather internalize and degrade it very quickly (Datta *et al.* 1992). Once differentiated (M0 macrophages), they can be incubated with IL-4 and IL-13 in order to obtain M2 polarized macrophages or with IFN-gamma and LPS for classical macrophage activation (M1) (Genin *et al.* 2015). Additionally, THP-1 cells are rapidly differentiated into mature dendritic cells (DCs) when cultured in serum-free medium containing granulocyte-macrophage colony-stimulating factor (GM-CSF), tumor necrosis factor-α (TNF-α) and ionomycin (Berges *et al.* 2005). The differentiation process is summarized in Figure 1.5.

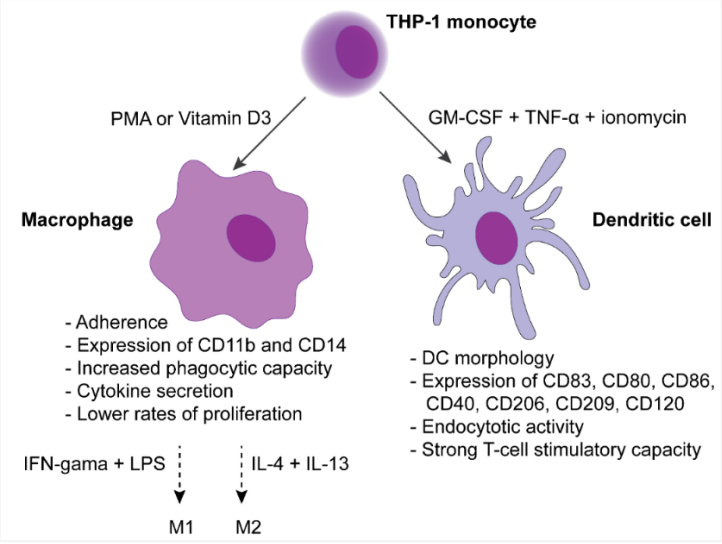

Figure 1.5 Differentiation of THP-1 cells. These monocytes-like cells can be stimulated toward macrophage or dendritic cell phenotypes. After incubation with specific activators, there are cellular effects on morphological, phenotypical, molecular and functional properties.

There has been a great engagement of screening research groups, allowing the identification of new active, selective and bioavailable compounds, which are now progressing into the development pipeline (DND*i* 2016). However, the path to be followed by a new chemical entity from discovery to registration is a long and costly process, there are high attrition throughout the pipeline, causing downstream failures of most candidates. As in the case of VL-2098, a molecule identified by DND*i* as very potent and safe, being selected for in-depth evaluation of its efficacy, pharmacokinetic, and early safety profile (Gupta *et al.* 2015). Later on, it was observed that VL-2098 causes testicular toxicity in mice models and therefore a decision was made to stop development of this drug (DND*i* 2015).

High quality compound collections can be composed by: fully synthetic molecules; naturally-occurring bioactive small molecules, derivate from natural products (extracts from plants, animals, microbes and minerals); and semi-synthetic molecules, hybrids of natural and synthetic sources. *In vitro* drug screening, regardless of the library composition, may select candidates for new drugs. The two new promising antileishmanial compounds, GNF6702 and DDD853651/GSK3186899, were identified from synthetic libraries (Wyllie *et al.* 2018; Khare *et al.* 2016). Leishmaniasis chemotherapy has been historically associated with natural products (revised in Rodrigues *et al.* 2015). Amphotericin B is extracted from the filamentous bacteria *Streptomyces nodusus* and paromomycin is extracted from *Streptomyces rimosus* (Rodrigues *et al.* 2015). The identification of natural products with antileishmanial activity is constantly reported, such as artemisinin and lissoclinotoxin E (Zulfiqar *et al.* 2017; Sen *et al.* 2010). However, the identification of a new molecular scaffold, also known as *de novo* drug discovery, is high cost and time-consuming. Thus, drug repurposing has been considered as a powerful approach to accelerate the process of novel candidates' identification and optimization. Several antileishmanials were primarily indicated for others pathologies: amphotericin B, pentamidine and paromomycin (revised in Charlton *et al.* 2018). Despite the often assignment of miltefosine as a repurposed medicine to leishmaniasis, the discovery of its antiprotozoal and antineoplastic activities occurred simultaneously but independently (Croft and Engel 2006). However, priority was given first to the development of miltefosine as a treatment for cancer, which highlights the negligence toward leishmaniasis. Drug repurposing continuously identify new antileishmanials, noteworthy, the example of tamoxifen. Tamoxifen is a broad spectrum antileishmanial with activity against clinical isolates from CL and VL patients (Miguel *et al.* 2011, 2009, 2007). Figure 1.6 shows the compounds exemplified here for each approach.

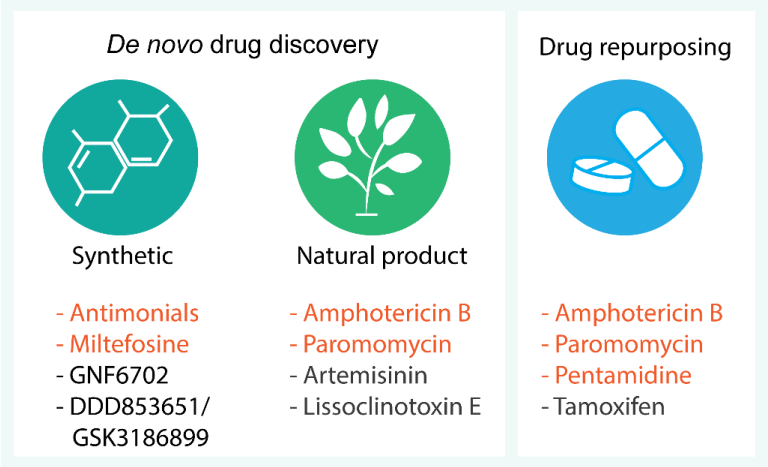

Figure 1.6 Drug discovery approaches. Examples of leishmnanial compounds for each category are shown. Current therapy is highlighted in red.

The use of animal models is still necessary to establish anti-protozoan activity, pharmacokinetic properties (absorption, distribution, metabolism, excretion- ADME) and safety profiles. Due to the complex pathophysiology of human leishmaniasis, developing and validating a relevant animal model is challenging. Hamsters are recognized as a promising model for VL, notably for *L. donovani*, as they mimic features of human visceral leishmaniasis showing progressive increase in parasite burden, cachexia, hepatosplenomegaly, pancytopenia, hypergammaglobulinaemia and ultimately death (Garg and Dube 2006). Post-kala-azar dermal leishmaniasis (PKDL) is a complication associated with VL caused by *L. donovani* and for which there is no animal model of infection established. Regarding CL, there are several species causing different clinical manifestations, which brings complexity to the establishment and validation of models with features similar to humans with respect to etiology, pathophysiology, symptomatology, and response to the therapeutic or prophylactic agents. Therefore, there is no validated animal model for CL (Mears *et al.* 2015).

The inconsistency observed in activity translation of compounds from *in vitro* to *in vivo* assays, as well from animal models to clinical research, is a major scientific gap in *Leishmania spp.* drug discovery. Improved translation might result from validation of more representative animal models.

Unfortunately, most of the compounds do not reach the clinical stage. A recent systematic review identified 145 published visceral leishmaniasis clinical trials from 1983 to 2015, with data from ~27k patients. Only 0.75% (203 patients) were enrolled in studies with other drugs excluding pentavalent antimonial, amphotericin B deoxycholate, miltefosine, amphotericin B lipid-associated formulations, paromomycin, pentamidine or sitamaquine

(Bush *et al.* 2017). Notwithstanding the current Public – Private – Partnerships (PPP) initiatives (revised in Alcântara *et al.* 2018), which combine academic knowledge and pharma/biotech expertise in an efficient *modus operandi* network addressing all aspects of *Leishmania* drug discovery, no drug candidate fulfilling DND*i* target product profile has been forwarded to clinical evaluation so far.

Once a molecule is defined as a drug candidate, it seems the most challenging steps have been trespassed (discovery, design, synthesis and clinical trial). However, a whole world of flaws arises: regulatory approval and commercialization. The drug must be manufactured according to high standards of purity and stability as established by regulations. In last instance, commercial price and supply strategies must assure availability. Miltefosine is an example of successful research and development (R&D) for a neglected tropical disease (NTD) that fails to reach the target population. The medicine price is not affordable for the majority of patients, most of them poor and marginalized. And even when provided for free by the public health system in the Indian subcontinent, the supply of the drug never quite met the demand. Furthermore, lack of the active pharmaceutical ingredient in generic capsules has been reported in Bangladesh (Sunyoto *et al.* 2018).

1.5 Cutaneous leishmaniasis: neglected within neglected tropical diseases

Neglected Tropical Diseases (NTD`s) are a group of infectious diseases which affect over one billion people globally, predominantly tropic and sub-tropic regions, but despite such scope, treatment options are partly investigated. The most affected people are the poorest population due to malnutrition, population displacement and lack of access to safe water, sanitation and basic health services. Therefore, pharmaceutical industry and academia present minor interest in this field because such diseases do not represent a substantial profitable market. Accordingly with the 10th meeting of the Strategic and Technical Advisory Group for Neglected Tropical Diseases, the World Health Organization (WHO) lists 20 poverty related diseases, including leishmaniasis (WHO 2017).

Due to the limited resources available for the development of new drugs against neglected diseases, for many years cutaneous leishmaniasis (CL) was not part of the research and development (R&D) agenda of most foundations, partnerships or the industrial sector. Correspondingly, the scientific community has focused on the screening of compounds against visceral species, considering its higher mortality rate. This scenario started to change after the creation of the Drugs for Neglected Diseases initiative (DND*i*) in 2003 and subsequent inclusion of all types of CL in the target diseases list in 2007 (Modabber et al. 2007). Although

CL is associated with low mortality, it causes very severe disfiguring scars in infected individuals, which most often leads to stigmatization. Such scars can be considered, in some societies, indicatives of low social status, further enhancing stigma. In a worse scenario, when leishmaniasis is believed to be contagious, infected individuals can be prevented from attending school, reinforcing the vicious cycle of disease and poverty (Alvar *et al.* 2006).

There are substantial differences in cell biology, biochemistry and immune response among *Leishmania* species, generating the wide spectrum of clinical manifestations. Apart from that, it is more likely that no single chemotherapy will be suitable for all species, which is evidenced by reference drugs variable efficacy depending on the clinical form and geographical location. Therefore, a species-specific approach should be considered. The lack of satisfactory therapeutic agents has prompted the engagement of pharmaceutical companies and research institutes in screening of millions of samples on cell-based systems trying to identify new chemical series for visceral leishmaniasis (Khare *et al*. 2016; Peña *et al.* 2015). By contrast, still, few screenings of large compound collections with novel chemical classes have been reported for cutaneous leishmaniasis species, which was one of the underlying driving motivations for this project.

2 Objectives

The purpose of this study was to establish a High Content Screening (HCS) assay for different *Leishmania* species and, in doing so, evaluate the impact of species-specificity in compound selection.

The specific aims of the present work were as follows:

- Development of a protocol for image analysis using commercial softwares;
- Establishment of the intracellular assay conditions for dermotropic species;
- Validation of the HCS assay for dermotropic species by evaluating the activity of a commercial library and widely used reference drugs, amphotericin B and miltefosine;
- Screening of two libraries (LOPAC and Pathogen Box) for dermotropic and vicerotropic species of *Leishmania*, followed by correlation analysis of selected compounds between species;
- Identification of pan-antileishmanial compounds.

3 Material and methods

Unless otherwise specified, all experimental conditions in 384-well plates were tested in at least 16 well-replicates per independent experiment. Dose-response curves are assessed in triplicates.

3.1 Cell lines and parasite lineages

The THP-1 cell line is a human monocytic cell line, derived from the peripheral blood of a human male child with acute monocytic leukemia. It is maintained in suspension and becomes adherent upon differentiation into macrophage-like cells. The differentiation process was induced by phorbol-12-myristate-13-acetate (PMA). The present cell stock was acquired from the Rio de Janeiro Cell Bank, Xerém-RJ, Brazil.

Raw 264.7 is a murine leukemia adherent macrophage cell line established from a tumor induced by the Abelson murine leukemia virus. This cell was kindly donated by Prof. Dr. André G. Tempone, Center for Parasitology and Mycology Institute Adolfo Lutz, Secretary of Health of São Paulo State.

J774A.1 is a murine adherent macrophage cell line derived from a tumor in a female BALB/c mouse. This cell line was donated by Prof. Dr. André G. Tempone, Center for Parasitology and Mycology Institute Adolfo Lutz, Secretary of Health of São Paulo State.

L. amazonensis strain MHOM/BR/1977/LTB0016, *L. braziliensis* strain MHOM/BR/75/M2903, *L. major* strain MHOM/SU/73/5-ASKH and *L. infantum* MHOM/BR/2002/LPC-RPV were obtained from the *Leishmania* collection of Fundação Oswaldo Cruz, Rio de Janeiro – RJ, Brazil ("Coleção de *Leishmania* do Instituto Oswaldo Cruz –CLIOC"). *L. donovani* (MHOM/IN/80/DD8) promastigotes were kindly provided by Prof. Silvia Uliana – USP, Brazil. These *Leishmania* strains were maintained *in vitro* as promastigotes. Their infectivity *in vivo* was not tested.

All cultures were routinely screened for mycoplasma contamination using MycoAlert™ Mycoplasma Detection Kit (Lonza).

3.2 Animals

Female mice of 8 to 12-week-old balb/c strain were used. The animals were kept without water or dietary restriction, in light/dark cycles under a temperature of 22 to 25 °C, in the experimental room of the Department of Parasitology UNICAMP. The experiments with animals were performed in collaboration with Prof. Danilo Ciccone in the Infection Biology Studies lab _ LEBIL. The protocol for the use of animals was approved by the Committee on

Ethics in the Use of Animals (CEUA), registered under N°. 4047-1 for use of animals under experimentation, 10/26/2015 (See Annex I and II).

3.3 Reference compounds

Stock solutions of amphotericin B and miltefosine (Sigma- Aldrich) were prepared by dissolving standardized powder in 100% dimethyl sulfoxide (DMSO) at 20 mM. VL-2098 was provided by DND*i*, and a stock solution of 20 mM was prepared in 100% DMSO. Aliquots were stored at – 20°C, under low-humidity conditions, and protected from light.

3.4 LOPAC library

LOPAC®1280 were purchased from Sigma- Aldrich. The library was acquired dissolved in 100% dimethyl sulfoxide (DMSO) at a stock concentration of 10 mM and was stored at – 20°C, under low-humidity conditions, and protected from light. At first, the LOPAC library was tested at the single concentration of 50µM. For potency determination of selected compounds, *cherry picking* was performed, followed by confirmatory dose-response studies.

3.5 Pathogen Box library

The library contains 400 molecules and is provided dissolved in 100% dimethyl sulfoxide (DMSO) at a stock concentration of 10 mM. The four 96-well plates were manually reformatted into 384-well plates and compounds were 2.5-fold diluted in 100% DMSO to final concentration of 4 mM. The library was kept frozen at – 20 °C, under low-humidity conditions, and protected from light. The Pathogen box library was tested at single-point concentration of 20 µM.

3.6 *Leishmania spp.* culture

Unless otherwise stated, *Leishmania spp.* promastigotes were cultured in M199 media supplemented with Hepes (40 mM), adenine (0.1 mM), biotin (1 µg/mL), hemin (25 µg/mL), L-glutamine (2 mM), 10% FBS (20% for *L. braziliensis*), penicillin G (100 U/mL) and streptomycin (100 µg/mL). Parasites were passaged at 5 x 10^6/mL every 2 to 3 days in T25 or T175-flasks and maintained at 26 °C under constant agitation (30 rpm).

At the infection day, promastigotes parasites from 6-day old (or 5-day/7-day old, when specified) cultures were counted, centrifuged (pelleted) at 2,200 x g for 5 min, resuspended and diluted to the correct density in RPMI 1640 media. The infection was performed with 50 promastigotes per cell (or 10/20/40, when specified) by adding 25 µL of the promastigote suspension in each well. The plates were incubated at 37 °C (34 °C for cutaneous

species), in a 5% CO_2 humidified incubator for 24h prior treatment with compounds.

3.7 Raw 264.7 and J774A.1 cell lines culture

Raw 264.7 and J774A.1 cell lines were maintained in RPMI 1640 medium supplemented with 10% of heat-inactivated Fetal Bovine Serum (FBS), Hepes (10 mM), sodium bicarbonate (1.5 g/L), sodium pyruvate (1 mM), penicillin G (100 U/mL) and streptomycin (100 µg/mL). at 37°C in a 5% CO_2 humidified incubator. Subcultures were prepared washing the cells twice with PBS, followed by the addition of trypsin for 5 minutes, then dilution in completed medium and thoroughly re-supension. The cells were counted and then plated at density of $1x10^5$/mL or at ratio of 1:10 every 3 to 4 days in T75 flasks.

3.8 Culture of L929 cells and recovery of supernatant

L929 cell line secretes macrophage colony stimulating factor (M-CSF), an important factor for the differentiation of bone marrow derived macrophages. In order to obtain their supernatant, the cells were cultured in 15 mL of RPMI 1640 medium, supplemented with 10% FBS, in a 75 cm^2 flask. The flask was maintained at 37 °C in the presence of 5% CO_2 for 7 days or until reaching maximum confluency. After, the culture was washed twice with PBS, followed by the addition of 3 mL 0.05% trypsin for 5 minutes at 37 °C to detache the cells. The reaction was blocked by adding 7 mL of RPMI 1640 medium supplemented with 10% FBS, stopping the action of the enzyme. Cells were resuspended and divided into 20 cell culture flasks of 175 cm^2 containing 40 mL of RPMI 1640 medium, supplemented with 10% FBS. After 14 days at 37 °C in the presence of 5% CO_2, the culture supernatant was collected, centrifuged at 524 x g for 10 min, filtered in a 0.2 µm filter and stored in aliquots at -20 °C until use.

3.9 BMDM isolation

Bone marrow-derived macrophages (BMDMs) were isolated from femurs of female BALB/c mice, as described previously (LUTZ *et al.*, 1999; CORTEZ *et al.*, 2011). Briefly, the mice were euthanized in a CO_2 chamber. The femurs and tibias were then withdrawn and immersed in 70 ° GL alcohol for 2 min, followed by immersion in PBS. Afterwards the two epiphyses were cut off and the bone flushes with 5ml RPMI 1640 medium. The flow-through was then collected. The cell suspension was centrifuged at 230 × g for 10 min at 4 ° C and next resuspended in RPMI 1640 medium supplemented with 20% of heat-inactivated Fetal Bovine Serum (FBS), Hepes (10 mM), sodium bicarbonate (1.5 g/L), sodium

pyruvate (1 mM), penicillin G (100 U/mL), streptomycin (100 µg/mL) and 20% of L929 cell supernatant. Cells were cultured in cell culture dishes of 100 mm in diameter at 4×10^6 cells in 10 mL of medium and incubated at 37 °C for 4 days in the presence of 5% CO_2. On the fourth day a further 10 mL of RPMI 1640 medium supplemented with 20% FBS and 20% supernatant of L929 cells were added to the plate. On the seventh day of culturing, adhered macrophages were detached by scraping with a cell scraper and used for assays. Cell viability was assessed using trypan blue (0.04 %) and a hemocytometer (Neubauer chamber). The plating was performed in 384 well plates at the density of 7,500 cells per well and maintained at 37 ° C for 24 hours prior to infection.

3.10 THP-1 culture and differentiation

THP-1 cells were cultured in RPMI 1640 medium supplemented with 20% of heat-inactivated Fetal Bovine Serum (FBS), Hepes (10 mM), sodium bicarbonate (1.5 g/L), sodium pyruvate (1 mM), penicillin G (100 U/mL) and streptomycin (100 µg/mL), at 37 °C in a 5 % CO_2 humidified incubator. Cells were seeded at 2 x 10^5/mL every 3 to 4 days in T-flasks and maintained in exponential growth up to 10 passages, after which the batch was discarded and a new culture was started from a frozen culture stock. The cellular density cannot exceed 1×10^6/mL.

THP-1 cells were differentiated from monocytes to macrophages 4 days after passaging in culture flasks. Unless otherwise noted, cells were washed once in RPMI media and plated onto 384 well plates (F-bottom, µCLEAR®, black, Greiner Bio-One—cat. no. 781091) at 7,000 cells/well in 25 µL of RMPI media containing 50 ng/mL PMA, and incubated at 37 °C/5 % CO_2 for 48 h before infection.

3.11 Intracellular amastigotes assay

THP-1 cells were plated onto assay plates (7,000 cells/well, 50 µL) in RPMI media (50 ng/mL PMA), and incubated at 37 °C/5 % CO_2 for 48 h. Then, cells were infected with day-6 promastigotes at a multiplicity of infection (MOI) of 50 by adding 25 µL of RPMI (without PMA) containing $1.4x10^7$ parasites/mL, thus decreasing PMA concentration to 25 ng/mL. After 24h of incubation at 37 °C (34 °C for cutaneous species), 10 µL of compounds were added to the plate, as well as 10 µL of the negative control-vehicle (0.5% DMSO) and the positive control (10 µM amphotericin b), according to a plate map. For dose-response curves, ten-points of serial dilution by a factor of 2 were tested. After 96h of compound exposure at 37 °C or 34 °C, plates were fixed with 4% paraformaldehyde (PFA) in PBS pH 7.4 and washed three times with PBS.

Following fixation and washing, plates were stained with 5 µM Draq5 in PBS, and processed for image analysis. The sequential steps are represented in Figure 3.1.

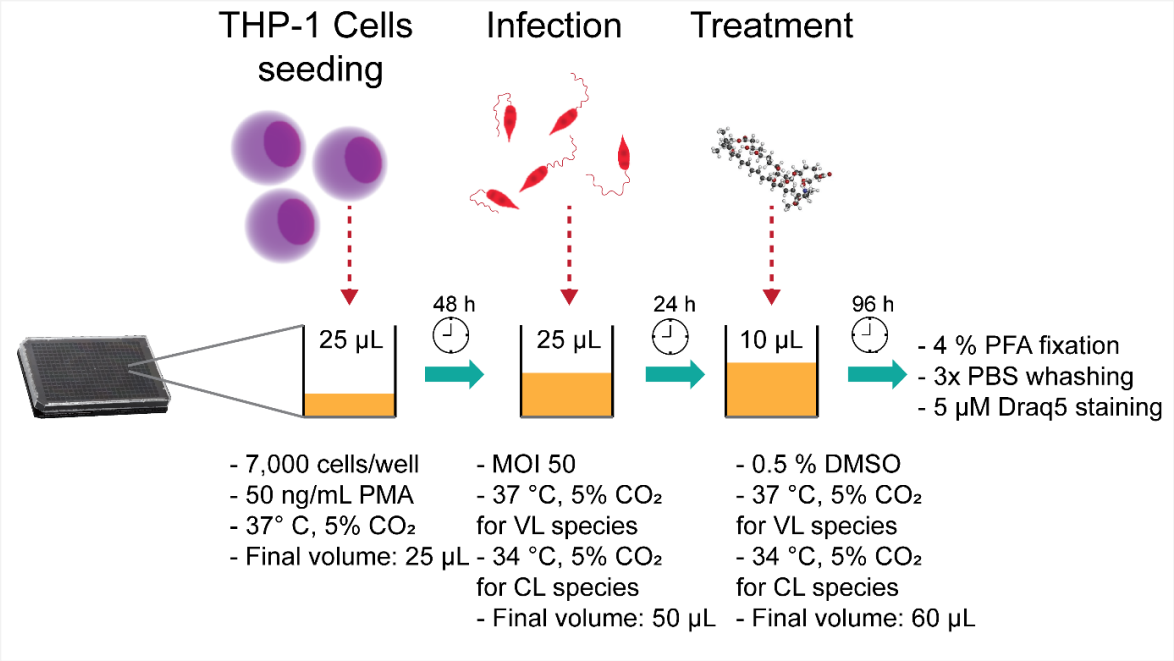

Figure 3.1 Intracellular amastigotes assay protocol.

3.12 High content image acquisition and data analysis

Four images from each well were acquired in the Operetta High Content Imaging System (PerkinElmer), version 3.1, or in the InCell Analyzer High Content Imaging System (GE), version 2200, using a 20x objective and filters optimized for far-red fluorescence (fluorescence filter: 635nm).

Next, images were analyzed by Harmony (PerkinElmer) or Investigator (GE) software, providing the following outputs: total number of cells, total number of infected cells, number of parasites (spots) per infected cell, the ratio of infected cells to the total number of cells, this is the Infection Ratio (IR), in all 4 images from a given well. The tables 3.1 and 3.2 display the parameters used for each software. The parameters values in the tables are mean values obtained for all species under the experimental conditions here described, each parameter was fine adjusted to optimize parasites detection for each specie. These values change according with the image objective, time of exposure, quality of the image.

Table 3.1 Parameters of Harmony software

Analysis steps	Parameters	Parameter value
Find nuclei (method B)	Common Threshold	0.50
	Area	>55µm^2
	Split factor	14.0
	Individual Threshold	0.65
	Contrast	> 0.20
Find cytoplasm (method B)	Common threshold	0.35
	Individual threshold	0.15
Select population I	Common filters	Remove the border objects
Find spots (method C)	Radius	≤1.43
	Contrast	>0.13
	Uncorrected spot to region intensity	>0.90
	Distance	≥1.20
	Spot peak radius	0.00
Select population II	Filter by property	Number of spots ≥ 1
Define results	Sets which information will be provided from image analysis.	Total cell number, Infected cells number, and total spots number

Table 3.2 Parameters of Investigator software

Analysis steps	Parameters	Parameter value
Nuclei	Segmentation	Top-hat
	Minimum area	80 µm^2
	Sensitivity	85
Cells	Segmentation	Collar
	Radius	15.6
Organelles	Segmentation	Multiscale top-hat
	Granule size	1.2-3
	#Scales	1
	Sensitivity	85
	Detect inclusions	In the cytoplasm
	Advanced _ sensitivity range	3.5
Summary	Sets which information will be provided from image analysis.	Total cell number, Infected cells number, and total spots number

To determine the normalized antileishmanial activity (NA), the raw data of infection ratio (IR) for the samples (S) was normalized to the IR mean of negative controls (NC), meaning 0.5% DMSO-treated infected cells, which is the concentration found in each well when compounds are added; and the IR mean of positive controls (PC), that is non-infected cells treated with 0.5% DMSO. Data normalization is performed per plate. NA is expressed as a percentage of activity in comparison to control wells, according to the equations below:

$$Normalized\ Acitivity = \left[1 - \left(\frac{IR(S) - mean\ IR(PC)}{mean\ IR(NC) - mean\ IR(PC)}\right)\right] \times 100$$

Normalized Activity values were processed with the Graphpad Prism software, version 6, for generation of sigmoidal dose-response (variable slope) nonlinear curve fitting. Potencies were expressed as $pEC_{50,}$ which is the negative log of the EC_{50} value in molar [pEC_{50} = -log EC_{50} (M)]. For the purpose of this study, pEC_{50} values were determined by interpolation, and EC_{50} defined as the compound concentration corresponding to 50% normalized activity after 96h of compound incubation. The pEC_{50} is the better option to evaluate and compare potencies, since the curve fitting actually solves for the logEC_{50}, not EC_{50}. The standard error for pEC_{50} are symmetrical (pEC_{50} 8.0 ± 0.6). Already EC_{50} values reported as molar values are on a linear scale, and the error becomes asymmetric, which may be confusing (10nM ± 30nM would mean EC_{50} ranges from -20nM to 40nM). The more potent the compound gets, its pEC_{50} increases (Murray 2013). Table 3.1 exemplify the correspondence between EC_{50} and pEC_{50} values.

Table 3.3 EC_{50} and pEC_{50} values

EC_{50}	EC_{50} (M)	pEC_{50}
1 nM	10^{-9}	9.0
10 nM	10^{-8}	8..0
30 nM	$10^{-7.5}$	7.5
100 nM	10^{-7}	7.0
1 µM	10^{-6}	6.0
10 µM	10^{-5}	5.0
30 µM	$10^{-4.5}$	4.5
100 µM	10^{-4}	4.0
1 mM	10^{-3}	3.0
10 mM	10^{-2}	2.0

The number of THP-1 cells are used for preliminary toxicity determination, named cell ratio (CR). The ratio between the total cell number in each sample (S) well and the mean cell number in the negative controls (NC), meaning 0.5% DMSO-treated infected cells, is calculated (see equation below). As closer to 1, there was no cell toxicity, comparing to control. Below 1 indicates a decrease in cell number, and above 1 suggest a relative increase in cell survival. The cell ratio values above 0.5 were considered acceptable.

$$Cell\ Ratio = \frac{cell\ number\ (S)}{mean\ cell\ number(\ NC\ )}$$

Plates were also submitted to quality control analysis using the Z´-factor, the equation is shown in Figure 3.2. The Z′-factor is a screening window coefficient. It describes how well separated the positive and negative controls are, and indicates the likelihood of false

positives or negatives (Zhang *et al.* 1999). A good assay has a large signal window or separation band (>3-fold) and clear separation between the tails of the distributions of the controls. Values between 0.5 and 1(large separation band) are excellent, values between 0 and 0.5 (small separation band) may be acceptable, and values less than 0 (no separation band – variation bands overlap) indicate the assay is unlikely to be usable in a high-throughput context. Individual assay plate Z'-factors were derived from the negative controls (infected cells threated with 0.5% DMSO) and positive controls (non-infected cells). An experimental run was considered successful only if the plates Z'-factors were >0.5.

$$Z'-factor = 1 - \frac{3.SD(PC)+3.SD(NC)}{|mean(PC)-mean(NC)|}$$

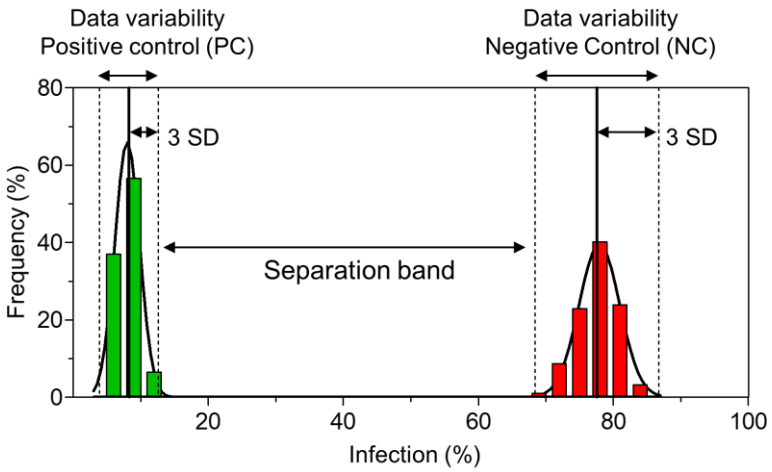

Figure 3.2 Z'-factor determination. Histogram representing controls infection distribution. X-axis shows infection bins (%) and y-axis shows the frequency (%) of compounds per bin. The solid line represents the mean value. The dashed lines represent 3 standard deviations above and below the means.

3.13 Resazurin assay

In order to evaluate the THP-1 cells viability at 34 °C and 37 °C, different THP-1 cell densities (2000, 4000, 6000, 8000 cells/well) were plated into 384-well plates and incubated at 37 °C/5 % CO_2 for 48 h. After this time, one plate was maintained at 37 °C and the other one was transferred to a 34 °C in a 5 % CO_2 humidified incubator. At 84 h post cell plating, resazurin (Sigma R7017) was added to the plates at a final concentration of 10 µM and incubated for further 12 h. Then, plates were fixed and stained with Draq5 (BioStatus). Wells containing only media and resazurin were used as background control.

3.14 Determination of the drug exposure window

On day 1, THP-1 cells were plated in 384 well plates at 7,000 cells/well in 25 µL

of RMPI complete media containing 50 ng/mL PMA, and incubated at 37 °C/5 % CO_2 for 48h to complete differentiation. On day 3, promastigotes were added to the plate at 50 parasites/cell in 25 µL of RPMI media per well and transferred to a 34 °C/ 5 % CO_2. On day 4, amphotericin B was serially diluted in 2-fold serial dilution in DMSO in 10 points in a polypropylene (PP) 384 well plate using a 16-channel manual pipette equipped with disposable tips, followed by a dilution of 16.6-fold in PBS ("intermediate dilution"). Then, 10 µL of intermediate plate content were transferred onto plates containing *Leishmania*-infected THP-1. The starting test concentration was 25 µM. Each concentration was tested in triplets in the same plate. The plates were incubated at 34 °C/5 % CO_2. Finally, plates fixed with 4 % paraformaldeh (PFA) at some time-point after experimental treatments (0, 24, 48, 72, 96 and 120h) and then subsequently washed, labeled and read in HCS instrument.

3.15 EdU incorporation test

In order to evaluate the EdU incorporation in cells infected with *L. amazonensis*, EdU (Click-iT® Plus Alexa Fluor® 488 kit, Life Technologies) was added in the assay plates at 100 µM for 24 hours. Plates were fixed with 4% PFA for 15 minutes and permeabilized with 0,5 % Triton X-100 in PBS for 20 minutes. Posteriorly, cultures were washed twice with 3% BSA and treated with Click-iT® reaction cocktail for 30 minutes, at room temperature, protected from light. For nuclear staining, cultures were incubated with with 5 µM Draq5 in PBS. Then plates were read in HCS instrument.

3.16 Tanimoto structural similarity index

In order to identify common scaffolds, the Tanimoto structural similarity index was calculated using the online service ChemMine Tools (http://chemmine.ucr.edu/).

4 Results and Discussion

There are two key points to be considered in a High Content Screening (HCS) assay: (i) the biologic model relevance and (ii) the imaging analysis. Although both aspects were developed concomitantly, in order to facilitate the understanding, this thesis approach them separately. Initially, it is described how two different commercial HCS systems were successfully used to generate quantitative data (section 4.1). Then, the establishment of the intracellular amastigote assay for dermotropic species is reported (section 4.2). The HCS assay for dermotropic species was validated by activity evaluating of a commercial library and widely used reference drugs, amphotericin B and miltefosine (section 4.3). The validation for viscerotropic species has been reported in the PhD thesis of Alcântara (Alcântara 2017). The section 4.4 gives an overview of the multi-species high content assay protocol. The sections 4.5 and 4.6 report the screening of two libraries: LOPAC and Pathogen Box, respectively. Finally, section 4.7 indicates pan-antileishmanial compounds.

4.1 Image analysis protocol

The HCS platforms are complex instruments with lots of components: the stage; the light source; the autofocus system; and the light path, including objectives, filters, mirrors, and the camera or photomultiplier tube. Firstly, and most important, is to use a calibrated equipment that always captures the same quality image, allowing to compare and reproduce data over time, for example, plate-to-plate and day-to- day. After the system is set up to acquire the best images possible, the next step is the optimization of image analysis parameters. The analysis software assign pixels to objects and characterize its features (intensity, color, size, shape, texture, or dynamics). Then, image analysis algorithms derive qualitative and quantitative measures of the features (Trask and Johnston 2015).

In the protocol here described, the goal is to count the number of cells and classify the ones containing intracellular amastigotes, a measurement named as infection ratio. So, two objects are identified based on its features: cell and parasite. The object “cell” has two subregions: nucleus and cytoplasm. Using Draq5, a far-red fluorescent DNA stain, both parasites and host cells are detected. Though Draq5 is a stain specific for DNA, its background on cell organelles is enough for cytoplasm delimitation. As plates can be read using a single channel for fluorescence, there is a reduction of time in both image acquisition and analysis, representing an advantage considering large scale screenings.

Fluorescence images were acquired using the Operetta system (Perkin Elmer). The objective has impact on performance and throughput, affecting the resolution, field of view,

detection sensitivity, and algorithm performance. Because resolution and field of view are inversely related, higher resolution results in a smaller field of view with fewer cells per image, requiring longer scan times to analyze acceptable number of cells. The 20x magnification was enough to identify cell and parasites. Higher magnifications would facilitate parasites detection, but it would also evidence artifacts. For Operetta 20x objective, the 384-well microplate can be subdivided into 35 imaging fields (each image with approximately 0.35 mm^2). The lowest number of images that statistically represented the whole well was 4 (~1,000 cells), therefore 4 images were acquired for each well. This correlation is only true if the distribution is homogenous throughout the well. Others acquisition parameters were also set up, such as: exposure time, focus and plate map. As the autofocus was not available in the device options, a multiple stacks imaging was performed, adjusting the focus to evidence the amastigotes.

Harmony high-content analysis software is a commercial software designed for Operetta, Operetta CLS and Opera Phenix high-content screening systems. Figure 4.1 shows a raw image followed by analysis segmentation. Each specific parameter is adjusted empirically by trial and error from among available options.

The single plan image analysis consists on the following sequential building block setups:

- Raw image (Figure 4.1 A): represents the pseudocolored original image acquired by Operetta at 20x magnification. Parameters such as exposition, excitation and focus stacking were determined at the acquisition time in order to provide high quality images.
- Find nuclei (Figure 4.1 B): responsible for detecting nuclei in the image. The detection is based on the highest nucleus intensity compared to its surrounding.
- Find cytoplasm (Figure 4.1 C): delimits the cytoplasm; especially based on nuclei/cell areas and minimal contrast/intensity threshold. Some multinucleated cells are splitted in more than one individual cell.
- Select population I (Figure 4.1 D): creates a subpopulation from the Find Nuclei population. This first “selection population” is applied in order to exclude cells that are not completely inserted in the image field.
- Find spots (Figure 4.1 E): identifies individual intense spots (parasites) inside the host cells. The spots detection in based on the strong signal from the labeled DNA of the parasite nucleus and kinetoplast (indistinguishable under this magnification), within the limits of the previously defined cytoplasm area. The selected script allows, after fine adjustments, to detect the individual spots without generating, however, an excessive

number of false positives (in this case commonly generated by natural differences in cytoplasmic contrast or presence of cellular debris).

•Select population II (Figure 4.1 F): selects infected cells from the whole population. The use of method "filter by properties" is adapted to consider as infected cells the ones presenting number of spots ≥ 1.

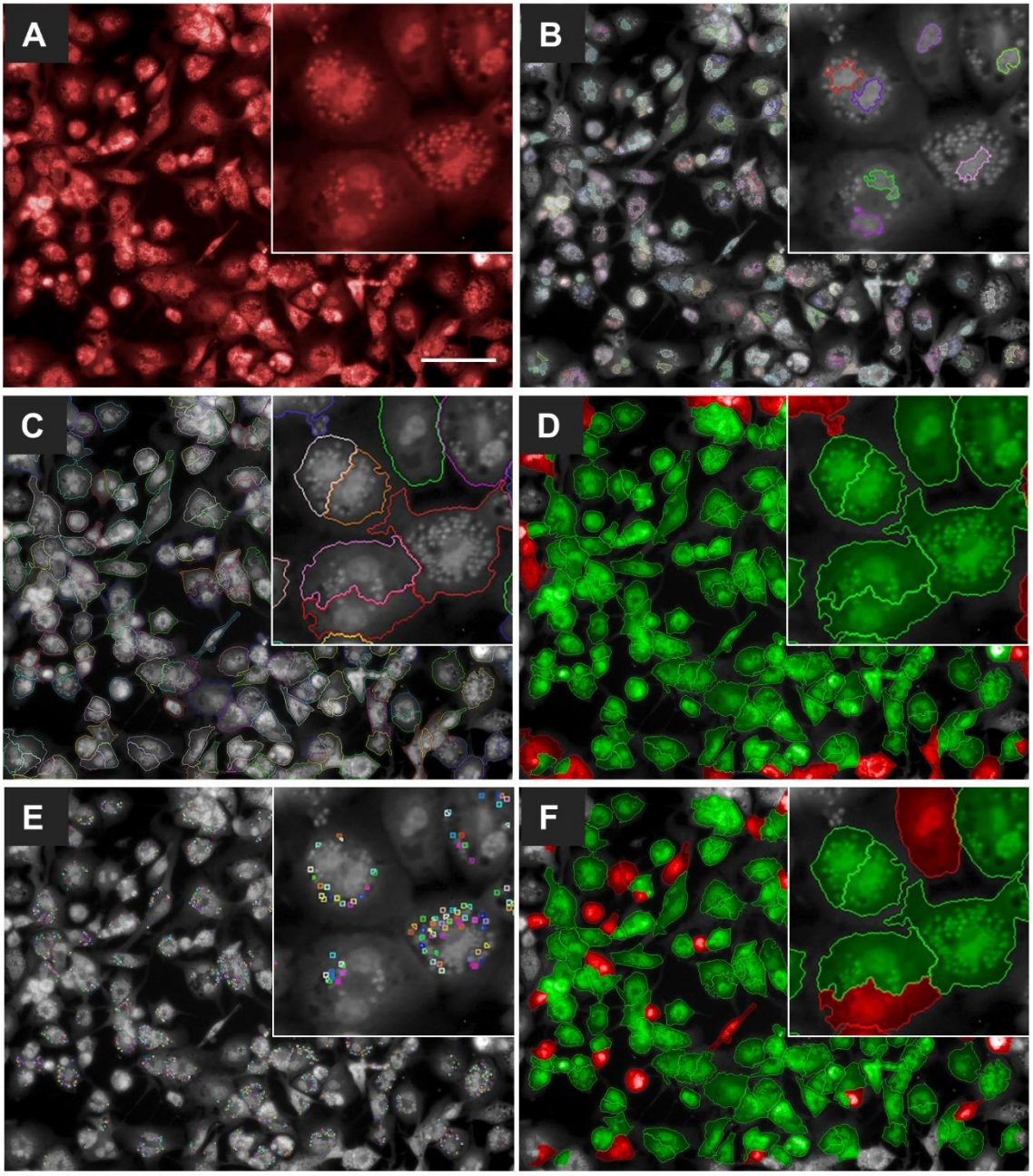

Figure 4.1 Harmony software image analysis building-blocks. Images of THP-1 cells infected with *L. braziliensis*. **A)** Pseudocolored raw image acquired from Operetta microscope with a 20x objective. **B)** Nuclei detection**. C)** Definition of the cytoplasmic region. **D)** Elimination of cells that are not completely inserted in the image field (red cells). **E)** Spot detection (parasites). **F)** Infected cells are highlighted in green, noninfected cells are in red. Scale bar: 100 µm.

After being configured, the whole script is tested on the positive and negative

controls in order to evaluate the detection of false positives false positives (non-infected cells are selected as infected cells due to cellular structures recognition as parasites by the software) and false negatives (infected cells are selected as a non-infected cells due to intracellular amastigotes that are not detected as a spot). For the infection ratio of non-infected cells, a maximum of 10% false positive was tolerated. The specific readouts chosen were: total host cells number, infected cells number, infection ratio and the number of parasites per each well.

The software sensitivity was evaluated by using different cell densities and different infections ratios. THP-1 cells were plated at 2000, 3000, 4000, 5000, 6000 and 7000 cells/well densities. The density of 7000 cells/well was infected with various multiplicities of infection (MOIs) _ 10, 20, 30, 40 and 50. The defined scripts were able to successfully measure the number of cells. Detection of cells increases as the number of seeded cells rises, which demonstrate a linear correlation (Figure 4.2 A). A linear increment was also observed in infection percentage and ratio of spots/cell when cells were infected with different MOIs, hereby validating the sensitivity of the system (Figure 4.2 B and C). As consequence of using a single channel for both cell and parasite delimitation, cellular debris and other non-specifically stained artifacts on cytoplasm lead to false positive detection of parasites. Therefore, the software sensitivity is reduced to prevent high ratios of false-positive. The reduction in sensitivity contributes to non-identification of some true parasites as spots, as can be seen in Figure 4.1 E. In addition, the parasites features used to identify spots (size, contrast, intensity threshold and the minimal distance between two spots to consider two independent objects) are heterogeneous, mainly because the images are acquired in a single plan and amastigotes present a tridimensional disposition in the parasitophorous vacuole. The discrepancy between the real number of infected cells and the software analysis is corrected by normalization of data with positive and negative controls (as described in material and methods, section 3.12), thus calculating the infection inhibition percentage (named normalized activity). When the infection ratio of a sample well is higher than the mean value of negative control, the compound normalized activity will be negative, indicating an increase in the infection ratio. In the same way, but less obvious, when the infection ratio of a sample well is lower than the mean value of the positive control, the compound normalized activity will be greater than 100%. A sample can have an infection ratio lower than the non-infected cells. It occurs when the compound eliminates the parasites and, somehow, also decrease the incidence of debris and artifacts that mislead the detection of spots.

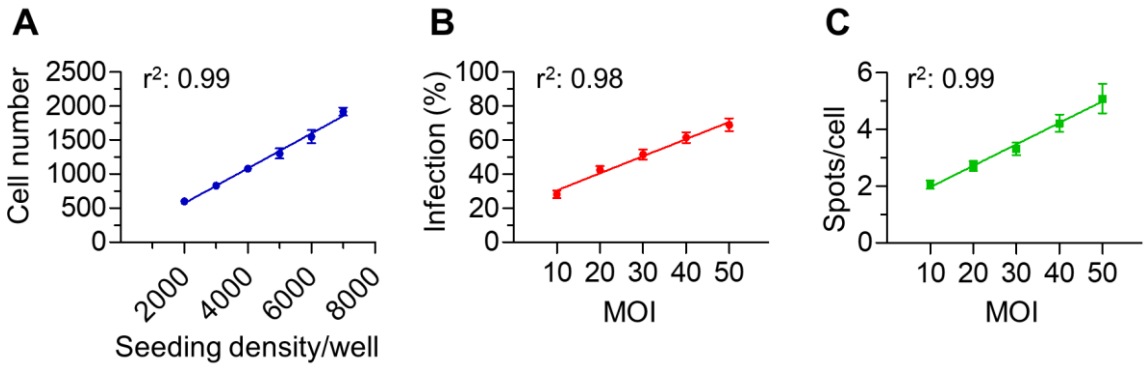

Figure 4.2 Harmony software sensitivity. THP-1 cells were seeded at different densities (2000, 3000, 4000, 5000, 6000 and 7000 cells/well). **A)** The number of cells in the 4 images was counted by the software for different seeding densities/well. Next, the 7,000 cells/well density was infected with multiples MOI of *L. braziliensis.* **B)** Infection percentage and **C)** spots per infected cell was measured by the software for different MOIs. Data points are means and error bars represent the standard deviation of 16 wells. The straight lines are linear regression lines, R-squared values above.

Some of the experiments here described used IN Cell Analyzer 2200 (General Electric) to acquire and analyze images instead of Operetta (Perkin Elmer). Each HCS instrument company has unique image analysis software. Image analysis algorithms from different sources may result in different EC_{50} values, even from the same image set. So, in order to check system-to-system variability, images of the same plates were acquired in the two equipment (Table 4.1). Then images were analyzed by Harmony software (Perkin Elmer) or Investigator software (General Electric). The Investigator software has a different interface and algorithm, but the steps of analysis are similar to those used in Harmony. Both image analysis softwares are intuitive and easy to navigate.

Table 4.1 Comparation between Operetta and IN Cell Analyzer analysis

		Z'-Factor	[a]Infection %	[b]Spots/cell
L. amazonensis	Operetta	0.89	89.81 (± 1.14)	17.77 (± 1.03)
	IN Cell	0.81	87. 42 (± 1.61)	11.36 (± 1.04)
L. braziliensis	Operetta	0.74	77.11 (± 4.01)	12.86 (± 1.21)
	IN Cell	0.73	78.93 (± 2.63)	8.13 (± 0.86)
L. donovani	Operetta	0.89	93.12 (± 1.31)	12.97 (± 0.76)
	IN Cell	0.78	86.78 (± 2.14)	7.41 (± 0.86)
Non-infected	Operetta	-	10.41 (± 1.69)	1.43 (± 0.14)
	IN Cell	-	14.33 (± 3.09)	0.21 (± 0.05)

[a] Means (± Standard Deviation).
[b] Means (± Standard Deviation) of spots per infected cell.

As evident in Table 4.1, there was no statistical difference in the percentage of infected cells detected using Operetta or IN Cell Analyzer. The Z'-factor were high for both

systems. Even though the spots/cell number differ, this is not the parameter used to evaluate compounds activity. Besides, as already mentioned, the determination of parasites (spots) is not absolute but proportional to the parasite load.

The most important aspect to be compared is compounds activity. Thus, the dose-response curve of two reference compounds for three species were assessed by Operetta and IN Cell Analyzer using the same assay plates to acquire and analyze images. As can be seen in Figure 4.3, the two generated curves are noticeably overlapping for all tested conditions. The data similarity is reinforced by the non-significant difference between pEC_{50} values (**Table 4.2**).

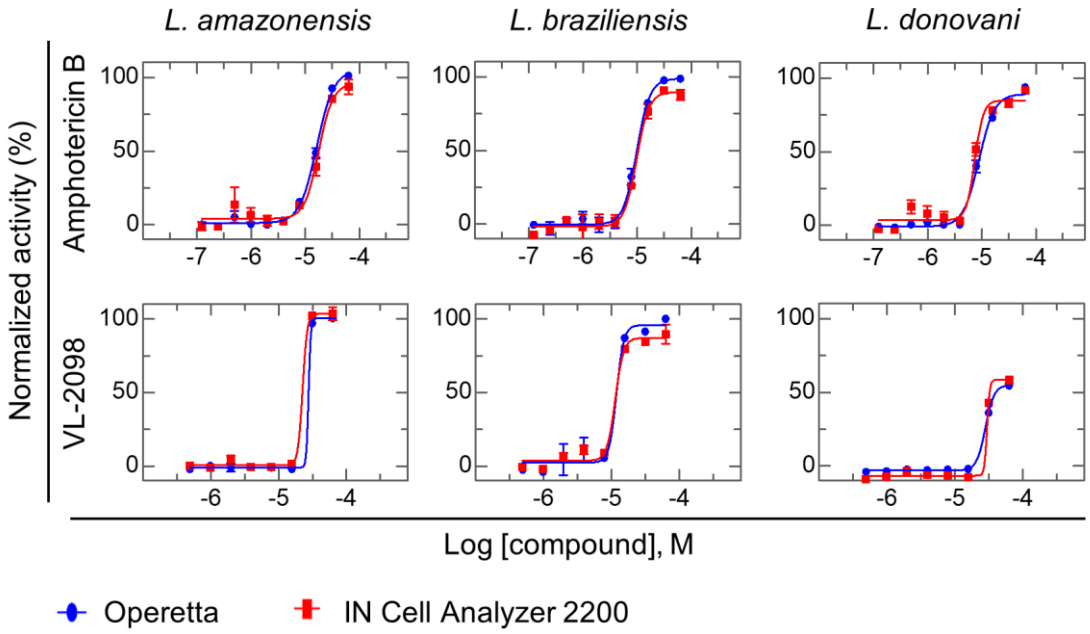

Figure 4.3 DRCs of reference compounds assessed by Operetta and IN Cell Analyzer. THP-1 cells were infected with *L. amazonensis*, *L. braziliensis* or *L. donovani* and treated with amphotericin b or VL-2098. The X-axis indicates the log of compounds concentration (molar) and Y-axis indicates the normalized antiparasitic activity, which represents the inhibition of infection in relation to controls. Data points are means and error bars represent standard deviations of triplicates.

Table 4.2 pEC_{50} values determined by Operetta and IN Cell Analyzer analysis

	L. amazonensis		*L. braziliensis*		*L. donovani*	
	Operetta	IN Cell	Operetta	IN Cell	Operetta	IN Cell
AMB	4.81	4.75	5.01	4.98	5.02	5.11
VL-2098	4.56	4.65	4.93	4.93	3.40	3.49

pEC_{50} = -log EC_{50} (M)

Commercial image analysis softwares are developed to be used in a variety of

assays. However, their development is based on limited number of cell lines, staining reagents, phenotypic changes, for which specific image analysis algorithms were developed to analyze a particular set of features and then extrapolated to similar assays. So, the difficulty for a precise recognition of a particular cellular phenotype is not surprising. Despite that, it is possible to configurate the script in order to improve accuracy. Certainly, some platforms provide more configuration flexibility by the user than others. The ideal would be to configurate a specific algorithm for each assay, increasing sensitivity and specificity. The development of *in house* software is an option, but it is time and resource consuming, besides, it requires high technical expertise.

Although the exact number of parasites per cell was not detected by neither of the commercial softwares here used, the event of interest, that is infection ratio reduction, was satisfactory assessed by both platforms. It should, however, be mentioned that precise number of parasites per cell would be crucial to evaluate the replicative dynamic of intracellular amastigotes. In that case, a second stain specific for amastigotes would be enough to achieve accuracy. Which is recommended for small sets of compounds, as in secondary assays or mechanism of action studies. However, in the case of primary screening, a second channel for fluorescence virtually doubles the time of image acquisition and analysis. Also, the higher number of images requires more storage space. Proper data storage and management is one of HCS challenges. It is highly recommended to keep backups of all images.

4.2 Establishment of the intracellular *Leishmania spp*. assay for dermotropic species

A range of tegumentary manifestations occurs due to *Leishmania spp.* infection. The most important determinant in the clinical outcome is the parasite species. Here the establishment of an intracellular assay is described for three species: *L. amazonensis*, *L. braziliensis* and *L. major*. When infected with *L. amazonensis*, patients often develop the severe syndrome termed diffuse cutaneous leishmaniasis. *L. braziliensis* is the species most often associated with the highly disfiguring mucocutaneous leishmaniasis. Despite *L. major* is most related to localized self-healing cutaneous leishmaniasis, its epidemiological importance is well known.

For drug discovery purpose, choosing the host cell is a decisive step in the establishment of an intracellular assay, as antileishmanial activity of compounds can be dependent of the host cell (Seifert *et al.* 2010). Beyond that, others aspects are also relevant in HCS assays context. The continuously requirement of large quantities of cell represents a bottleneck for the use of primary cells. Cell lines provide high densities of homogeneous

populations, an attractive for high-throughput assays, and no animals are involved, which is ethically attractive. Also, some morphological features are desired for image analysis: a monolayer growth, enabling proper cells individualization, and large cytoplasm, so amastigotes can be easily identified. To select the cell host, three cell lines were examined: Raw 264.7 and J774A.1 from murine origin, and THP-1 of human origin.

The RAW 264.7 and J774A.1 cell lines have a very small cytoplasm, what is problematic to spots identification. Furthermore, even after extensively effort to de-clumping before plating, both cell lines display multilayer points before achieving confluence regardless initial density, as indicated in Figure 4.4. At the end, no further attempts were performed to overcome such difficulties and these cell lines were not further considered for assay development.

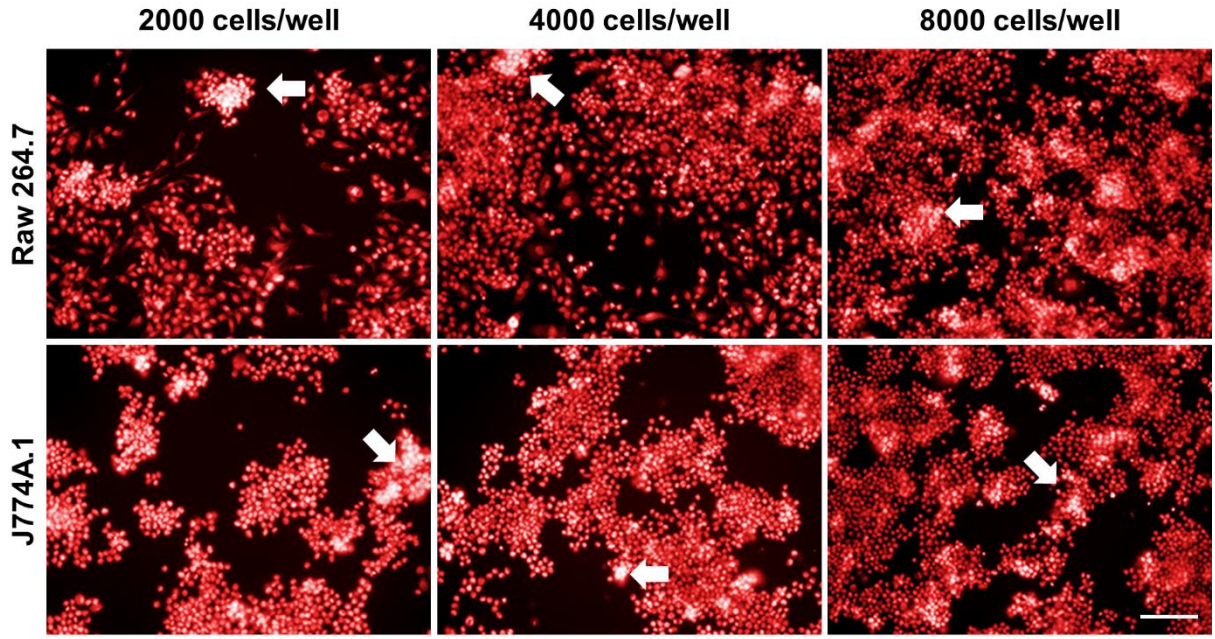

Figure 4.4 Standardization of RAW 264.7 and J774A.1 cell lines density in 384-well plates. Cells were plated at three different densities: 2000, 4000 and 80000 cells/well. After 96 hours, the plates were fixed and stained. Images were acquired by Operetta High Content System (Perkim Elmer). Arrows indicates cell clusters. Scale bar: 100 µm.

Regarding THP-1, in order to determine the cell seeding density to achieve confluence, different cell densities were plated into 384-well plates in presence of 50 ng/mL PMA (data reported in Alcântara, 2017). The density of 4,000 cells/well did not reach complete confluence. The formation of cell clusters at the density of 10,000 cells/well impaired the cells individualization by the analysis software. The density of 7,000 cells/well provided an optimum confluence. Hence, 7,000 cells/well was the established density for 384-well plates (see figure in Appendix 1).

The phenotype of PMA-differentiated THP-1 macrophages is dose and time dependent, thus several protocols has been reported (Starr *et al.* 2018). Their phagocytic capacity is a central function for *Leishmania spp*. infection assay. To measure differentiated THP-1 phagocytosis, cells were exposed to 50 ng/mL PMA for 24h, 48 h or 72h, followed by 1 h incubation with fluorescent zymosan particles, and subsequent washing with PBS to remove non-internalized particles. These zymosan particles are trypsin-treated cell wall preparation of *Saccharomyces cerevisiae*. Their phagocytosis is mediated by a repertoire of different receptors that recognize the different components of the particle and mediate internalization (Underhill 2003). Figure 4.5 shows the results. After 48h of differentiation a reasonable number of particles were phagocyted. Although the phagocytic capacity peaked at 72h-differentiation induces highest phagocytic capacity, 48h was chosen for the regular assay. This is because the longer the assay window, the greater the chances of variability due to external interferences. It is worth pointing out that cell differentiation is the first of a series of sequential steps, therefore, 48 h is not the assay total period.

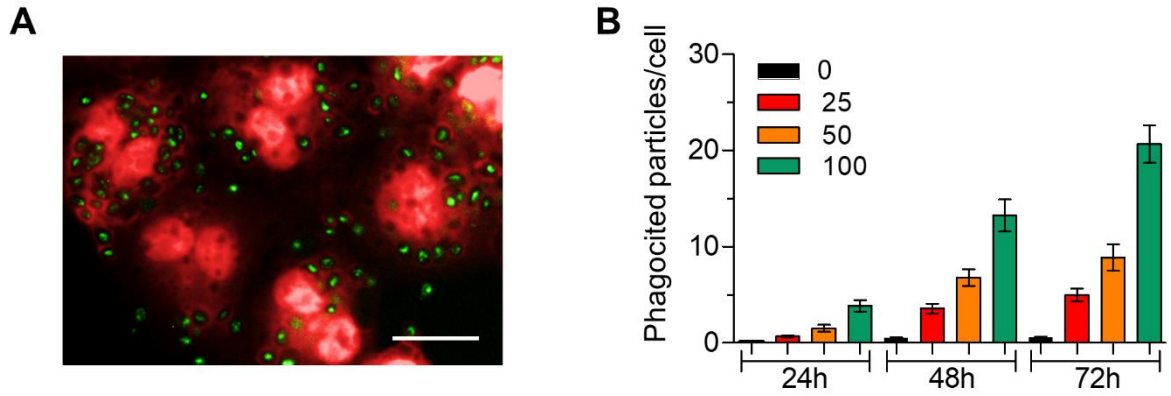

Figure 4.5 Evaluation of THP-1 cells fagocytic capacity after PMA differentiation. Cells were activated with 50ng/ml PMA for 24, 48 or 72h, and then incubated with 25, 50 or 100 fluorescent zymosan particles/cell for 1h. **A)** Psedocolored image of 48h-diferentiated cells incubated with 25 particles/cell (green). Nuclear staining with Draq5 (red). Scale bar: 25 µm. **B)** The number of phagocited particles for each zymosan density incubation (25, 50 or 100) were mesured by Harmony software. Bars are means and error bars represent the standard deviations from one experiment.

Stimulation with PMA for 48 h was sufficient for differentiation of THP-1 into macrophage-like cells, as demonstrated by cell adherence, cytoplasmatic area enlargement and phagocytic capacity. A washing step after differentiation process has been reported by other researchers in order to remove PMA and avoid unexpected interferences (Duffy *et al.* 2017; Jain *et al.* 2012; De Muylder *et al.* 2011). Thereby, the effect of removing PMA after 48h of differentiation was investigated (data reported in Alcântara, 2017). Cultures in which PMA had been washed off were more similar to undifferentiated monocytes, as evidenced by lower cell

adherence, smaller cytoplasmatic area and increase in population growth rate (see figure in Appendix 1). Accordingly, maintenance of PMA in the culture medium throughout the duration of the biological assay ensured morphologically macrophages-like cells.

It is well known that *Leishmania spp.* present different temperature tolerances for intracellular growth (Berman and Neva 1981; Sacks *et al.* 1983). This thermosensitive influence the parasite localization in the human host, as skin temperature is lower than internal temperature. In order to confirm the best temperature for cutaneous species infection, experiments were conducted at two temperatures: 34 and 37 °C. The THP-1 cells were differentiated in two 384-well plates at 37°C for 48h. Next, cells were infected with late-stationary phase promastigotes of *L. amazonensis*, *L. braziliensis* or *L. major* at different multiplicities of infection (MOIs) _ 10, 20 or 40. Immediately, one plate was incubated at 34 °C and the other at 37°C for further 96h. Figure 4.6 shows representative images from both conditions.

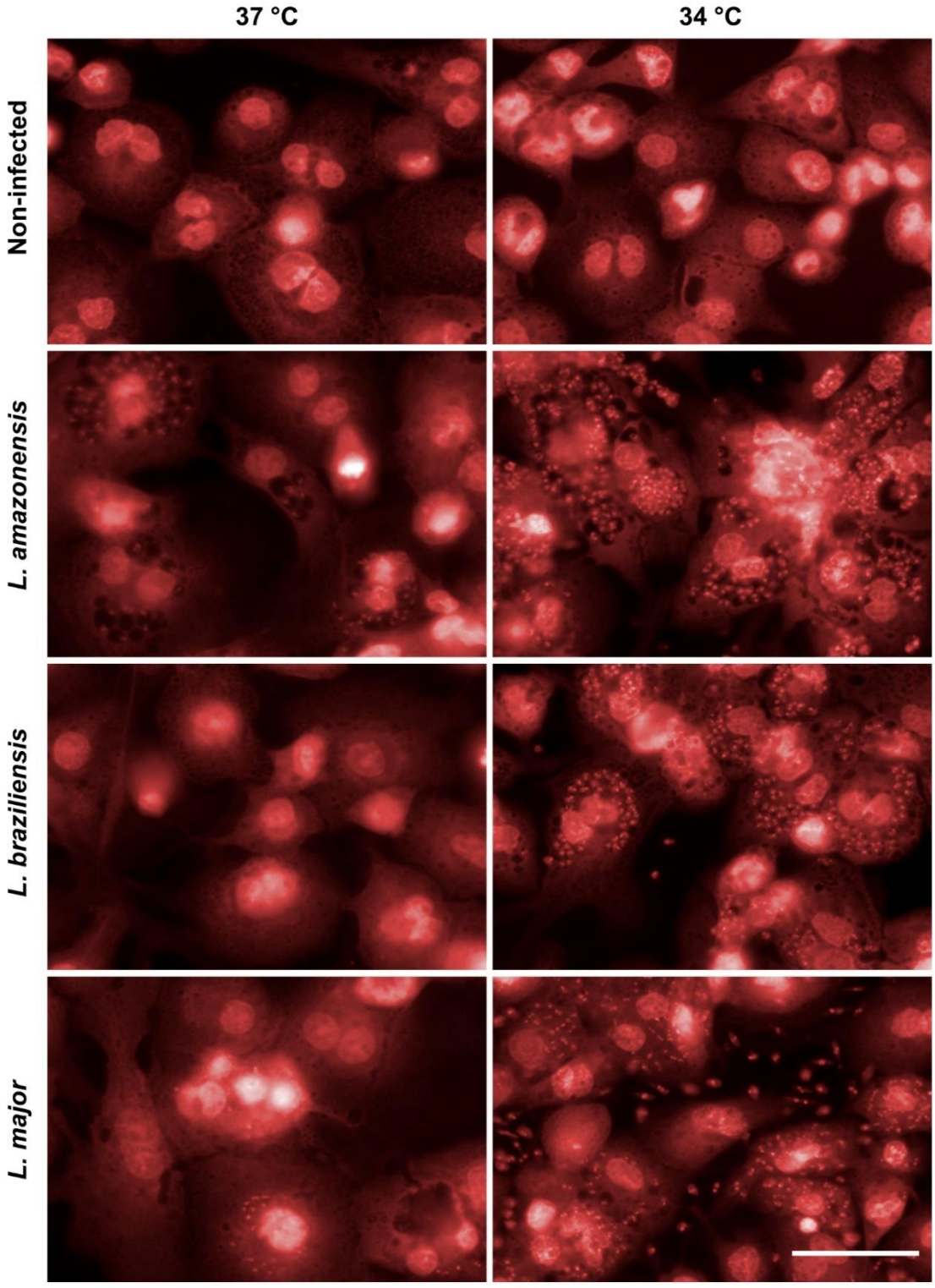

Figure 4.6 Infection performed at 34°C is better for CL species. Representative images of THP-1 cells infection with *L. amazonensis*, *L. braziliensis* and *L. major* at 34 or 37°C after 96 h of infection. Raw images acquired with Operetta. Scale bar: 50 µm.

As can be seen in Figure 4.7, clearly, incubation at 34°C resulted in increased infection ratios as well as increased numbers of intracellular amastigotes when compared with results at 37°C. *L. braziliensis* was the most thermosensitive species, intracellular amastigotes were completely eliminated after 96 hours incubation at 37°C.

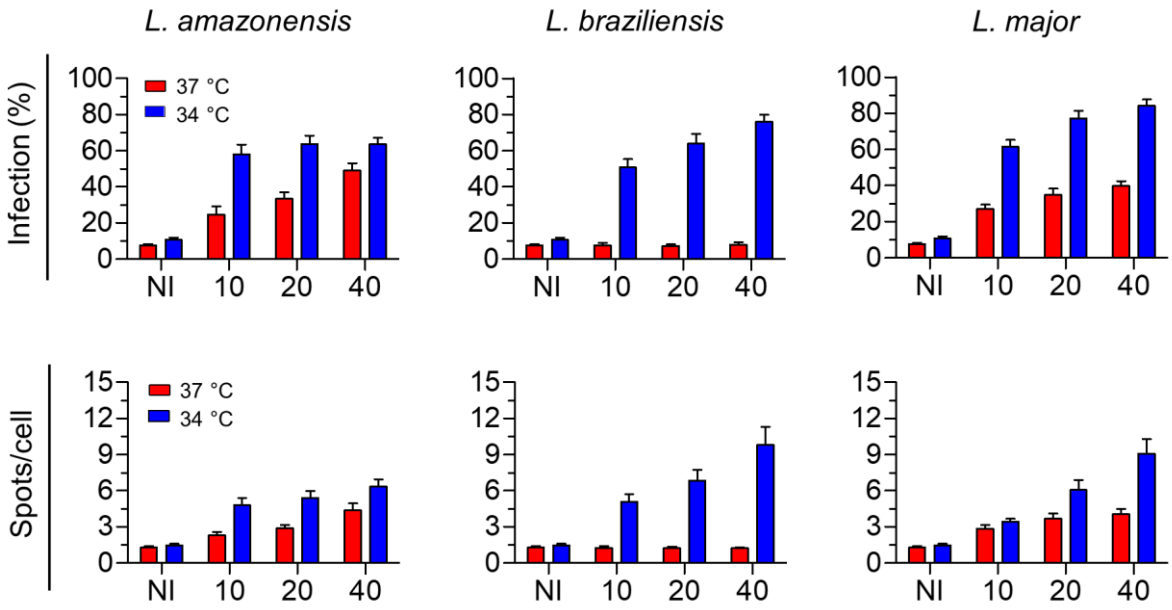

Figure 4.7 Infection performed at 34°C increases CL species infectivity. A) Infection Ratio of THP-1 cells infected with different MOIs of *L. amazonensis*, *L. braziliensis* and *L. major* at 34 or 37°C (96 h of infection). **B)** Spots/cell of THP-1 cells infected with different MOIs of *L. amazonensis*, *L. braziliensis* and *L. major* at 34 or 37°C (96 h of infection). Bars are means and error bars represent the standard errors. Three independent experiments were performed.

Mammalian cells are usually cultured at 37°C in the incubator supplied with 5% CO_2 unless specific research purpose is required. Thus, the THP-1 cells viability was investigated in both temperatures. The viability analysis following incubation at 34 or 37 °C was performed by a resazurin assay, as described in material and methods section 3.13. The number of cells was also evaluated using the Harmony software analysis in order to prove there was the same number of cells in both plates. There was no difference in the cell counts or cell viability between the two conditions (Figure 4.8 A and B). Nevertheless, the cells presented slightly smaller nucleus and cytoplasm areas at 34 °C (Figure 4.8 C). This morphological change is expected, since cell metabolism decreases at lower temperatures, and metabolism affects cell size (Miettinen and Björklund 2017).

In accordance with previous reports, 34° C was established as the temperature to infect THP-1 cells with dermotropic species of *Leishmania*.

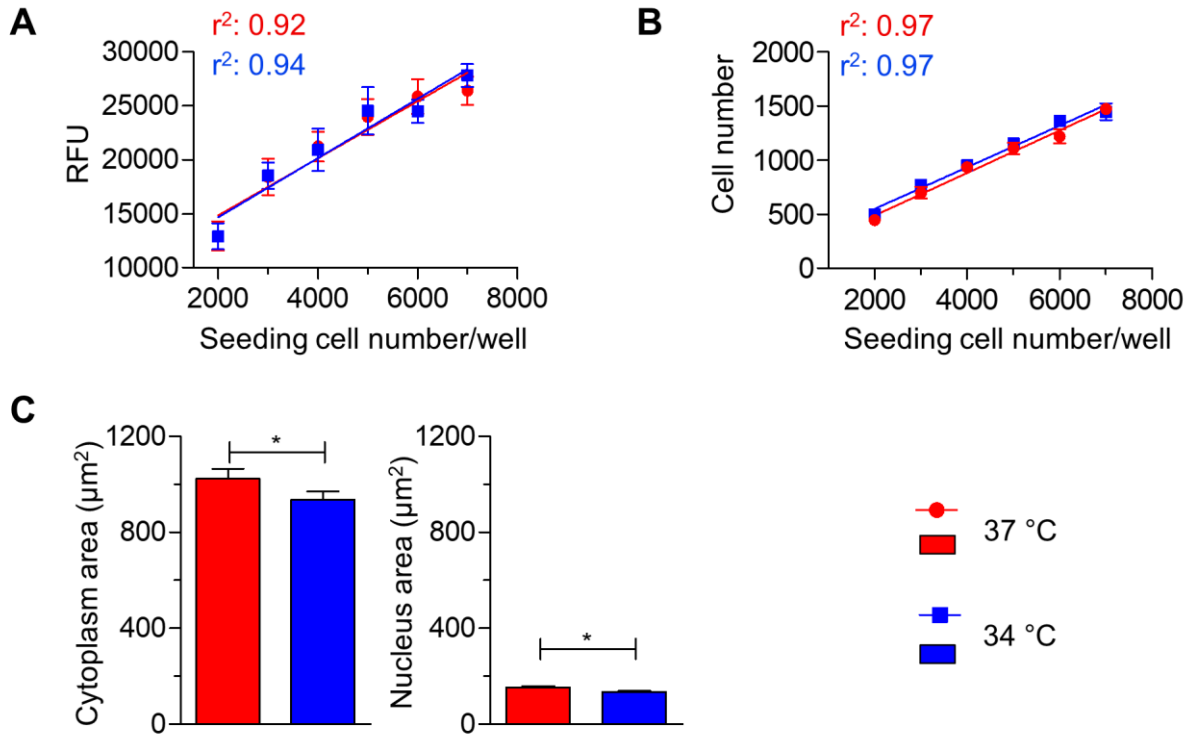

Figure 4.8 THP-1 cells incubated at 34 °are viable. **A)** Fluorescence (560/590nm) signal after 12-hour incubation of THP-1 cells with resazurin at 34 and 37°C. It shows a linear correlation between fluorescence and cell number. **B)** Total number of cells in 7 fields of the well at 34 and 37°C. It shows a linear correlation between seeding cell number and the software analysis. **C)** Nucleus Area and Cytoplasm Area of THP-1 cells plated at 34 and 37°C. Squares and bars are means and error bars represent the standard errors. Three independent experiments were performed. *$p < 0.05$, t-test.

Several culture media are currently used for maintenance of *Leishmania spp*. promastigotes, which are determinants for culture viability and parasite infectivity (Castelli *et al.* 2014; Childs *et al.* 1978; Merlen *et al.* 1999). More specifically, studies by Santarem *et al.* showed that parasites cultured in distinct culture media may exhibit changes in metacyclic gene expression, resulting in different levels of infectivity *in vitro* and *in vivo* (Santarém *et al.* 2014). Considering this, different promastigote culturing media (LIT, RPMI, M199, Grace's and Schneider's) were tested and compared in terms of promastigote growth curve and infection profile. Starting from the same original stock, *L. amazonensis*, *L. braziliensis* and *L. major* promastigotes were cultured for 8 passages in the different media to ensure that parasites were fully adapted to the individual culture media composition, and only then their growth curves and infectivity were evaluated. The results are summarized in Figure 4.9. Only M199 and LIT media were able to support growth of all three species.

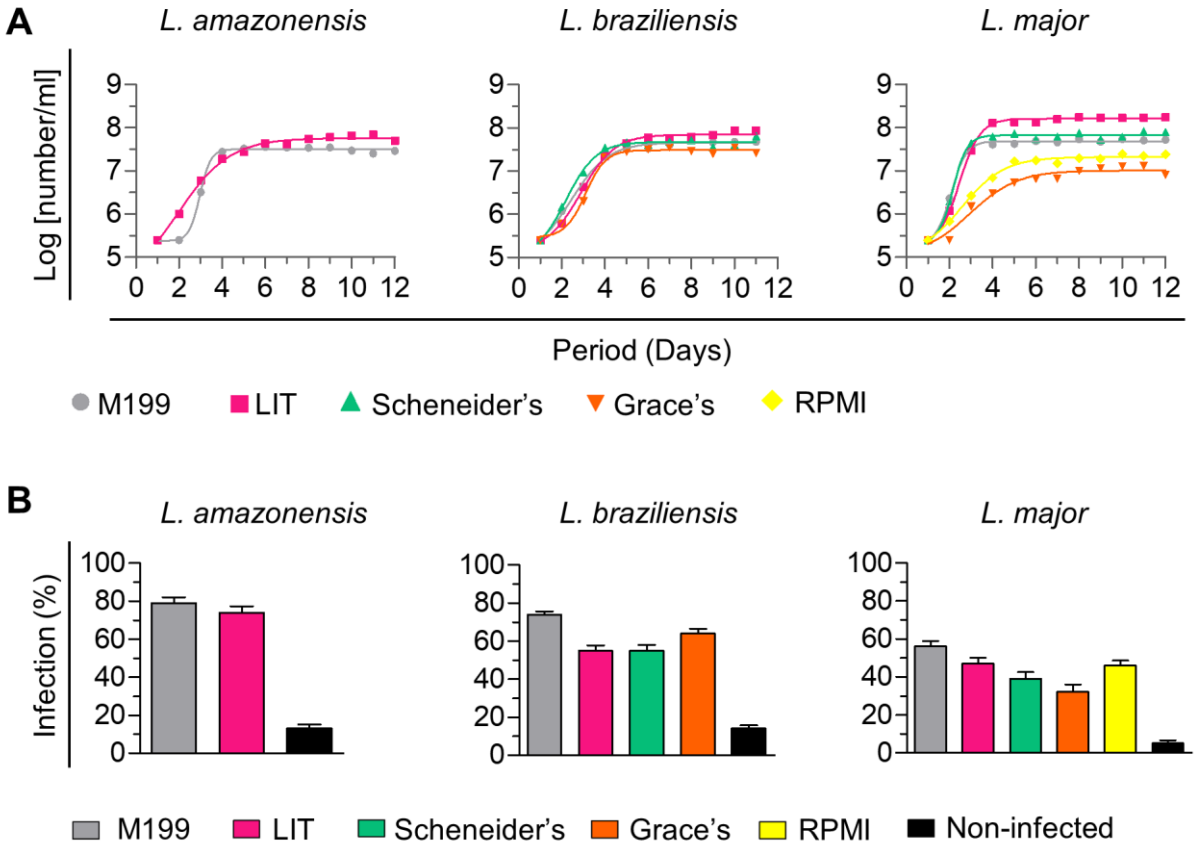

Figure 4.9 Evaluation of growth and infectivity of promastigotes cultured in different media. **A)** Growth curves of *L. braziliensis*, *L. amazonensis* and *L. major* in different insect cell culture media. **B)** Infection ratios of THP-1 cells infected with *L. braziliensis*, *L. amazonensis* and *L. major* cultivated in different media (MOI 20) after 120 h of infection. Bars are means and error bars represent the standard errors of two independent experiments.

The promastigotes entered stationary phase around day 6 in all media; from seven days onward, the parasites viability decreased (observed by visual inspection), so 6-day old promastigote culture was chosen for test the infection in THP-1. It was previously reported, that stationary phase promastigote culture results in higher infection ratios because of the enrichment of metacyclic promastigotes in the culture media (da Luz *et al.* 2009). Promastigotes cultured in M199 achieved higher infection ratios, followed by those cultured in LIT (Figure 4.9 B). Therefore, M199 was chosen as the culture media for all species.

In order to confirm 6-days as the best period of promastigotes culture before infection, 5-day, 6-day and 7-day old parasites were used to infect THP-1 cells at a MOI 20. The infection ratios were evaluated at 96 h post-infection (see Figure 4.10 A). Only *L. major* proved to be more infective with a 5-day old culture, instead of 6-day and 7-day old ones. For *L. braziliensis* and *L. amazonensis* there was no significative difference.

As all the standardization experiments were performed using 25 cm^2 (T25) flasks to culture promastigotes, a test with different flask sizes (T25, T75 and T175) was performed

to determine whether promastigote culture scaling up would affect metacyclogenesis and, consequently, the infection ratios. No relevant impact on infection ratio was observed, showing that any size of flasks could be used to culture the parasites (Figure 4.10 B).

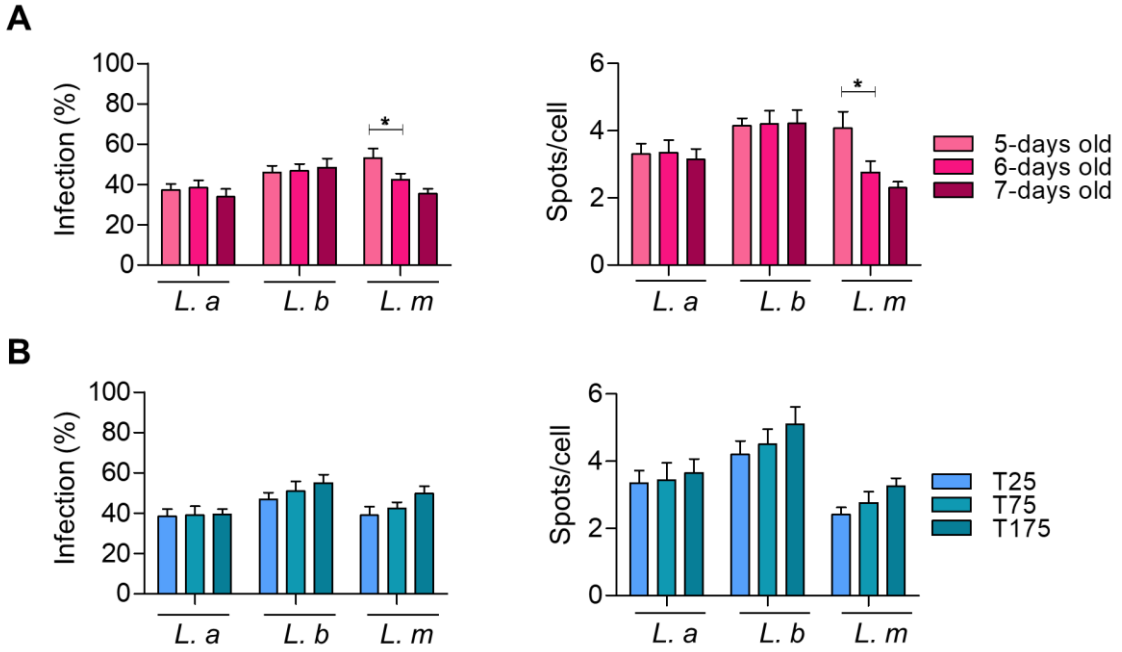

Figure 4.10 Infection parameters standardization. A) Infection ratio and spots/cell of infected THP-1 cells with day-5, 6 or 7 *Leishmania spp* promatigotes (MOI 20), 96h after infection. **C)** Infection ratio and spots/cell of infected THP-1 cells with day-6 promastigotes cultured in different flask sizes (25, 75 and 175 cm^2), 96 h after infection. Bars are means and error bars represent the standard errors of two independent experiments. *$p < 0.05$, t-test.

As a mean to choose the assay multiplicity of infection (MOI), infection ratio dynamic was evaluated. Figure 4.11 shows results for *L. braziliensis*. There was a linear increment in infection ratio correlated with the MOI, reaching saturation at MOI 50 (Figure 4.11 A). This correlation is sustained over time. The number of spots/cell was also proportional to the MOI up to MOI 50 (Figure 4.11B). Both infection ratio and spots/cell slightly increased after 8 days of infection. But at the same time there was an accentuated decrease of the cell number (Figure 4.11 C). The infected cells tend to have a better survival than the non-infected ones, which may explain the apparent increase in the infection ratio. Interestingly, cytoplasm area enlargement stabilized only after 8 days of infection, which may be related to complete THP-1 differentiation process (Figure 4.11D). Similar results were obtained for *L. amazonensis* and *L. major* (Data not shown).

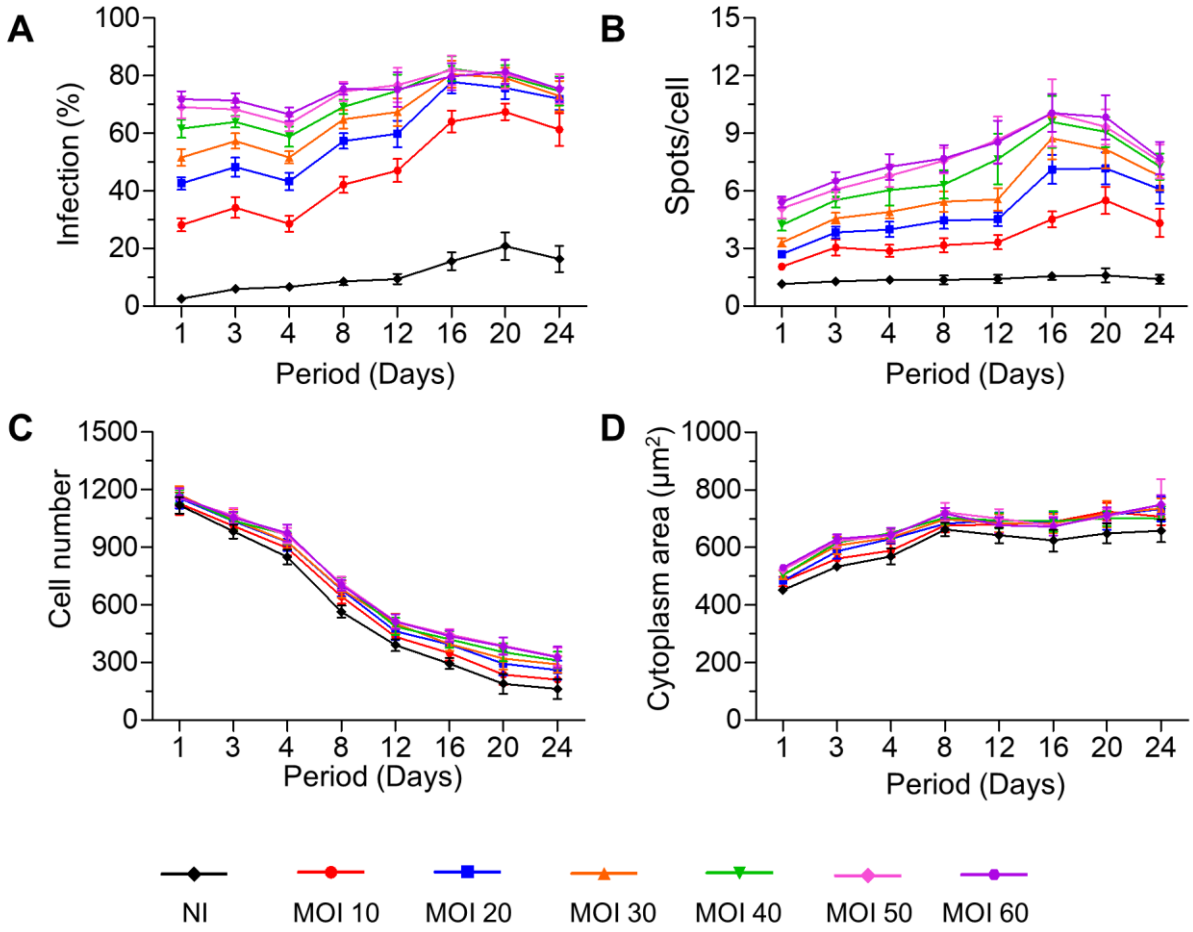

Figure 4.11 *L. braziliensis* infection ratio dynamic over time. A) Infection Ratio. **B)** Mean number of parasites/cell. **C)** Mean cell number of THP-1 cells. **D)** Mean Cyptoplasm Area of THP-1 cells. Dots are means and error bars represent the standard deviations of one experiment.

The plateau of infection ratio and intracellular amastigotes at high MOIs is expected, since macrophages have a limited uptake capacity. The MOI 50 was enough to achieve the highest infection possible for all species under the assay conditions. Thus MOI 50 was chosen for further experiments. The standardization of different MOIs for each model aiming to get more physiologically representative rates would be extremely laborious, and probably would lead to great differences in infection ratio and number of intracellular amastigotes among species.

The assay treatment window was determined by evaluating the time needed for reference compounds (amphotericin B, miltefosine or pentamidine) reaching maximum effect under these *in vitro* experimental conditions. Infected macrophages were exposed to nine different concentrations of serially diluted drugs. Copies of identical plates were prepared to allow determination of infection ratio each 24 hours up to 192h of treatment exposure. A representative panel of images from infected cells is shown in Figure 4.12.

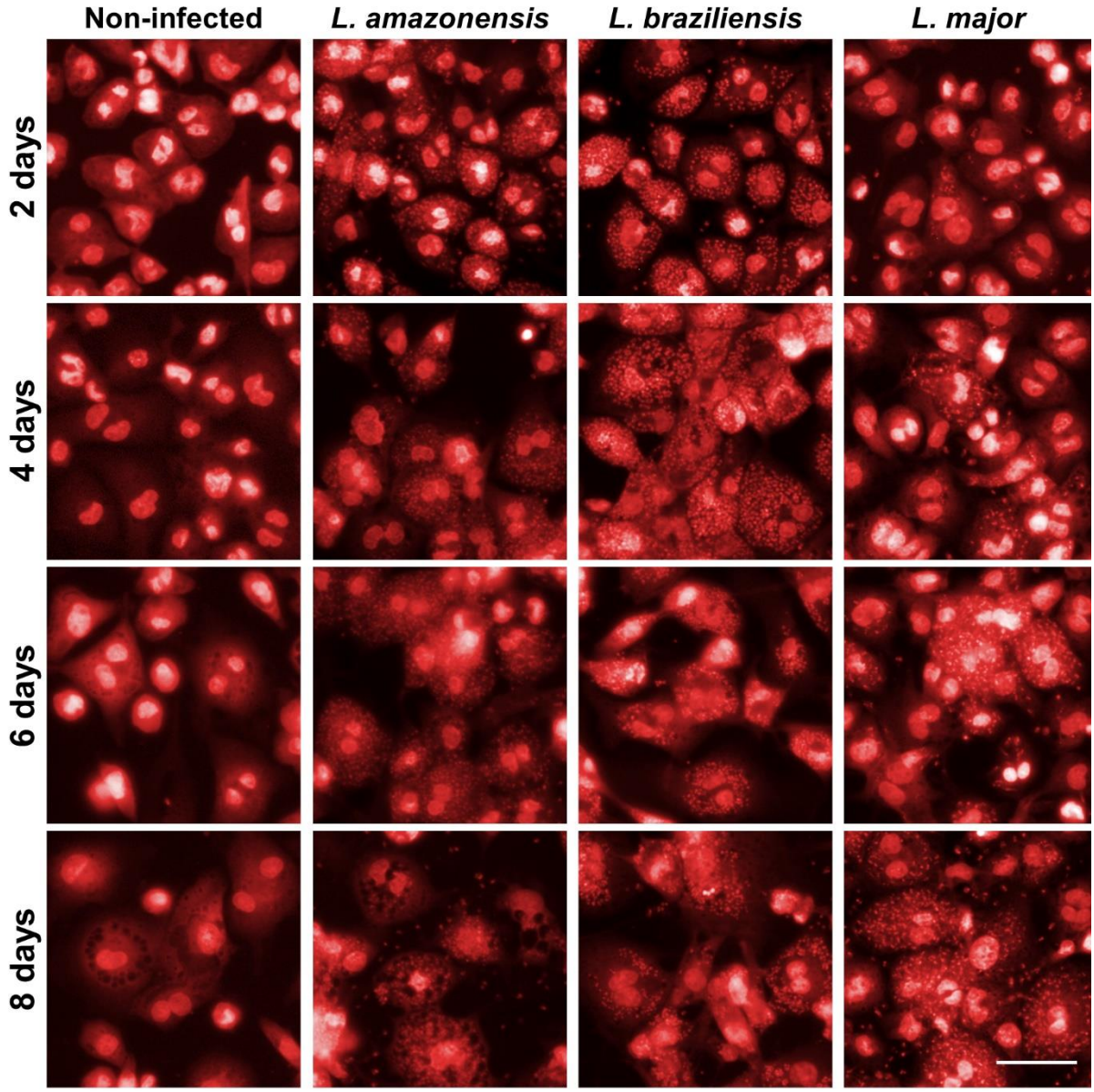

Figure 4.12 Representative images panel of THP-1 cells infected with *Leishmania spp*. Pseudocolored raw images acquired with Operetta microscope (20x objective). The images are from the 0.5% DMSO control of each specific time point after infection. Scale bar: 50 µm.

The cidal dynamics ('time-kill') plot for each drug is presented in Figure 4.13 and pEC_{50} values are in Table 4.3. The data show both concentration and time-dependent activity for amphotericin B and miltefosine. Amphotericin B was the drug with broader activity spectrum. Miltefosine was most active against *L. braziliensis* and only partially active against *L. amazonensis*. Apparently, *L. major* showed resistence to all tested drugs. At least 96 h were necessary to fully achieve the elimination of *L. amazonensis* amastigotes under amphotericin B exposure. Although the plot for *L. braziliensis* shows a borderline infection ratio at 96h due to software detection limitation (spots false-positive detection), amphotericin B completely eliminated parasite infection, as inferred by visual images inspection. Thus, for *L. amazonensis*

and *L. brazilienis*, based on amphotericin results, 96 hours was defined as drug exposure window to detect unambiguous activity/efficacy for compounds under these conditions. Also, the minimal-effective concentration of 10 µM was determined as a positive control. The lack of activity for pentamidine is not surprising, since it is reported that this drug only reduces the number of intracellular amastigotes but not the number of infected cells, and here infection ratio is the parameter evaluated (Wang *et al.* 2010).

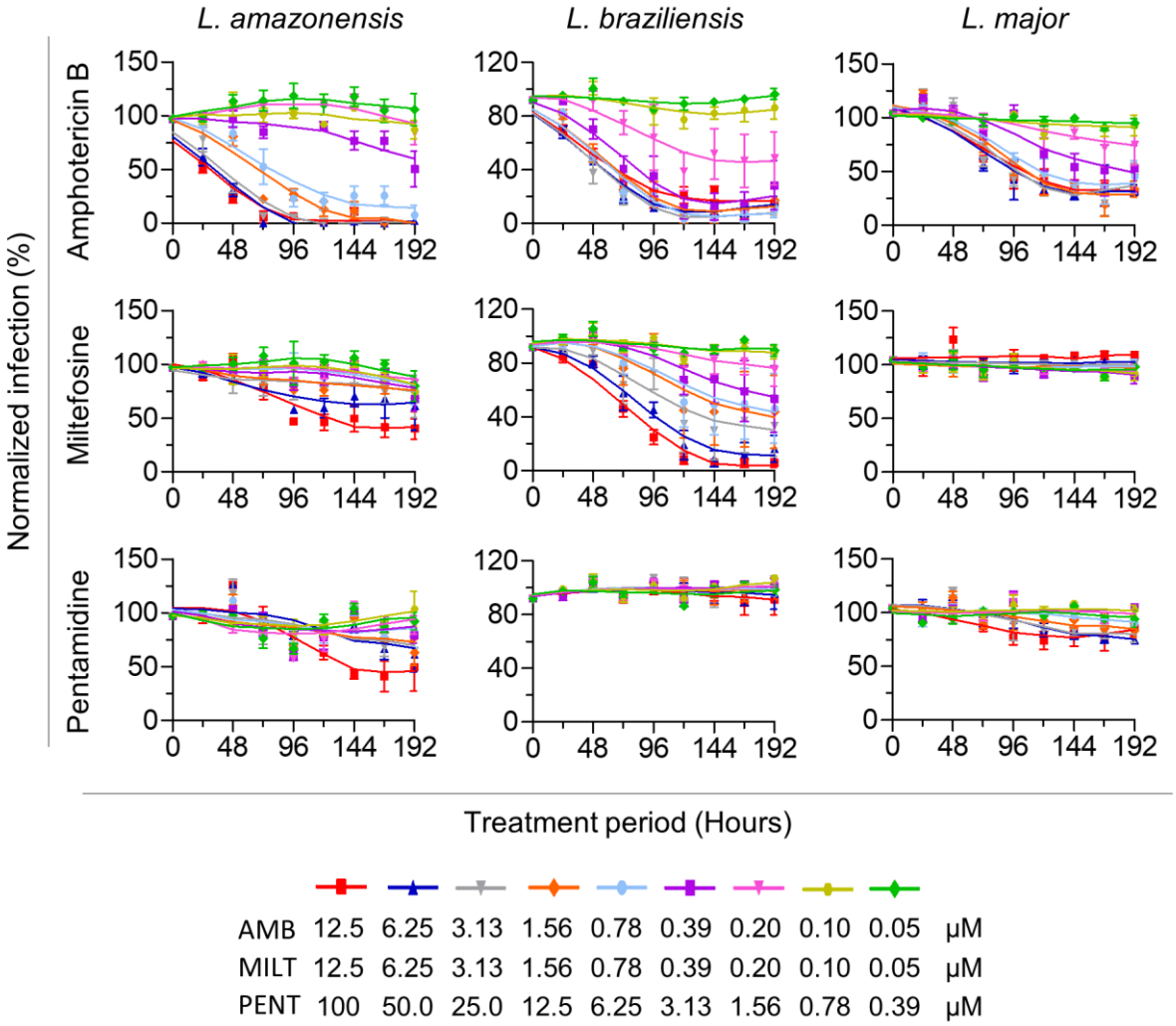

Figure 4.13 Determination of the drug exposure window. THP-1 cells were infected with *L. amazonensi*, *L. braziliensis* and *L. major* (MOI 50) for 24 h prior to addition of compound (previously serially diluted by the factor of 2-fold, as indicated the by the colors legend). Activity was analyzed every 24 h, starting right after compound addition (time point 0 h), up to 192 h. Data points are means and error bars represent standard errors of two independent experiments.

Table 4.3 pEC_{50} values at 72-, 96-, and 144-h of continuous reference compounds exposure

	Amphotericin B			Miltefosine			Pentamidine		
	72h	**96h**	**144h**	**72h**	**96h**	**144h**	**72h**	**96h**	**144h**
L. amazonensis	5.78	6.08	6.06	-	4.65	4.76	-	-	-
L. braziliensis	6.20	6.26	6.40	-	5.01	5.74	-	-	-
L. major	-	5.77	6.08	-	-	-	-	-	-

Data refer to pEC_{50} mean from two independent experiments. pEC_{50} = -log EC_{50} (M)

The time- and concentration-dependent activity of the compounds are in line with recently reported data. Maes and collaborators demonstrated that more than 240 h are required for miltefosine (10 mM) and amphotericin B (2 mM) to completely eliminate all viable amastigotes. Their protocol used *L. donovani* and *L. infantum* spleen-derived amastigotes to infect primary peritoneal mouse macrophages, and cydal dynamics was assessed by the quantification of recovered amastigotes differentiated to promastigotes (Maes *et al.* 2017). In another work, Voak *et al.* reported infection of bone marrow derived macrophages with *L. donovani* amastigotes freshly harvested from the spleen, and subsequent evaluation of infected cells percentage for different amphotericin B and miltefosine concentrations along with measurement of cellular drug accumulation. The time to reach 50% of maximum drug penetration (t50) was 55.72 h for amphotericin B and 100.01 h for miltefosine. Highlighting that at 10 µM miltefosine, the timepoint of maximum total cellular drug concentrations preceded the timepoint at which maximum parasite killing was observed (Voak *et al.* 2018).

The apparent resistance of *L. major* might be related to its high multiplication rate even at 34 °C (Eren *et al.* 2018). So, the growth curve of parasites with or without PMA was assessed. The initial density was comparable to parasite density used to infect cells at MOI 50. As can be inferred by Figure 4.14, PMA presented no effect on growth curve of all species. *L. major* keep multiplying at 34 °C during the incubation period. As there is no washing step to remove non-internalized parasites in the protocol here reported, the remain extracellular promastigotes can multiply and re-infect neighboring cells, misleading the compounds activity measurement. No further investigation was conducted. At the end, it was decided afterwards to not continue experiments with *L. major*, given that promastigotes multiplication at 34 °C might interfere with compounds activity.

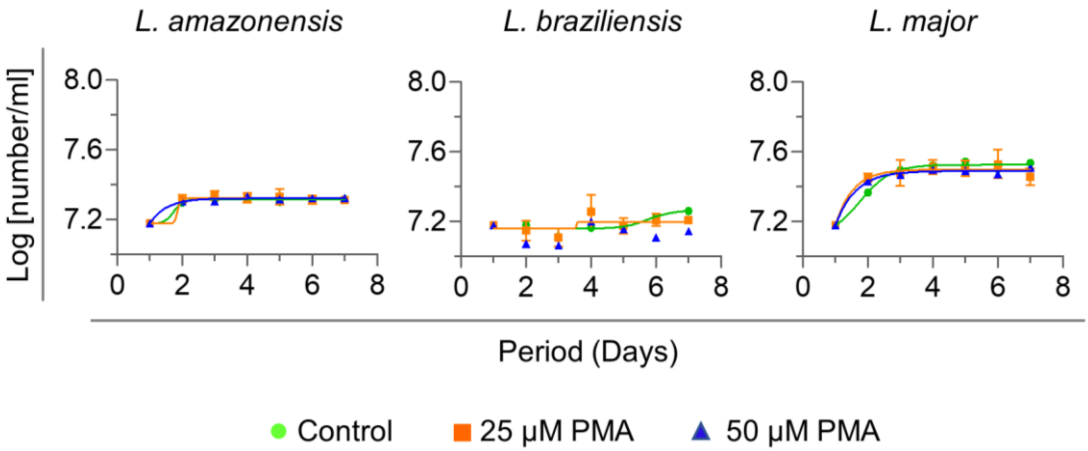

Figure 4.14 Growth curve of promastigotes at 34° C. The initial density of $1.5x10^7$ parasites/mL is comparable to parasite density used to infect cells at MOI 50. Data points are means and error bars represent standard errors of two independent experiments

The attempts to remove non-internalized promastigotes by washing the microplates resulted in high rates of cell detachment, which drastically elevated variability in cell number among wells replicates, thus impairing the use of cell ratio data, an essential parameter in HCS approach (data not shown). Lastly, by not adding a washing step, the reliability on the cell viability prediction was assured.

L. amazonensis is well known by its large parasitophorous vacuoles hosting several amastigotes, a strategy to subvert host cell defenses, providing an environment with lower activities and/or concentrations of hydrolytic enzymes vacuoles (Real and Mortara 2012). The biogenesis mechanisms behind the formation of these communal vacuoles in not totally elucidated. As such feature could not easily be seen in the assay images, and representative images of *L. amazonensis* infecting THP-1 was not found in the literature, it was questioned if THP-1 cells were able to generate such large vacuoles or if the high MOIs impaired to observe them. So, differentiated THP-1 cells were infected with one parasite per cell ratio in T25 flasks, and incubated until observation of vacuoles could be done under the microscope. After 13 days, infected cells were harvested and plated in 384-well plates for 24h. At this time point, treatment with amphotericin was added for 96h. In the last 24 h of the experiment, EdU reagent was added to some wells, as described in material and methods section 3.15. Typical *L. amazonensis* vacuoles were successfully observed in THP-1 cells (Figure 4.15 A). Also, EdU incorporation in 31.27% of parasites after 17 days of infection indicate an active process of replication. Amphotericin B activity was noticeable the same when compared with the conventional assay (infection with MOI 50 for 24h directly on 384-well plate) concomitantly performed (Figure 4.15 B).

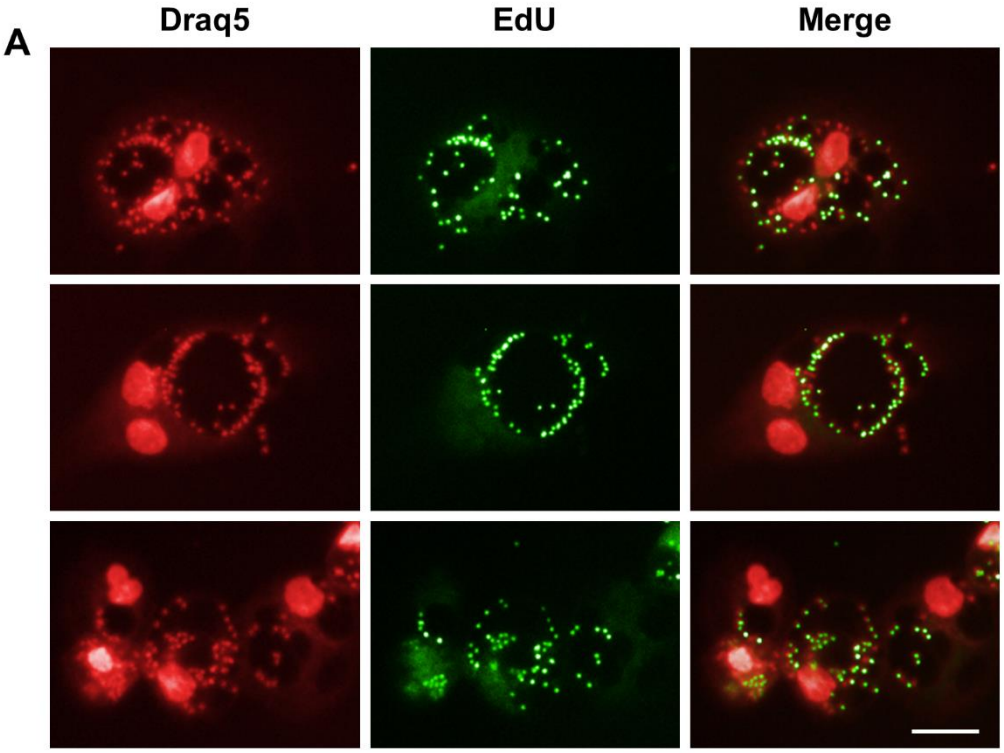

Figure 4.15 *L. amazonensis* communal parasitophorous vacuoles in infected THP-1 cells. **A)** Representative images of THP-1 cells after 17 days of infection. Pseudocolored raw images acquired with Operetta microscope (20x objective). Scale bar: 25 µm **B)** Amphotericin B dose response curve for MOI 1 (blue) and conventional protocol _MOI 50 (red). Data from one experiment.

Albeit THP-1 cell line is currently used as the host cell in the majority of *Leishmania* HCS assays, their use is not without concerns. THP-1 cells differ from primary macrophages in the phagocytic activity, the cytokines production and the regulation of the oxidative burst. Ideally, primary macrophages of human origin would be preferable. However,

it is difficult to obtain a reliable and homogeneous supply of human primary cells at a scale suitable for routine screening. An alternative is to use murine primary mouse macrophages. In order to investigate the impact of the host cell on compounds selection against *Leihsmania spp.*, an attempt of using bone marrow derived macrophage (BMDM) was done. Initially, the infection profile of *L. amazonensis* and *L. braziliensis* was evaluated. The differentiation of the BMDM was performed as described in the methodology, section 3.9. Primary macrophages were plated 24 hours prior to infection and THP-1 cells 48 hours prior. Stationary phase promastigotes were used to infect cells at different MOIs. The plates were fixed every 24h post-infection.

Both species were able to establish infection in both cell types. Representative images of the infection after 120 hours are shown in Figure 4.16.

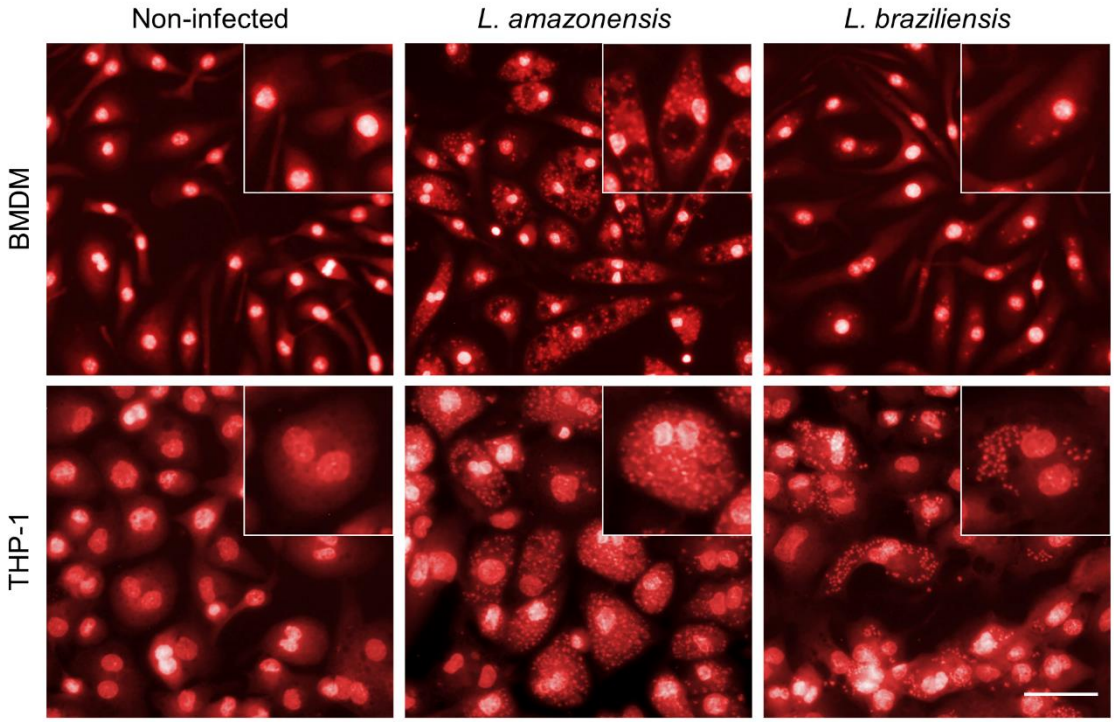

Figure 4.16 Representative images of infected THP-1 and BMDM cells. Pseudocolored raw images acquired with Operetta microscope (20x objective). Infection with *L.amazonensis* or *L. braziliensis* at MOI 20. Scale bar: 50 µm.

Infected THP-1-derived macrophages inhibit *Leishmania* species growth but do not eliminate them, infection ratio and number of amastigotes were stable up to 120 hours. By contrast, primary macrophages derived from murine bone marrow were able to contain *L. braziliensis*, a significant decrease in the rate of infection in BMDM begins after 48h, almost completely eliminating all amastigotes at 120 h time point (Figure 4.17). The decrease in *L. braziliensis* BMDM infection data are in agreement with previous report (Novais *et al.* 2009).

L. amazonensis causes chronic infection in balb/c mouse, but in contrast the animals cure from infection by *L. braziliensis*. This death of *L. braziliensis* occurs by an interferon gamma-dependent mechanism (DaMata *et al.* 2015; DeKrey *et al.* 1998). Possibly, the results obtained *in vitro* reflect what occurs *in vivo.*

Altogether, these results indicate THP-1 cells as a more robust model to assess activity against various species of *Leishmania.*

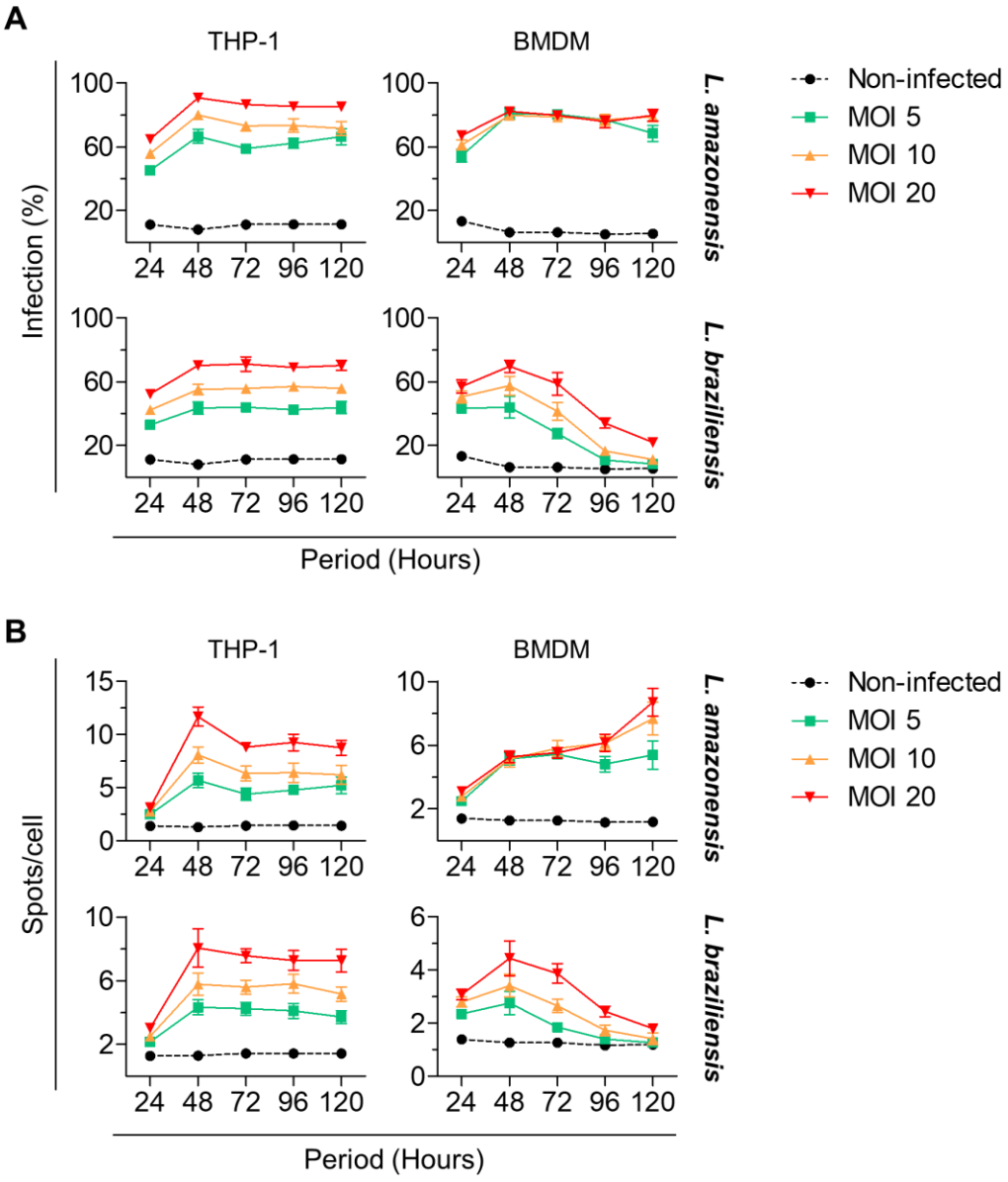

Figure 4.17 Infection dynamic of *L. amazonensis* and *L. braziliensis* in THP-1 and BMDM cells. Data points are means and error bars represent standard errors of two independent experiments.

4.3 HCS assay validation for dermotropic species

After careful standardization of biological models and image analysis, the next step

is the assay validation. The validation consists of experiments and subsequent data analysis to ensure that the assay is acceptable for its intended purpose, which in this case is reliability and robustness in compound activity detection.

The dose-response curves (DRCs) of amphotericin B and miltefosine were assessed in ten independent experiments. Figure 4.18 shows a fairly consistent determination of pEC_{50} values over time.

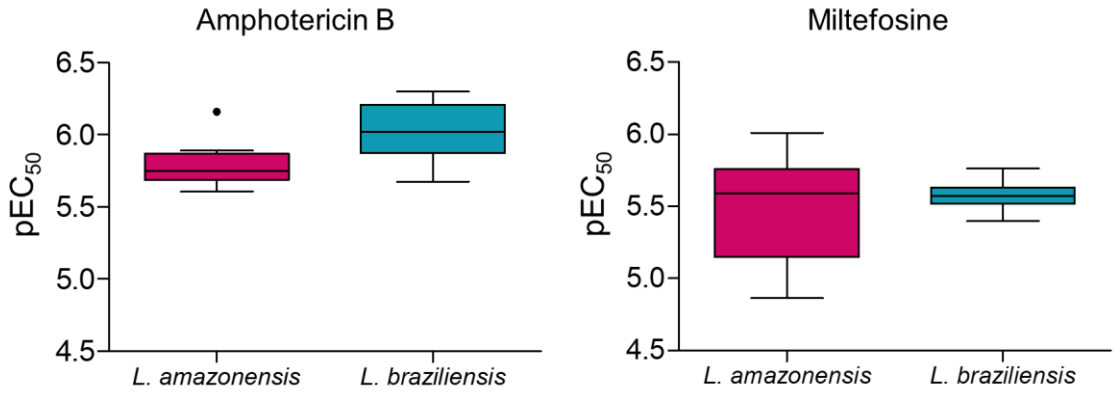

Figure 4.18 Validation of potency determination. Box plots of ten independently determined pEC_{50} values of amphotericin B and miltefosine for *L. amazonensis* and *L. braziliensis*. The plot shows median (line within box), 25th and 75th percentiles (box), and minimum and maximum (whiskers). Circles indicate outliers.

To further characterize the assay reproductivity, the pEC_{50} of a small library composed by 30 compounds from collaborators were determined in two independent experiments. A Bland-Altman plot was used to evaluate the agreement between two experimental runs. In such cases, the use of correlation coefficients is misleading, because correlation quantifies the degree to which two variables are related. But a high correlation does not automatically imply that there is good agreement between the two data sets. The Bland-Altman statistical method constructs limits of agreement based on the mean and the standard deviation. The resulting graph is a scatter plot XY, in which the difference of the two paired measurements is plotted against the mean of the two measurements (Bland and Altman 1986). A confidence interval of 95% is used to determine limits of agreement.

The Bland-Altman plot (Figure 4.19) showed that the mean difference in pEC_{50} is 0.01 for both species, which is very close to 0, so there is no significant variation from one experiment to the other. The limits of agreement, 0.14/-0.16 for *L. amazonensis*, and 0.21/-0.21 for *L. braziliensis* are acceptable. Calculated MSD (minimum significant difference) of all the compounds tested were lower than the reported to most cell-based assays (0.4-0.5). The MSD indicates the largest potency difference that can be considered random (Murray 2013). Thus, in this assay, the required difference should be greater than 0.21 between two compounds pEC50

values to assure that the pEC_{50} for one compound is truly different to that of another compound.

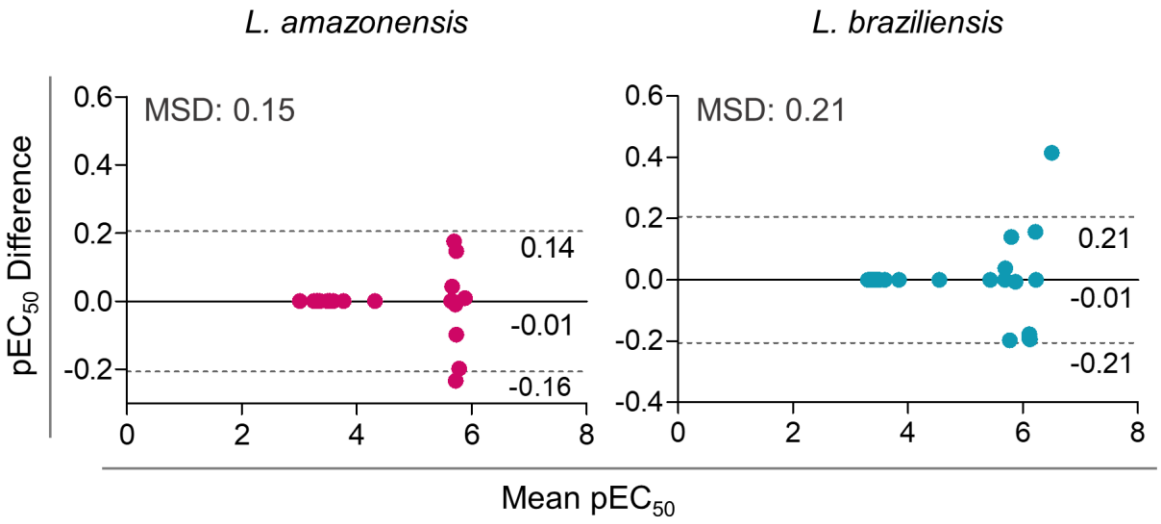

Figure 4.19 Determination of Minimum Significant Difference (MSD). Bland Altman plot of the log potency differences vs the mean data of two independent experiments. The continuous line is the mean difference between measurements, and doted lines represent the 95% confidence interval limits of agreement. MSD is defined as 2*SD of log potency differences. pEC_{50} = -log EC_{50} (M).

The current protocol was also validated to single-point test by screening a commercial library of pharmaceutically active compounds (LOPAC). This biologically annotated collection of inhibitors, receptor ligands, and approved drugs impacts most signaling pathways and covers all major drug target classes. Highly pure compounds are widely used to validate screening assays because the reproducibility is better assessed. The library is composed by 1,280 compounds, which were distributed in 4 plates. Compounds activities were assessed twice in independent runs.

For each screening run, three control plates were prepared: two plates of reference compounds dose-response curves, which allow to verify inter-plates activity variation during the assay. In addition, to evaluate the infection ratio consistence within the same plate, all wells of one plate were treated with 0.5 % DMSO (negative control). Because systematic bias that yields higher values in a pattern across a plate can mask the real differences between wells, thus hiding important information. All pipetting steps are always performed in the same sequence: (i) DRC1 plate, (ii) DMSO plate, (iii) compounds plates, and (iv) DRC2 plate. See plate maps on Figure 4.20.

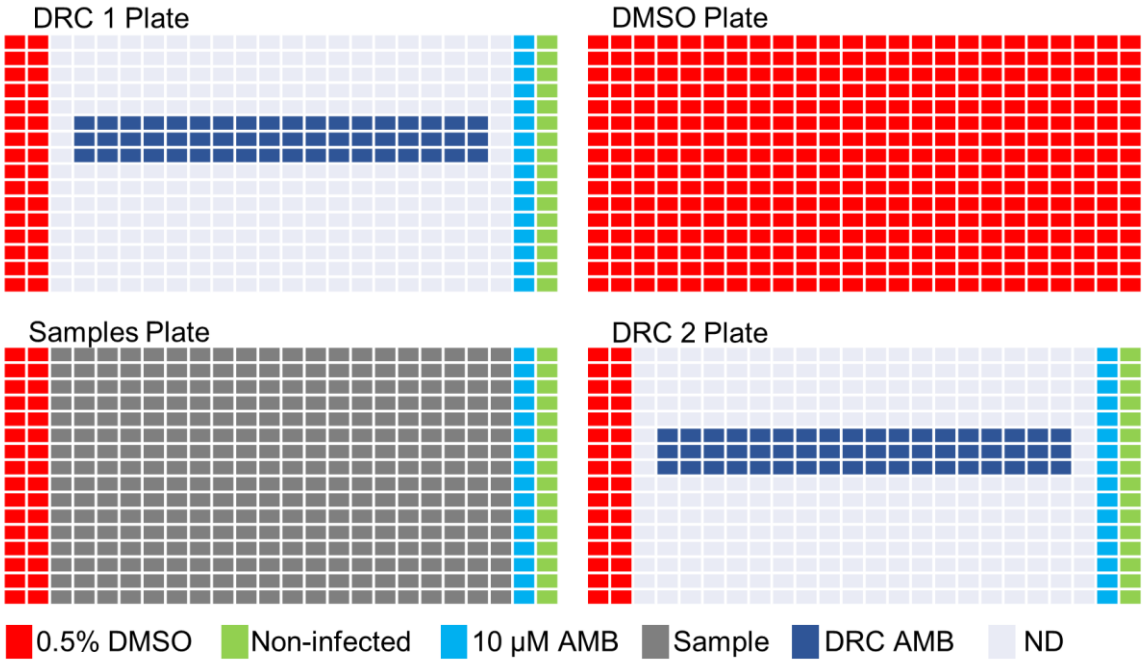

Figure 4.20 Plate maps showing controls and samples positioning. As indicated in the legend, colours represent: 0.5% DMSO treated infected cells – negative control (red), non-infected cells (green), 10µM amphotericin B treated wells – positive control (light blue), samples (grey) and DRC amphotericin B (dark blue). ND = non determined.

The criteria for approving a screening run was dependent on Z'-factor values (> 0.5); coefficients of variance (< 20%); pharmacological validation as assessed by dose response curves for amphotericin B (EC_{50} value and maximum activity); and evaluation of any type of plate position effects such as edge effects, particularly important for assays with long incubation periods. The statistics data for both species are shown in TTable 4.4.

Table 4.4 LOPAC screening for *L. amazonensis* and *L. braziliensis*

	L. amazonensis	*L. braziliensis*
Z'-factor	0.65 ± 0.04	0.76 ± 0.07
CV cell number (%)	5.2	4.7
CV infection ratio (%)	11.74	11.38
IR 0.5% DMSO	63.27 ± 6.17	69.83 ± 9.25
IR Non-infected	10.15 ± 2.27	9.49 ± 2.19
IR 10 µM AMB	15.03 ± 4.01	22.31 ± 8.86

Coefficient of variation (CV) is relative to cell number and infection ratio from all wells of two 0.5% DMSO plates (one from each run). Z'-factor and IR data are Mean ± Standard Deviation from 12 plates (6 from each independent run).

In summary, both species had a good window between the positive and negative controls and had a robust and reproducible performance between runs (Figure 4.21 A). The mean ± standard deviation of Z'-factor values of both runs was 0.65 ± 0.04 for *L. amazonensis* and 0.76 ± 0.07 for *L. braziliensis*, which give confidence in the reproducibility and the quality

of the assay (Figure 4.21 B). The Bland Altman plot shows that the mean difference of normalized activity for both species was very close to 0 and the limits of agreement are acceptable, considering a highly complex biological assay (Figure 4.21 C).

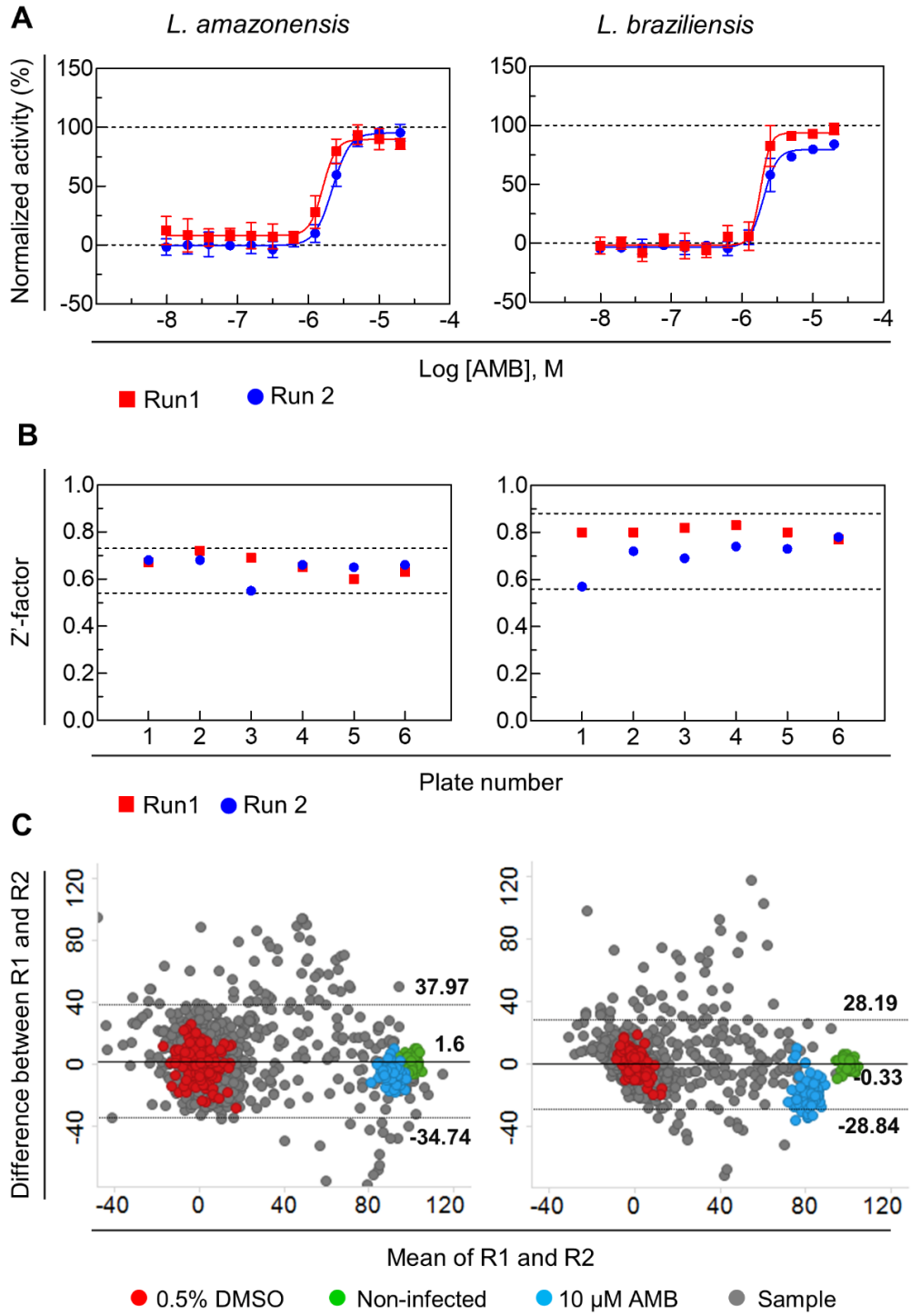

Figure 4.21 Single point screening validation for *L. amazonensis* and *L. brazililensis*. A) Amphotericin B dose-response curves. **B)** Z-factor values. **C)** Bland Altman plot of the normalized activity differences vs the mean between the data of two runs. R1: run 1 and R2: run 2. The continuous line is the mean difference between measurements, and doted lines represent the 95% confidence interval limits of agreement.

Overall, the HCS assay here described was successfully validate for two cutaneous species of *Leishmania*. The validation for visceral species (*L. donovani* and *L. infantum*) has been reported in the PhD thesis of Alcantâra (Alcântara 2017).

4.4 The multi-species high content assay

A multi-species high content assay was established and validated for some of the most clinically relevant *Leishmania* species: *L. amazonensis*, *L. braziliensis*. *L. donovani* and *L. infantum*. Figure 4.22 shows an overview of the HCS assay, a more detailed description can be found in the materials and methods (section 3.11). THP-1 differentiated macrophages are infected with stationary phase promastigotes in 384-well plates. After 24 hours of infection the cells are exposed to compounds. Plates are fixed after 96 hours of experimental treatments and then subsequently washed, labeled and read in an HCS instrument. The images are processed by a software analysis, providing specific readouts: total host cells number, infected cells number, infection ratio and the number of parasites per each well. Data are subsequently plotted in proper graphs in order to facilitate visualization.

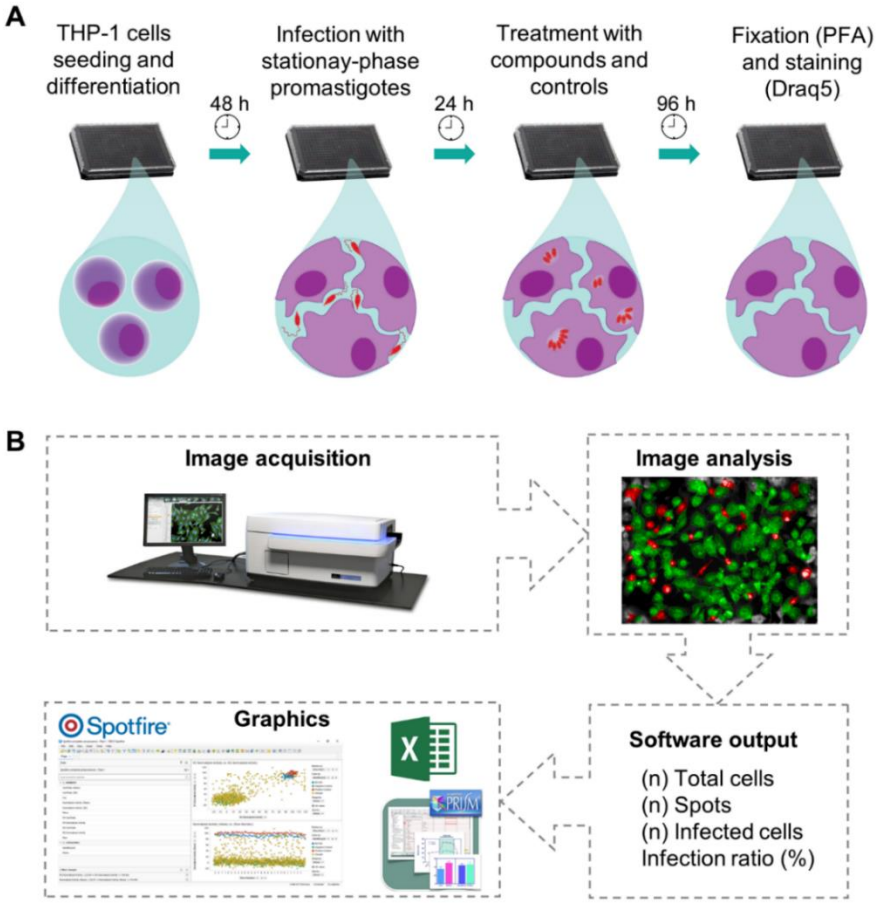

Figure 4.22 General scheme of *Leishmania* high content assay. A) Biological *in vitro* assay steps. **B)** High content imaging workflow.

As mentioned before, the parasites features used by the analysis software to designate amastigotes as objects (spots) are heterogeneous. *Leishmania* species generated different infection profiles bringing forth morphological variations in the host cells, as staining differences for amastigotes (size, contrast, intensity threshold and distance between two spots). For instance, *L. amazonensis* nucleus/kinetoplast DNA is weakly stained by draq5, meaning the threshold between spots and cytoplasm background is low, which result in poor detection of intracellular amastigotes despite the high infection level, as observed by images inspection (Data not shown). Therefore, the software script parameters were optimized for each species in order to obtain an appropriate cell segmentation as well as the best parasite detection possible. Thus, ensuring a good separation between the controls and, consequently, good z'-factor. Nevertheless, comparison of data between species can be made only in terms of normalized activity. There is a bias in any conclusion based on comparison of the infection ratio or spots/cell number. Even so, the raw data of infection ratio and spots/cell are important to evaluate the assay variability.

The differences in the pattern observed for Draq5 staining was not further investigated. The same protocol was used to dye all plates (volume, concentration and time of incubation) as well as the reading filter and exposure time. Probably, the multiplication ratio of each species plays a role in this matter, since Draq5 staining is stoichiometric and can be used for DNA content analysis in cell proliferation studies.

The activity of amphotericin B and miltefosine was evaluated for the four species. Figure 4.23 shows the DRCs and Table 4.5 displays the pEC_{50} values. The amphotericin B activity was highly consistent to all species, reaching 100% of effectiveness and similar pEC_{50} values (6.3 ± 0.1), while miltefosine showed variable interspecies efficacy (78-100%) and potency (6.0 ± 0.32). Variation in miltefosine sensitivity for both promastigote and amastigote stages has been extensively reported (revised in Croft *et al.* 2006).

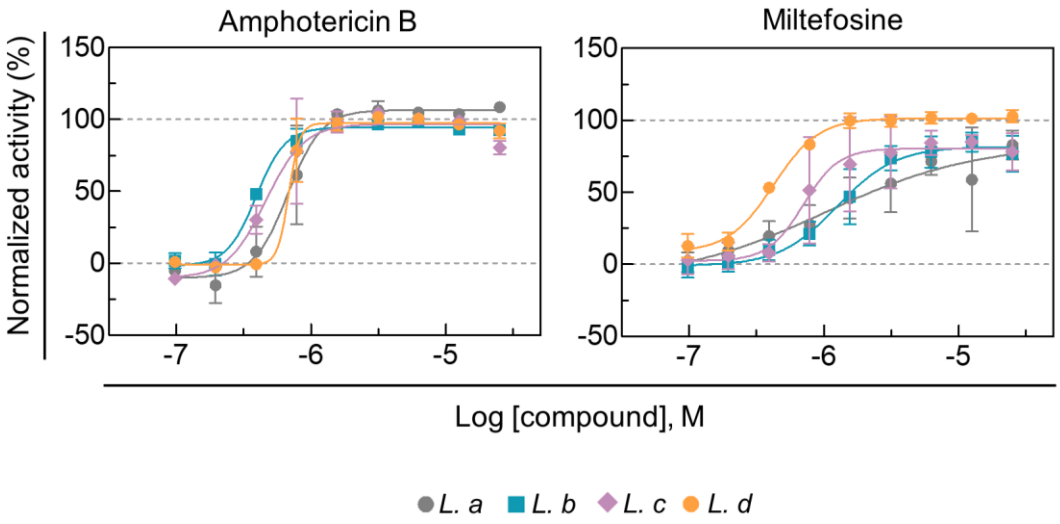

Figure 4.23 Dose-response curves of reference compounds for *Leishmania* species.

Table 4.5 pEC 50 values of reference compounds for *Leishmania* species.

	L. amazonensis	*L. braziliensis*	*L. donovani*	*L. infantum*
Amphotericin B	6.2	6.4	6.3	6.2
Miltefosine	5.7	5.8	6.1	6.4

pEC_{50} = -log EC_{50} (M)

The pEC_{50} values obtained for amphotericin B (6.3 ± 0.1) are quite in agreement with the mean data previous reported (6.8 ± 0.4, see Table 1.4). The variance in compounds potency is expected due to differences in the assay formats. Particularly, the variation in MOI, the distinction of cell host and the disparity in treatment exposure. More important than precise equivalence with others reports is the reproductivity of the data, which is shown in Figure 4.18.

In order to evaluate the correlation of compound library screenings for different species, the results obtained for two distinct collections were analyzed. Although the principal motivation for screening of the LOPAC library was to validate the assay, this library contains FDA-approved drugs and pharmaceutically relevant compound structures, providing predictable activity profiles against a wide range of drug targets (kinases, proteases, GPCR's, etc.). The Pathogen Box (PBox) is an open-access collection provided by Medicines for Malaria Venture (MMV). It contains ~400 diverse, drug-like molecules previously reported as active against a range of different pathogens, predominantly *Plasmodium*, *Mycobacterium*, and kinetoplastid parasites (*T. brucei*, *Leishmania spp*., and *T. cruzi*).

4.5 Library of Pharmaceutically Active Compounds (LOPAC)

This library was screened twice against *L. amazonensis*, *L. braziliensis* and *L.*

donovani intracellular amastigotes at 50 µM. Despite interspecies phenotypic variations, all models presented a good window between the positive/negative controls and had a robust and reproducible performance between runs (Table 4.6).

Table 4.6 LOPAC primary screening quantitative data

	L. amazonensis	*L. braziliensis*	*L. donovani*
Z'-factor	0.65 ± 0.04	0.76 ± 0.07	0.77 ± 0.05
IR 0.5% DMSO	63.27 ± 6.17	69.83 ± 9.25	76.55 ± 4.73
IR Non-infected	10.15 ± 2.27	9.49 ± 2.19	7.02 ± 1.47
IR 10 µM AMB	15.03 ± 4.01	22.31 ± 8.86	11.40 ± 2.30

Z'-factor and IR data are Mean ± Standard Deviation from 12 plates (6 from each independent run).

There are two common strategies to select the compounds from a primary screening that will be tested in confirmatory assays: determination of a cut-off score (e.g. 50% of activity) and taking compounds with activity values within three standard deviation of the positive controls. Due to variable sensivity among species, a cut-off of 50 % activity and 0.5 cell ratio would result in the selection of significantly divergent number of compounds for each species: *L. amazonensis* (61), *L. braziliensis* (39) and *L. donovani* (31). The great difference in the number of compounds selected for each specie diffilcults the comparasion of results. The selection based on positive controls (infected cells treated with 10µM amphotericin B) standard deviations led to a similar trend. Hence, aiming to correlate compounds activity among species latter, selection of the forty most active compounds with cell ratio ≥0.5, approximately 3% of the library, was a better option. The *L. amazonensis* was the most sensitive species, with the 40 selected compounds presenting mean activity of 81.5 %, followed by *L. donovani* and *L. braziliensis*, 63.5 and 61.5%, respectively. In total, with no duplication, 71 compounds were chosen for be assessed in dose-response curve, from which only 27 (38%) were selected in all three models.

The therapeutic profile of selected compounds was compared with the general library distribution of pharmacological classes. Within the ten therapeutic categories (classification provided by supplier support datasheet) drugs related with neurotransmission showed the most expressive percentage (70%) for the selected compounds, followed by phosphorylation (8%), ion channels (7%), apoptosis/cell cycle (6%), and gene regulation (3%). Only within the hormones class no compound was selected. As can be better observed in Figure 4.24, the selected compounds were quite representative of the library general diversity.

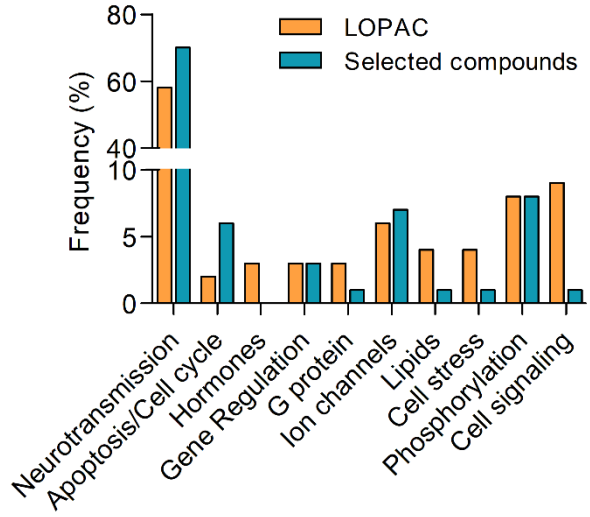

Figure 4.24 Therapeutic profile of LOPAC selected compounds. Classes frequency distribution of LOPAC and selected compounds from primary screening.

As mentioned in the introduction, drug repurposing is an appealing alternative to find new antileishmanial compounds. In this context, several medicines involved with neurotransmission have been tested against *Leishmania* models. Among them, clomipramine (Zilberstein and Dwyer 1984), cyclobenzaprine (Cunha-Júnior *et al.* 2017), sertraline *(*Lima *et al.* 2018), imipramine (Zilberstein and Dwyer 1984), mianserin (Dinesh *et al.* 2014), ketanserin (Singh *et al.* 2014) and domperidone (Gómez-Ochoa *et al.* 2009). Such compounds were present in the LOPAC set, and Table 4.7 shows the results of the primary screening for them.

Table 4.7 Compounds related with neurotransmission reported as active against *Leishmania spp*.

Name	PubChem CID	*L. a*		*L. b*		*L. d*		Reference
		NA	CR	NA	CR	NA	CR	
Clomipramine	68539	101	0.8	73.5	0.8	87.1	1.2	(Zilberstein and Dwyer 1984)
Cyclobenzaprine	22576	83.4	1.0	43.1	0.9	37.1	1.1	(Cunha-Júnior *et al.* 2017)
Imipramine	8228	52.8	1.0	19.0	1.0	19.2	1.2	(Mukherjee *et al.* 2012)
Sertraline	63009	17.6	0.1	34.8	0.0	62.9	0.2	(Lima *et al.* 2018)
Mianserin	68551	9.5	1.0	12.9	1.1	0.7	1.1	(Dinesh *et al.* 2014)
Ketanserin	135348	5.5	1.0	-7.7	1.2	6.9	1.0	(Singh *et al.* 2014)
Domperidone	3151	9.1	1.1	14.8	1.2	-12	1.0	(Gómez-Ochoa *et al.* 2009)

The results obtained in this study are displayed. [a]NA: Normalized Activity (%); [b]CR: Cell Ratio. The values are mean of two independent experiments. Green color indicates compounds that presented normalized activity >40 and cell ratio >0.5. Red color indicates compounds with cell ratio < 0.5.

Clomipramine was the only compound with broad-spectrum activity for the tested

species. This tricyclic antidepressant drug has reported antileishmanial activity against amastigotes of *L. major* and *L. donovani* within peritoneal macrophages from BALB/c mice (pEC_{50} of 5.9 and 6.22 , respectively) (Zilberstein and Dwyer 1984). Cyclobenzaprine, another tricyclic antidepressant, demonstrated pEC_{50} of 4.9 in intracellular amastigotes of *L. infantum*, also in a model with peritoneal macrophages collected from BALB/c mice (Cunha-Júnior *et al.* 2017). But, in the present study, cyclobenzaprine was active only against *L. amazonensis* and *L. braziliensis*. Imipramine, also a tricyclic antidepressant, has demonstrated *in vitro* activity against *L. donovani* intracellular amastigotes using peritoneal macrophages from BALB/c mice as host cells (pEC_{50} of 4.8), and when administered orally it was found to be active against both antimony sensitive and antimony resistant clinical isolates in a hamster model *(*Mukherjee *et al.* 2012). However, only *L. amazonensis* was susceptible to imipramine in the experiments here reported. The mode of action of these compounds have been linked to inhibition of trypanothione reductase, a key enzyme in the redox metabolism of pathogenic trypanosomes (Pandey *et al.* 2015).

Sertraline, another well-known antidepressant, has a tetrahydronaphthalene core as a chemical scaffold, and has been reported as active against intramacrophage *L. infatum* (pEC_{50} of 5.4) and *L. donovani* (pEC_{50} of 5.1) using peritoneal macrophages from BALB/c mice as cell hosts (Lima *et al.* 2018; Palit and Ali 2008). This drug has been also reported as effective in eliminating splenic (72%) and liver (70%) parasite loads in BALB/c mice infected with *L. donovani* (Palit and Ali 2008). Unexpectedly, in the present study, sertraline was toxic for THP-1 cells, impairing the assessment of its activity for all three tested species. Lima and collaborators reported that sertraline induce respiration uncoupling, a significant decrease of intracellular ATP level, and oxidative stress in *L. infantum* promastigotes (Lima *et al.* 2018).

The other three drugs were ineffective against all tested species here reported. Mianserin, a tetracyclic antidepressant, has reported activity against *L. donovani* infected THP-1 cells (pEC_{50} of 4.3), with its mode of action via depletion of ergosterol levels (Dinesh *et al.* 2014). Ketanserin, a tricyclic serotonin S2-receptor antagonist, which is used as antihypertensive agent, has been tested against *L. donovani* infected THP-1 cell (pEC_{50} of 4.6), and observations suggest that its lethal effect is due to inhibition of 3-hydroxy-3-methylglutaryl coenzyme A reductase (HMGR) (Singh *et al.* 2014).

On the other hand, the lack of *in vitro* antileishmanial activity for domperidone was not surprising, since the therapeutic use of this drug has been proposed as an immunomodulation approach (Gómez-Ochoa *et al.* 2009). Domperidone is a gastric prokinetic and antiemetic drug and is also a selective dopamine D2 receptor antagonist. The drug, as a

secondary effect, stimulates prolactin production due to release of serotonin. The prolactin is a hormone that stimulates milk production in mammals, and plays a central role in the immune system as a pro-inflammatory cytokine. It stimulates a protective CD4 + Th1cell-mediated immune response by increasing the production of INF-γ, IL2, IL12, and TNF-α; which would help dogs to control and reduce clinical signs, and decrease anti-*Leishmania* antibody titers (revised in Travi and Miró 2018).

In order to evaluate how similar is the LOPAC screening activity among species, the correlation between activity of paired species was measured by the Pearson-coefficient, represented by the lowercase letter 'r'. This parameter is a statistical measure that can show whether, and how strongly, pairs of variables are related. It is expressed as values between +1 and -1. A perfect positive correlation between variables is indicated by +1 value. Conversely, a perfect negative correlation (when variable increases and the other decreases) is represented by -1 value. The zero indicates there is no discernable relationship. As can be seen in Figure 4.25 A, regarding LOPAC compounds, there was a strong correlation for all species pairing, with the highest value of Pearson-coefficient for *L. amazonensis* x *L. braziliensis* (0.76), followed by *L. amazonensis* x *L. donovani* (0.74) and *L. braziliensis* x *L. donovani* (0.68). However, the majority of compounds did not present activity (or presented only a marginal score) against parasites, which bias the index. When the same analysis is performed with the 71 selected compounds, there was low or none correlation in all cases (Figure 4.25 B). These results highlight the discrepancy of compounds activity for different species, which has an impact on the selection of compounds from a primary screening.

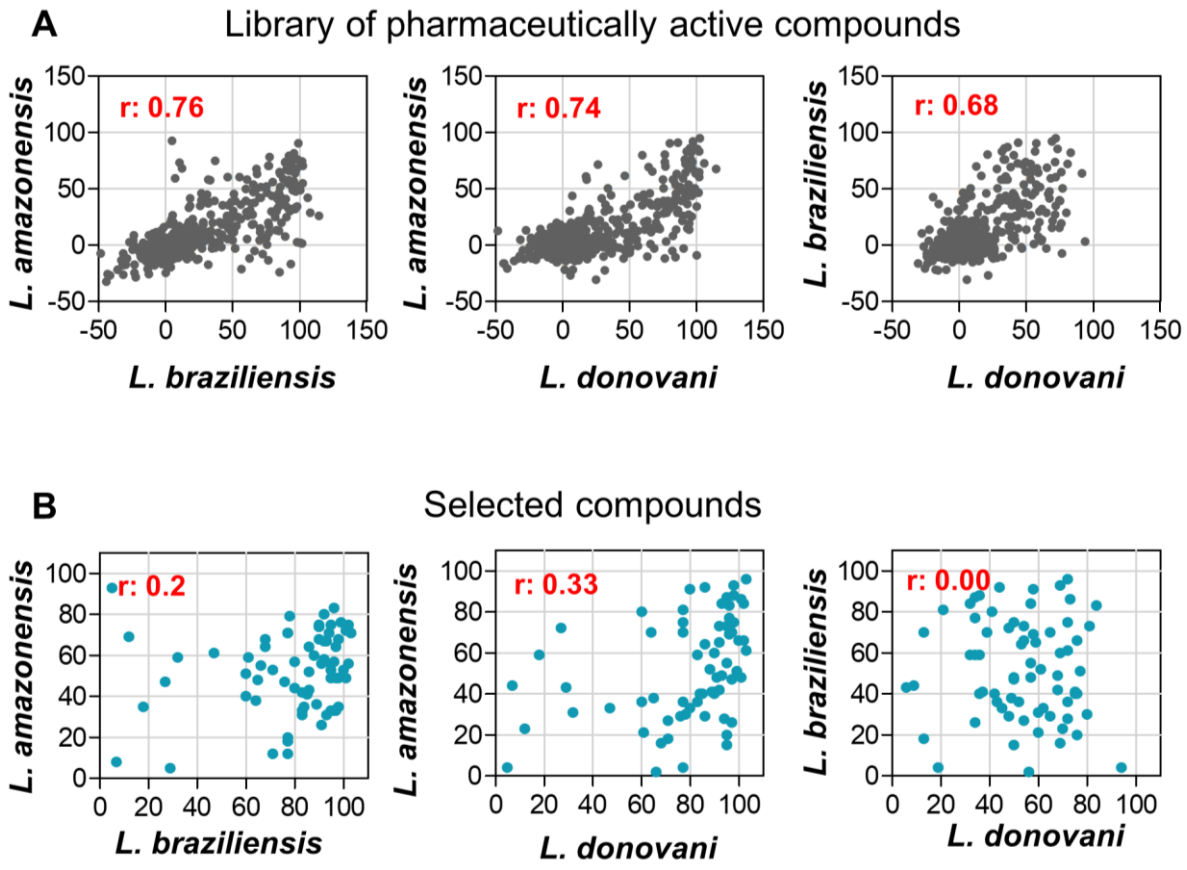

Figure 4.25 Differential activity of LOPAC compounds for *Leishmania* species. Plots show the compounds activity correlation between paired species. **A)** 1280 LOPAC compounds **B)** 71 selected compounds from primary screening.

The next step was to determine compounds potency. Two independent dose-response experiments were carried out. On account of limited compound availability, the top tested concentration was 50 µM. From the 71 compounds, it was possible to determine EC_{50} values for 51. Figure 4.26 summarizes the results obtained for the LOPAC screening. The overall compound potency was only marginal against *Leishmania* parasites, most compounds presented EC_{50} values higher than 30 µM, meaning pEC_{50} around 4.5 or lower. Inspection of maximum activity and pEC_{50} data, reported in Table 4.8, indicates as few as 14 (27.5%) broad-spectrum candidates out of the 51. Other 14 (27.5%) shared activity between two species and 23 (45%) were species-specific.

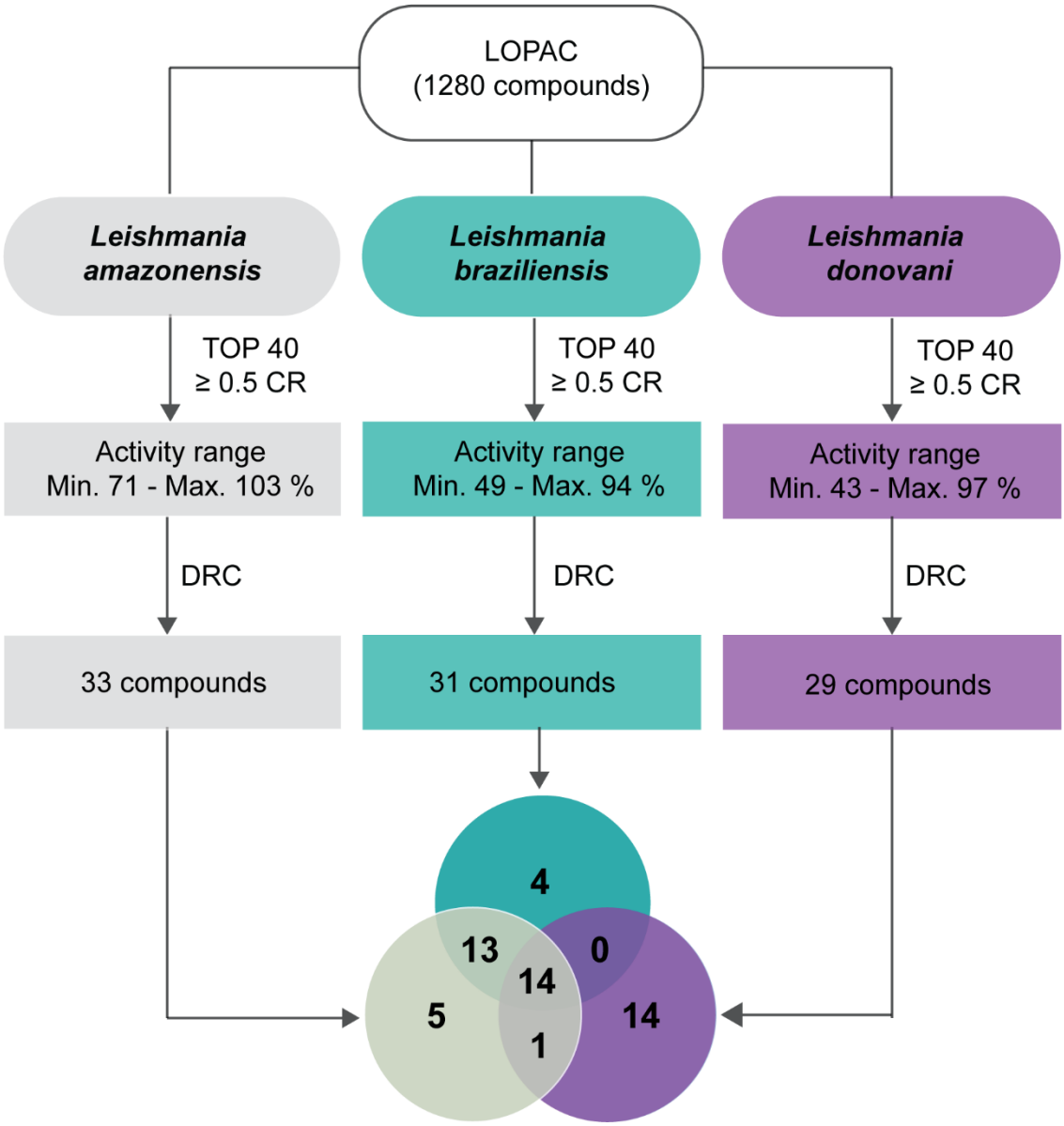

Figure 4.26 Summary of LOPAC screening against *Leishmania spp.* species. After primary screening at single-point concentration (50 µM), the 40 most active compounds with cell ratio (CR) greater than 0.5were tested in dose-response curve (DRC) for activity confirmation. The compounds with determined EC_{50} values were used to plot the Venn Diagram.

Table 4.8 LOPAC compounds maximum activity and pEC50 values

#	PubChem CID	Max. Activity (%)			pEC50 M		
		L. a	*L. b*	*L. d*	*L. a*	*L. b*	*L. d*
1	**89105**	70	78	78	4.51	5.66	5.43
2	**11957564**	100	80	93	4.54	4.49	4.59
3	**68539**	101	81	75	4.44	4.52	4.58
4	**71478**	91	72	85	4.44	4.50	4.56
5	**6603149**	100	82	58	4.41	4.43	4.53
6	**108047**	96	89	76	4.45	4.48	4.41
7	**11957654**	101	64	60	4.34	4.54	4.36
8	**11957471**	98	71	93	4.40	4.38	4.44
9	**9823846**	87	70	62	4.44	4.41	4.36
10	**9803932**	80	86	57	4.59	4.39	4.36
11	**5282318**	76	59	50	4.40	4.55	4.39
12	**122824**	86	64	44	4.34	4.43	4.50
13	**11957725**	83	62	59	4.37	4.58	4.31
14	**6438352**	78	71	52	4.38	4.42	4.31
15	**2585**	100	61		4.45	4.79	
16	**65327**	80	75		4.56	4.49	
17	**238053**	73	72		4.49	4.54	
18	**11957719**	64	66		4.55	4.46	
19	**24351**	80	70		4.46	4.51	
20	**441358**	82	63		4.53	4.44	
21	**2820**	95	79		4.42	4.52	
22	**2170**	89	63		4.42	4.51	
23	**13770**	84	73		4.53	4.39	
24	**67356**	96		82	4.42		4.42
25	**31100**	92	57		4.43	4.41	
26	**6014**	81	70		4.40	4.40	
27	**71311765**	77	75		4.40	4.34	
28	**2818**	61	60		4.31	4.39	
29	**10314472**			77			4.74
30	**11723708**	77			4.62		
31	**909822**		59			4.59	
32	**66062**			81			4.58
33	**71420**			87			4.57
34	**148177**			66			4.56
35	**4748**			77			4.56
36	**66069**			84			4.55
37	**60839**	94			4.54		
38	**62878**			76			4.50
39	**28693**			80			4.49
40	**3039995**			87			4.47
41	**133633**			58			4.46
42	**5282483**			88			4.46
43	**66064**			87			4.42
44	**11957588**		57			4.41	
45	**6918119**		94			4.40	
46	**2858523**			72			4.35
47	**5887**		67			4.34	
48	**672296**			62			4.33
49	**11973707**	64			4.31		
50	**11225543**	76			4.30		
51	**65341**	71			4.30		

Max. Activity is the mean value of normalized activity percentage at 50 µM of four independent experiments. pEC50 is the mean value of two independent experiments. Colors code: max. activity > 90% (green), 70% < max. activity < 90% (orange) and max. activity < 70% (grey). Blank represent no activity. pEC_{50} = -log EC_{50} (M).

4.6 Pathogen Box library

The Pathogen Box library (Pbox) was tested at single-point concentration of 20 µM against *L. amazonensis*, *L. braziliensis*, *L. donovani* and *L. infantum*. Table 4.9 shows the screening statistics data for each species.

Table 4.9 Pathogen Box primary screening quantitative data

	L. amazonensis	*L. braziliensis*	*L. donovani*	*L. infantum*
Z'-factor	0.63±0.01	0.63±0.01	0.65±0.04	0.79±0.03
IR - 0.5% DMSO	50.60 ± 4.33	64.46±4.78	79.89±5.25	83.65±3.50
IR - Non-infected	6.81 ± 1.76	9.56±2.36	10.10±2.45	5.27±1.55

Values expressed as Mean ± Standard Deviation

All models presented a satisfactory window between negative and positive controls, which resulted in Z'-factor values greater than 0.6 for all assay plates: 0.63 for *L. amazonensis*, 0.63 for *L. braziliensis*, 0.65 for *L. donovani* and 0.79 for *L. infantum*.

Analysis of general compounds distribution per normalized activity showed that more than 80.2% (± 7.8) of compounds were completely inactive against *Leishmania spp*, and only 3.6 % (± 0.4) presented activity higher than 75% (Figure 4.27 A).

The support information of PBox clusters the compounds according to the antiparasitic activity firstly described. Seventy compounds within the PBox have been reported as active against *L. donovani*, T. *b. brucei* and/or *T. cruzi*, and are grouped within a single set (kinetoplastids). The twenty most active compounds (approximately 10% of the library) for each species were selected to evaluate their distribution within these groups, adding up to 41 compounds (without duplications) (Figure 4.27 B). Most of the compounds selected were within the tuberculosis group (29%), followed by kinetoplastids (27%) and Malaria (20%). Furthermore, 7 reference compounds were within the selected list, which correspond to 17%.

The reference set within PBox is composed of 26 compounds from which 7 have reported antileishmanial activity, including drugs used in current therapeutics: amphotericin B, miltefosine, pentamidine, nifurtimox, clofazimine, sitamaquine and buparvaquone. The in-library amphotericin B, miltefosine and sitamaquine were inactive for all species. Pentamidine was active against *L. amazonensis* (activity of 60%) and Nifurtimox against *L. braziliensis* (82%). Clofazimine was effective against visceral agents, *L. donovani* (95%) and *L. infantum* (62%). Only buparvaquone presented broad-spectrum activity: *L. amazonensis* (106 %), *L. braziliensis* (104 %), *L. donovani* (97 %) and *L. infantum* (89 %). The ineffectiveness of amphotericin B and miltefosine within the PBox is not a point of concern, because compound degradation may occur with the repeated thawing-freezing cycles, and the *in-house* controls of

both compounds, tested in the same assay as dose-response curves, were active as expected. Similar issue has been reported in the PBox screening by Duffy *et al.* 2017.

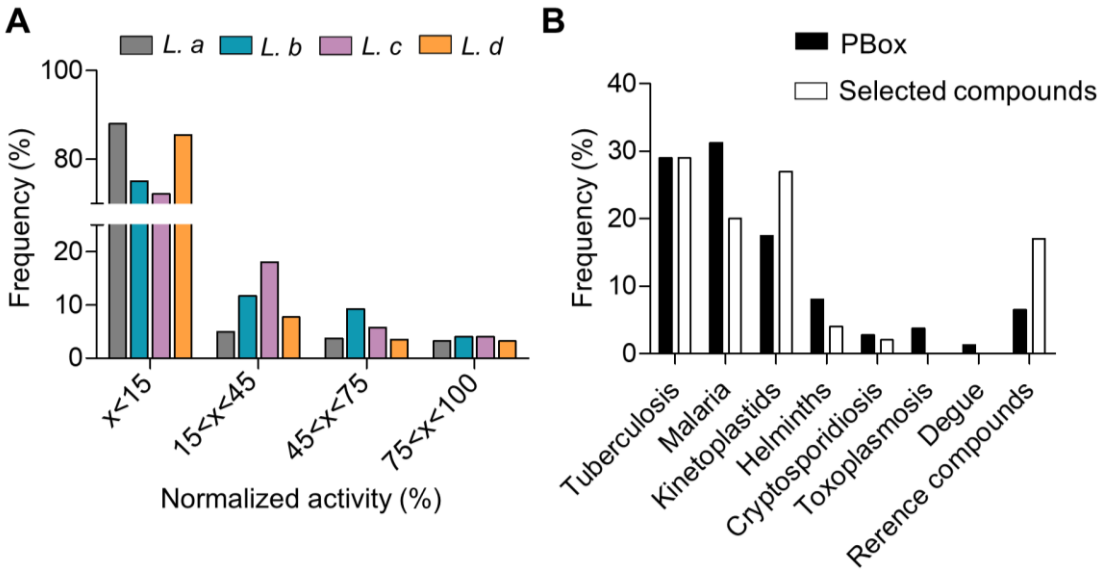

Figure 4.27 Profile of PBox screening. A) General distribution of all 400 compounds per normalized activity against *Leishmania* species. X-axis shows the binned normalized activity of compounds and Y-axis shows the frequency in percentage. **B)** General distribution of all PBox compounds in diseases sets (black) and the 41 most active compounds selected in the *Leishmania spp.* screening (white). X-axis shows the antiparasitic categories and Y-axis shows the frequency in percentage.

Regarding correlations between paired species, on the whole there was a considerable correlation for the PBox library (r = 0.62 ± 0.08), which is not surprising due to the substantial percentage of inactive compounds (Figure 4.28 A). In contrast, the correlation data for the 41 selected compounds varied depending on the species pair (Figure 4.28 B). The *L. donovani*/*L. infantum* pair maintained a high correlation coefficient (r = 0.74). The same occurred to *L. amazonensis*/*L. donovani* (r = 0.51). The complete loss of correlation was noticed only to *L. braziliensis* paired with *L. donovani* and *L. infantum.*

The maintenance of correlation between some pair of species for the most active compounds of the PBox contrasts with the results for LOPAC screening, for which no correlation at all was found between the species. This conflicting outcome highlights the impact of the library composition in the correlation. The LOPAC is a commercial library without any focus on leishmaniasis. In contrast, the PBox is an open access collection constituted by 17.5% of active compounds against kinetoplastid parasites and 6.5 % of reference compounds. Additionally, the PBox has one third of compound numbers (400) when compared with the LOPAC (1200). Thus, as bigger and less focused the compound collection is, the more divergent the selection of compounds will be for different species of *Leishmania*, and that also likely increases the chance of selection of species-specific molecules over broad-spectrum ones in single model platforms.

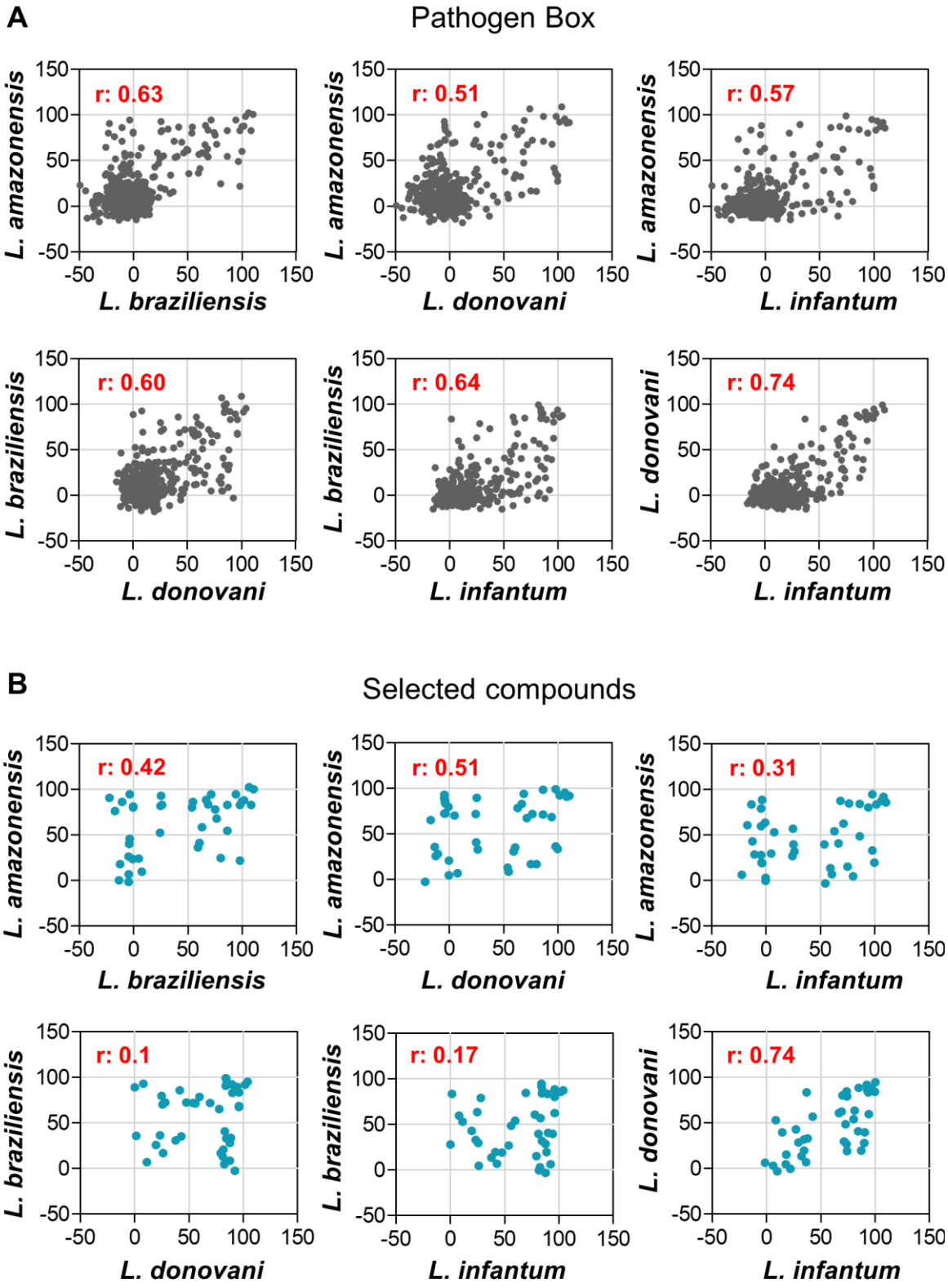

Figure 4.28 Differential activity of the PBox compounds for *Leishmania* species. Plots show the compounds activity correlation between paired species. **A)** 400 PBox compounds **B)** 31 selected compounds from primary screening.

Table 4.10 compares each species normalized activity of all 41 most active selected compounds. In view of the fact that the PBox was tested once at single concentration, compounds with normalized activity greater than 40% were considered actives.

Table 4.10 PBox most active compounds list

#	MMV ID	PubChem CID	*L. a*	*L. b*	*L. d*	*L. i*
1	MMV689480	71768	106	104	97	89
2	MMV689437	129011774	111	102	93	87
3	MMV021660	44523242	99	84	100	97
4	MMV688262	6480466	108	84	93	94
5	MMV690102	122196562	102	90	94	85
6	MMV688279	129011770	87	85	100	86
7	MMV011903	3110698	95	96	70	82
8	MMV690103	122196561	69	85	96	89
9	MMV687765	70695572	77	70	74	86
10	MMV687807	71508634	72	97	69	64
11	MMV675968	461917	67	90	85	43
12	MMV1030799	17399080	-3	96	85	90
13	MMV688372	72710598	87	56	73	50
14	MMV688978	24199313	63	60	80	56
15	MMV637229	68896369	25	95	91	41
16	MMV676477	8518466	100	89	35	21
17	MMV687749	122196546	25	83	43	58
18	MMV688991	41684	98	23	38	35
19	MMV676512	16360478	54	82	15	41
20	MMV676558	7354360	75	80	18	17
21	MMV658988	12004233	-17	78	67	62
22	MMV676401	644385	24	54	74	29
23	MMV595321	18568993	27	85	35	34
24	MMV023233	44525694	-4	28	74	80
25	MMV687730	50994378	-1	25	81	65
26	MMV687800	2794	-4	8	95	61
27	MMV026550	44530521	55	88	10	-2
28	MMV688467	23627030	61	43	37	9
29	MMV024311	129011762	-4	42	88	21
30	MMV000062	4735	60	38	32	15
31	MMV011511	24732616	-4	48	74	21
32	MMV688283	122196557	-11	88	30	30
33	MMV688514	16658982	5	26	72	31
34	MMV687776	129011775	80	26	18	7
35	MMV688990	3599	-4	0	90	30
36	MMV024406	44527543	-13	2	37	85
37	MMV001499	6604371	0	82	22	1
38	MMV676057	23656964	0	83	6	5
39	MMV019790	7080312	8	11	9	55
40	MMV023388	129011766	-12	20	27	45
41	MMV688755	456199	-22	93	-1	8

Values of activity were classified by colors: activity > 80% (green), 40 < activity < 80 (yellow) and activity < 40% (red).

Thirteen molecules (31.7%) presented species-specific activity, other 10 (24.39%) were active against two species, and 18 (43.9%) against three or four species (Figure 4.29).

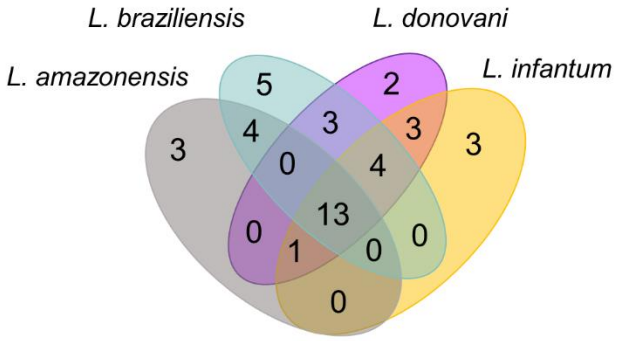

Figure 4.29 Venn Diagram comparing the selected compounds for each specie. Each colour represents the twenty most active compounds for one species.

The PBox supporting information lists 27 compounds that were reported with $pEC_{50} > 4.7$ ($EC_{50} < 20$ µM) for intracellular *L.infantum* in murine primary cells. Table 4.11 lists such compounds, their pEC_{50} and the obtained results for them in the present study.

Table 4.11 Compounds within PBox supporting information with $pEC_{50} > 4.7$

MMV ID	*L. infantum* pEC_{50}	*L. a*		*L. b*		*L. d*		*L. i*	
		[a]NA	[b]CR	NA	CR	NA	CR	NA	CR
MMV690102	7.5	102	1.3	90	1.0	94	0.8	85	0.7
MMV688372	6.7	87	0.7	56	0.4	73	0.6	50	0.5
MMV690103	6.3	69	1.2	85	1.0	96	0.9	89	0.9
MMV689437	6.3	111	1.3	102	0.8	93	0.8	87	0.5
MMV688371	6.2	32	0.7	86	0.0	102	0.1	91	0.1
MMV676602	6.0	28	0.4	57	0.5	67	0.2	47	0.1
MMV688179	6.0	-15	1.1	19	0.8	52	0.7	21	0.7
MMV688180	6.0	51	1.0	38	1.1	39	1.3	6	0.8
MMV676604	5.9	50	0.0	63	0.0	78	0.1	70	0.1
MMV652003	5.9	38	0.7	73	0.7	60	0.7	24	0.7
MMV689061	5.8	-20	1.0	26	1.0	9	1.0	0	0.9
MMV688283	5.6	-11	1.1	88	0.8	30	1.1	30	1.0
MMV688514	5.6	5	1.0	26	1.0	72	1.0	31	1.0
MMV659004	5.4	-23	1.0	82	0.4	6	1.0	20	0.7
MMV658988	5.4	-17	1.2	78	0.4	67	0.5	62	0.7
MMV676600	5.4	-9	0.8	40	0.9	20	0.5	0	0.8
MMV687706	5.4	-11	1.0	73	1.1	69	1.2	13	1.0
MMV688279	5.4	87	1.0	85	0.8	100	0.9	86	1.0
MMV595321	5.2	27	0.7	85	1.0	35	0.9	34	0.9
MMV688410	5.0	3	1.1	25	1.1	28	0.9	1	0.9
MMV676057	5.0	0	1.2	83	1.2	6	1.2	5	1.0
MMV688271	5.0	-16	1.1	8	1.1	17	1.0	5	0.8
MMV001561	4.9	-16	1.1	9	1.1	54	1.1	37	1.0
MMV688467	4.9	61	0.9	43	0.7	37	1.1	9	0.9
MMV676048	4.8	-11	0.9	3	1.0	5	0.9	0	0.9
MMV659010	4.8	-12	1.1	16	1.1	26	1.0	-7	1.1
MMV688415	4.8	-27	1.0	2	1.0	23	1.2	9	1.0

*In grey the pEC50 values reported in the supporting information onbtainded in the Laboratory of Microbiology, Parasitology and Hygiene (LMPH), Univ. of Antwerp are shown. The other columns are the results obtained in this study. [a]NA: Normalized Activity (%); [b]CR: Cell Ratio. Green color indicates compounds that presented normalized activity >40 and cell ratio >0.5. Red color indicates compounds that presented cell rate < 0.5. pEC_{50} = -log EC_{50} (M).

Table 4.11 inspection reveals that only five compounds (18.52%) presented normalized ≥ 40% activity and ≥ 0.5 cell ratio for all species. Still, 12 compounds (44%) were active against at least one representant without cell toxicity.

The Pathogen Box has been also screened against *L. donovani* THP-1 infected cells in an HCS assay more or less similar to the protocol here reported (Duffy *et al.* 2017). Table 4.12 displays pEC_{50} values of the 16 most potent compounds identified by the study and the results obtained in the present study. From which 9 (56%) were active in at least one model, with cell ratio ≥ 0.5, being 5 (31.25 %) active against at least 3 species.

Table 4.12 Activity of the 16 most potent PBox compounds reported by (Duffy *et al.* 2017)

	L. donovani	*L a*		*L. b*		*L d*		*L i*	
MMV ID	pEC_{50}	[a]NA	[b]CR	NA	CR	NA	CR	NA	CR
MMV690102	6.3	102	1.4	90	1.0	94	0.8	85	0.7
MMV652003	5.9	38	0.7	73	0.7	60	0.7	24	0.7
MMV676602	5.8	28	0.4	57	0.5	67	0.2	47	0.1
MMV021013	5.8	66.	0.1	69	0.1	34	0.5	55	0.4
MMV688372	5.8	86.	0.7	56	0.4	73	0.6	50	0.5
MMV688763	5.7	100.	0.1	62	0.2	29	0.5	24	0.4
MMV688271	5.5	-16	1.1	7.7	1.1	17	1.0	5	0.8
MMV687273	5.5	74	0.0	82	0.0	109	0.1	100	0.1
MMV676604	5.3	51	0.0	63	0.0	78	0.1	70	0.1
MMV022478	5.3	104	0.0	100	0.0	111	0.1	95	0.1
MMV022029	5.3	61	0.2	59	0.1	87	0.2	88	0.1
MMV687807	5.3	72	0.8	96	0.8	69	0.2	64	0.2
MMV010576	5.3	49	0.9	64	0.8	53	1.1	6	0.8
MMV690103	5.3	69	1.2	85	1.0	96	0.9	89	0.9
MMV688768	5.3	68	0.0	65	0.1	61	0.5	4	0.7
MMV689437	5.2	11	1.3	102	0.8	93	0.8	87	0.5

*In grey the pEC50 values reported by (Duffy *et al.* 2017) are shown. The other columns are the results obtained in this study. [a]NA: Normalized Activity (%); [b]CR: Cell Ratio. Green indicate compounds that presented normalized activity ≥ 40 and cell ratio ≥ 0.5. Red indicate compounds that presented cell rate < 0.5. pEC50 = -log EC50 (M).

Analyzing the values of normalized activity and cell ratio for the same compounds reported by Duffy *et al.*, it was noticed that most of them were cytotoxic for THP-1 cells. But it is worth pointing out that Duffy *et al.* have not reported the toxicity on infected THP-1 cells for the tested molecules. They reported toxicity data relative to a viability assay against HEK cells. It is certainly of most importance further investigation of toxicity in a panel of uninfected cells. But the bias of evaluating activity of a compound that, in addition to reducing infection rate and parasitic load, also significantly decreases the number of host cells cannot be ignored in intracellular assays. When a compound has toxic effect on the cell, it is impossible to distinguish whether the activity against the intracellular parasite is a consequence of host cell (upcoming) death or a direct effect of the compound; therefore, in these cases the activity data

are not reliable. The viability of the infected and treated cell is a crucial step in avoiding the selection of non-selective compounds. This is the major advantage of HCS methodology, the power of simultaneously providing critical and quantitative information for each tested compound concerning amastigote load and toxic effects on host cell at the single cell level, and such data must be included in all reports.

More recently, the PBox was tested against both axenic and intracellular amastigotes of *L. mexicana* expressing the luciferase NanoLuc-PEST (Berry *et al.* 2018). The most potent identified compounds are listed in Table 4.13. All seven compounds were active against at least one species here tested, and did not present toxicity against THP-1 cells. Additionally, 4 compounds presented broad-spectrum activity.

Table 4.13 Activity of the 7 most potent PBox compounds reported by (Berry *et al.* 2018)

MMV ID	*L. mexicana* pEC_{50}		L a		L. b		L d		L i	
	Axenic	Intra.	[a]NA	[b]CR	NA	CR	NA	CR	NA	CR
MMV676477	7.2	5.3	100	0.7	89	0.7	35	0.9	21	0.8
MMV652003	7.1	5.4	38	0.7	73	0.7	60	0.7	24	0.7
MMV011903	6.7	5.7	95	1.0	96	1.0	70	0.5	82	0.2
MMV689480	8.7	6.4	106	1.3	104	1.2	97	0.8	89	0.9
MMV595321	6.8	5.3	27	0.7	85	1.0	35	0.9	34	0.9
MMV690102	7.2	7.0	102	1.4	90	1.0	94	0.8	85	0.7
MMV688262	7.5	5.7	108	0.8	84	0.9	93	0.7	94	0.7

*In grey the pEC50 values reported by (Berry *et al.* 2018) are shown. The other columns are the results obtained in this study. [a]NA: Normalized Activity (%); [b]CR: Cell Ratio. pEC_{50} = -log EC_{50} (M). Green color indicates compounds that presented normalized activity ≥ 40 and cell ratio ≥ 0.5.

When all the compounds with reported antileishmanial activity from Tables 4.11, 4.12 and 4.13 are analyzed together, after removing duplications, there are 39 compounds. A disappointing number of 9 (23%) was found to have activity against at least 3 of the species here tested. This find is quite unsettling, since these 39 compounds are considered starting points for drug discovery and development, including modification of the compounds guided by medicinal chemistry and target identification, by the scientific community.

Most of the available assays rely on a single endpoint determination of compound potency against only one *Leishmania* species/strain. As a consequence of the sophisticated *Leishmania spp* cycle, is not feasible to standardize a single biological assay that perfectly represents the physiopathology, and at same time enables the prospection of great collections of samples. The better option is to expand the arsenal of relevant secondary assays. Such assays empower the prioritization of compounds based on crucial aspects besides the filters traditionally applied (mainly physico-chemical properties and toxicity). Thus, accelerating the

progression of best compounds. It is important to include recent isolates of *Leishmania* species/strains from the field for *in vitro* as well as *in vivo* tests, avoiding selection of hits against laboratory-adapted parasites (Hefnawy *et al.* 2018). Although it is known that reference isolated organisms present consistency and uniformity, *Leishmania* virulence fluctuates over time after several *in vitro* passages (Miguel *et al.* 2011; Zauli-Nascimento *et al.* 2010). Additionally, assessment of the minimal exposure time required to exert full antileishmanial activity, also known as "time-kill" assay, has been reported (*et al.;* Maes *et al.* 2017; Tegazzini *et al.* 2017) and should be considered a trend for future *in vitro* assays. Unraveling the relation of the time-kill assay to drug resistance and treatment outcome can be a powerful tool to prioritize selected drug candidates. Finally, neither human cell lines or primary murine cells fully mimic human origin primary macrophages, the ideal *in vitro* model. Additionally, antileishmanial activity of compounds can be dependent of the host cell (Seifert *et al.* 2010). Thus, the test in peripheral blood mononuclear cells (PBMCs) is important to eliminate cell-specific compounds.

On the whole, based on our results and recent reports, here we highlight four imperative secondary *in vitro* assays to assist compounds prioritization in early drug discovery: (i) broad-spectrum activity evaluation; (ii) activity against drug-resistant clinical isolates; (iii) evaluation of the rate of action; and (iv) activity in human primary cells (Figure 4.30).

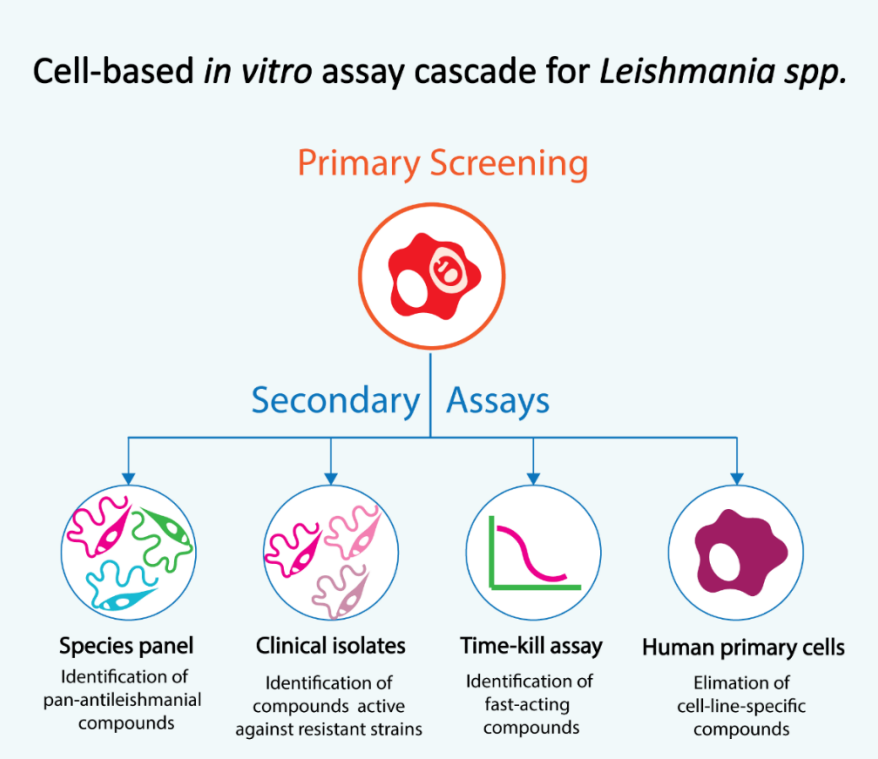

Figure 4.30 Cell-based assay cascade for *Leishmania spp*. in early drug discovery.

4.7 Pan-antileishmanial compounds

Taking in account data from both libraries (LOPAC and PBox), 32 compounds presented broad-spectrum activity against three or four species. Their molecular structures are displayed in Figures 4.31 and 4.32, and Table 4.14 shows their normalized activity at 20 µM.

Confronting Table 4.8, which display LOPAC compounds normalized activity at 50 µM, and Table 4.14, it is clear that most LOPAC compounds were active only at 50 µM, presenting a marginal activity at 20 µM. Only CB1954 (PubChem CID 89105), a nitroheterocyclic prodrug, previously reported as an antitrypanosomatidic agent (Voak *et al.* 2013, 2014; Bot *et al.* 2010), demonstrated a persistent broad-spectrum activity at 20 µM.

Table 4.14 List of compounds with broad-spectrum activity

#	Library	PubChem CID	*L. a*	*L. b*	*L. d*	*L. i*	Mean
1	PBox	71768	106	104	97	89	99
2	PBox	129011774	111	102	93	87	98
3	PBox	44523242	99	84	100	97	95
4	PBox	6480466	108	84	93	94	95
5	PBox	122196562	102	90	94	85	93
6	PBox	129011770	87	85	100	86	89
7	PBox	3110698	95	96	70	82	86
8	PBox	122196561	69	85	96	89	85
9	PBox	70695572	77	70	74	86	77
10	PBox	71508634	72	97	69	64	75
11	PBox	461917	67	90	85	43	71
12	LOPAC	89105	49	82	73		68
13	PBox	17399080	-3	96	85	90	67
14	PBox	72710598	87	56	73	50	67
15	PBox	24199313	63	60	80	56	65
16	PBox	68896369	25	95	91	41	63
17	PBox	122196546	25	83	43	58	52
18	PBox	16360478	54	82	15	41	48
19	PBox	12004233	-17	78	67	62	47
20	LOPAC	11957564	24	34	37		32
21	LOPAC	108047	38	21	22		27
22	LOPAC	68539	31	35	7		24
23	LOPAC	71478	2	36	29		22
24	LOPAC	9823846	37	21	0		19
25	LOPAC	11957725	19	28	4		17
26	LOPAC	6603149	17	21	3		14
27	LOPAC	9803932	26	11	1		12
28	LOPAC	11957471	3	18	13		11
29	LOPAC	5282318	5	19	7		10
30	LOPAC	6438352	9	14	4		9
31	LOPAC	122824	1	12	14		9
32	LOPAC	11957654	3	8	5		5

Heat map of normalized activity at 20 µM. Blank indicates the compound was not tested for *L .infantum*.

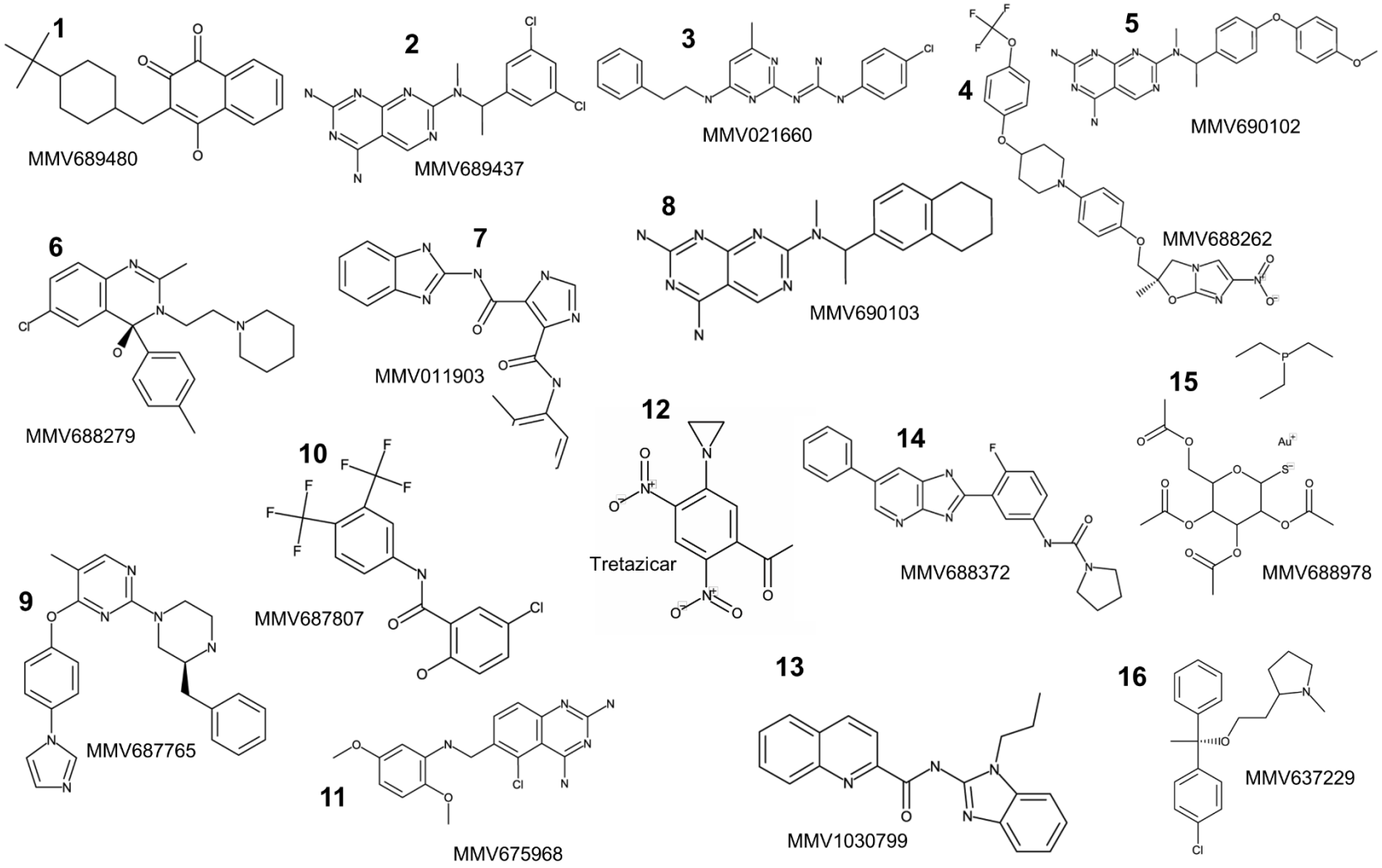

Figure 4.31 Molecular structure of compounds with broad-spectrum activity (1-16).

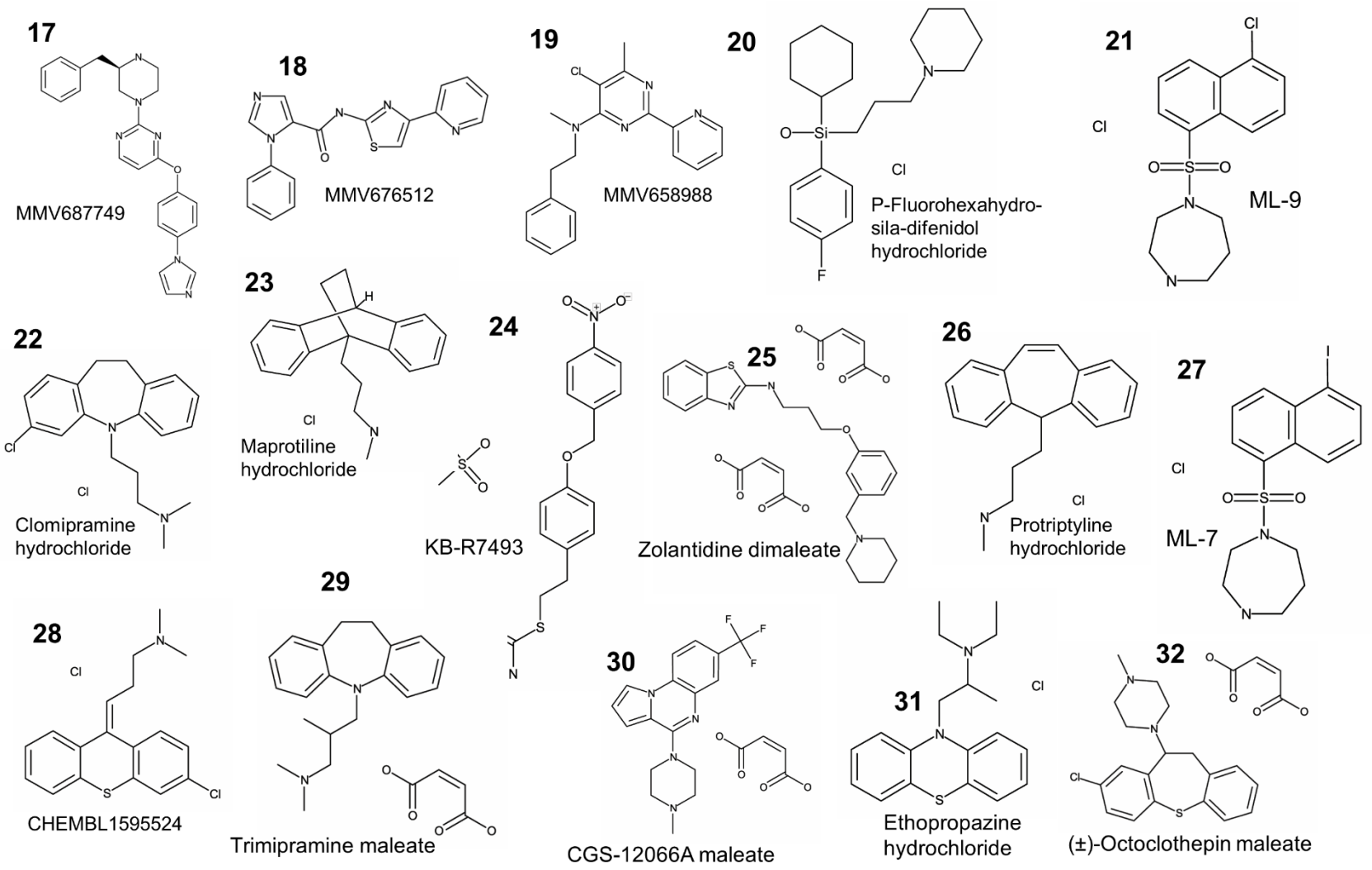

Figure 4.32 Molecular structure of compounds with broad-spectrum activity (17-32).

Nitroheterocyclic drugs are structurally characterized by one or more nitro substituents attached to an aromatic ring. Among the expressive variety of indications for protozoan and bacterial (anaerobic) infections, nitroheterocyclic molecules have been assessed as potential antileishmanial candidates. For instance, fexinidazole, the oral treatment recently recommended by the European Medicines Agency (EMA) for sleeping sickness (DND*i* 2018a), has been tested in a phase II clinical trial against visceral leishmaniasis, but it failed to demonstrate efficacy in patients (Musa and Khalil 2015). Delamanid, a nitro-dihydro-imidazooxazole derivative formerly reported as antimycobacterial agent, has been shown to be effective against leishmania (Patterson *et al.* 2016). Additionally, a nitroimidazole backup of VL-2098 compound (DNDi-0690) is under clinical trial phase I (DND*i* 2018b).

In order to identify an explorable scaffold for further optimization, the similarity index of the compounds chemical structure was calculated (Figure 4.33).

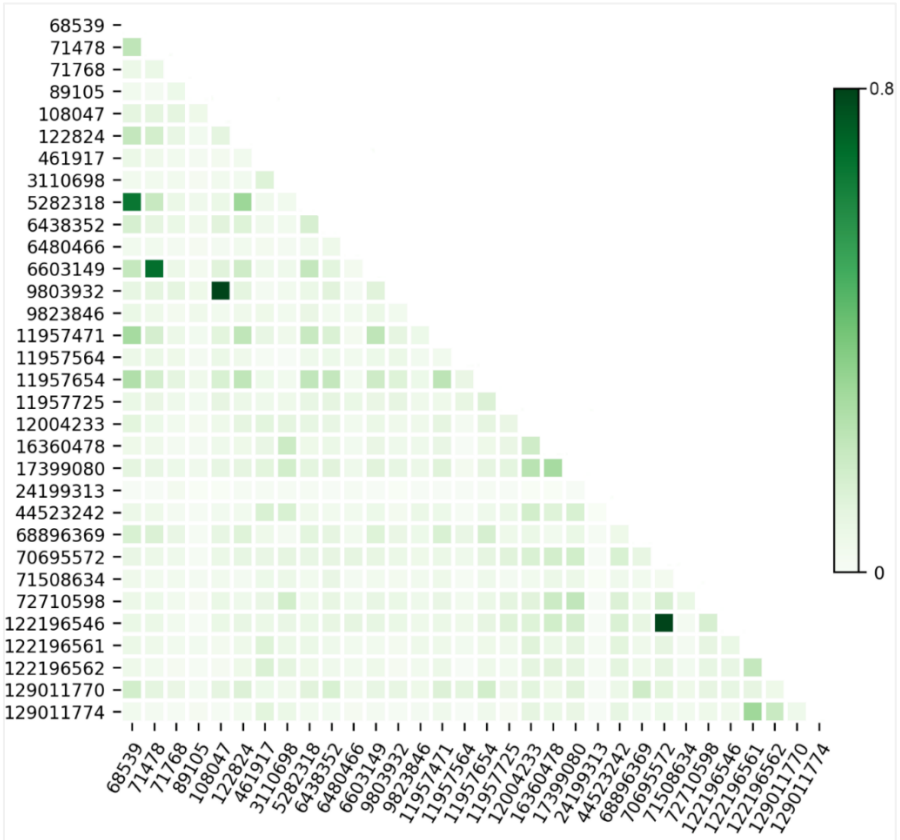

Figure 4.33 Heatmap based on chemical structure similarity determined by Tanimoto coefficient. The axes show the PubChem CID. Tanimoto similarity coefficient was calculated using (http://chemminetools.ucr.edu).

The analysis of compounds' chemical structures similarities did not reveal any cluster, only four pairs of compounds with Tanimoto similarity coefficient greater than 0.5 were identified: 70695572/122196546 (0.83); 108047/9803932 (0.83); 71478/6603149 (0.62); and

68539/5282318 (0.58).

Overall, PBox compounds were the most active (see Table 4.14). Taking into consideration activity for all four species, it was considered pan-antileishmanial compounds those which presented activity greater than 70% for all species in this study, without cell toxicity. A second analysis considered also as pan-antileishmanial compounds those that presented activity greater than 40% for at least three species in this study and potency determined by at least one of the following reported studies: Pbox supporting information data, Duffy *et al.* 2017 or Berry *et al.* 2018. Accordingly, 12 pan-antileishmanial compounds were identified (Table 4.15).

Table 4.15 Pan-antileishmanial compounds

MMV ID	*L. a*		*L. b*		*L. d*		*L. i*		[c]*L. i*	[d]*L. d*	[e]*L. m*
	[a]NA	[b]CR	NA	CR	NA	CR	NA	CR	pEC_{50}	pEC_{50}	pEC_{50}
MMV689480	106	1.3	104	1.2	97	0.8	89	0.9	-	-	6.4
MMV689437	111	1.3	102	0.8	93	0.8	87	0.5	6.3	5.2	-
MMV021660	99	1.1	84	0.6	100	1.0	97	0.9	-	-	-
MMV688262	108	0.8	84	0.9	93	0.7	94	0.7	-	-	5.7
MMV690102	102	1.3	90	1.0	94	0.8	85	0.7	7.5	6.3	7.0
MMV688279	87	1.0	85	0.8	100	0.9	86	1.0	5.4	-	-
MMV011903	95	1.0	96	1.0	70	0.5	82	0.2	-	-	5.7
MMV690103	69	1.2	85	1.0	96	0.9	89	0.9	6.3	5.3	-
MMV687765	77	1.1	70	0.7	74	0.9	86	0.9	-	-	-
MMV688372	87	0.7	56	0.4	73	0.6	50	0.5	6.7	5.8	-
MMV652003	38	0.7	73	0.7	60	0.7	24	0.7	5.9	5.9	5.4
MMV010576	49	0.9	64	0.8	53	1.2	6	0.8	-	5.3	-

[a]NA: Normalized Activity (%); [b]CR: Cell Ratio. Green color indicates compounds that presented normalized activity ≥ 70 and cell ratio ≥ 0.5. In grey the pEC50 values reported by [c] PBox supporting information; [d] Duffy *et al.* 2017 and [e] Berry *et al.* 2018 are shown. pEC_{50} = -logEC_{50} (M).

Representative images of infected cells treated with each of the 12 pan-antileishmanial compounds are shown in the Appendix 2.

Buparvaquone (MMV689480), an antiprotozoal drug related to primaquine hydroxynaphthoquinone and atovaquone, was found to be the most effective compound in this study, with mean activity of 99% for all species. Croft *et al.* (Croft *et al.* 1992) demonstrated for the first time the *in vitro* activity of buparvaquone against *L. donovani*; however, the drug showed limited *in vivo* efficacy in the BALB/c mouse model. There are some studies attempting to improve its efficacy by using liposomal formulations (da Costa-Silva *et al.* 2017).

MMV690102, MMV690103 and MMV689437, belonging to the chemical group

pyrimido [4,5-d] pyrimidine-2,4,7-triamine, demonstrated activity greater than 85% for all tested species. These compounds were previously identified from GSK screening against *Leishmania*, *T. cruzi* and *T. brucei*. Structurally related compounds have been shown to be dihydrofolate reductase (DHFR) inhibitors isolated from mammals (Gebauer *et al.* 2003), which is potentially the target in kinetoplastid parasites.

MMV021660, MMV688262 and MMV687765 were previously described as inhibitors of *M. tuberculosis* (Ballell *et al.* 2013; Li *et al.* 2014; Palmer *et al.* 2015). Here, these compounds were also active against all four species, with activities greater than 70%.

MMV688279 showed antitrypanosomal activity against bloodstream forms of *T. brucei* and inhibited the *T. brucei* recombinant trypanothionein S427 reductase (Patterson *et al.* 2011). This compound presented broad-spectrum activity in the presented study, the lowest activity was 85%. MMV688372 is a substituted 2-(3-aminophenyl) oxazolopyridines analogue and is active against *T. brucei*. Another analogue of the same series demonstrated efficacy in a mouse model of trypanosomiasis (Tatipaka *et al.* 2014). MMV652003 was able to cure the late-stage of central nervous system african trypanosomiasis in a murine model when administered intraperitoneally or orally (Nare *et al.* 2010). MMV688372 and MMV652003 presented marginal activities for some species in the present study, however their potency was demonstrated by others reports (see Table 5.11), therefore, they were also considered pan-antileishmanial compounds.

MMV011903 was identified through the development of a class of agents based on a polyaromatic pharmacophore structurally related to clotrimazole as an antimalarial (Gemma *et al.* 2008). Here, it was active (>70%) for all *Leishmania* species. MMV010576 is a representative of a novel class of orally active antimalarials, presenting activity against a chloroquine-resistant strain (Gamo *et al.* 2010; Younis *et al.* 2012). MMV010576 had marginal antileishmanial activity in the present report, but had potency reported by Duffy *et al.* 2017.

From the 12 pan-antileishmanial compounds, four compounds (MMV690102, MMV690103, MMV689437 and MMV011903) were also active against three *T. cruzi* strains:Y, CL Brener and Sylvio (data not shown). Interestingly, MMV690102, MMV690103, MMV689437 have activity reported against *Leishmania spp.*, *T. cruzi* and *T. brucei*. The activity against the three kinetoplastids possibly indicates a conserved molecular/metabolic target, since these parasites have many common core metabolic functions (Aslett *et al.* 2010). On the other hand, no report about MMV011903 activity in the extracellular parasite *T. brucei* was found, only for the intracellular parasites *Leishmania spp*. and *T. cruzi*, which might indicate a mechanism of action related to cell host modulation.

5 Final considerations

Leishmania infections constitute a complex model from biological, ecological, and epidemiological point of view. This parasite has multiple strategies to subvert the host defense mechanisms and survive in such a harsh intracellular niche (parasitophorous vacuole). Besides, these parasites keep evolving, adapting themselves to new environmental and hosts, and developing resistance to drugs. In face of such complexity, it is not surprising that the scientific community struggles to understand the paradox of *Leishmania* infection, multiplication in the professional phagocytic cells, and to develop efficient therapeutic options.

The standardization of a *Leishmania spp.* high content screening assay was a laborious and complex process. It is necessary to find a balance between biologically relevant infectious system, practicality and reproducibility. The HCS assay here described is based on a protocol previously established by our group at the Institute Pasteur Korea in 2010, the first HCS reported to *Leishmania spp.* (Siqueira-Neto *et al.* 2010).

Careful standardization was carried out aiming to achieve robustness and reproducibility, based on both: (i) the biological model, determining the best condition for parasite and host cell culture, infection and drug exposure, and (ii) the image analysis algorithm, which after several adjustments was able to provide useful and proper quantitative data for the infection models. This semi-automated assay is based on the infection of THP-1 macrophages with stationary phase promastigotes. It was demonstrated that, for the purpose of this study, Draq5 staining is sufficient for detection of macrophage nuclei, parasite nuclei/kinetoplast, and cytosolic delimitation. However, adjustment of specific image analysis settings was required for each species. As a result, all models presented significant robustness and reproducibility, as observed by high values of Z´-factor, and acceptable agreement between runs data.

As no reporter gene is required, this assay can be virtually adapted to any *in vitro* infective *Leishmania* species, including clinical isolates. Despite the advantages of engineered parasites in the development and improvement of biological assays, it has been reported that genetic modifications can lead to modifications in parasite metabolism, including loss of virulence (Rocha *et al.* 2013). Also, the genetic alteration of parasites could require culturing with selection antibiotic for post-transfection selection, which can lead to uncounted pharmacological interactions (Dagley *et al.* 2015). Nevertheless, this image-based assay can also be used to assist functional analysis studies of *Leishmania spp*. transgenic or knockout mutants. Targeted mutation approach is a key tool in basic parasite biology, pathogenicity mechanisms and drug resistance studies. The new technology for gene editing by Clustered

Regularly Interspaced Short Palindromic Repeats (CRISPR) associated gene 9 (Cas9) enables rapid large-scale screening of mutant phenotypes in *Leishmania spp*., thus accelerating the characterization of *Leishmania* genes for new drugs development (Zhang *et al.* 2017).

The multi-species high content assay was established for some of the most clinically relevant agents: *L. amazonensis, L. braziliensis, L. donovani, and L. infantum*. This is the first time that libraries are concomitantly screened against intracellular models of different dermotropic and viscerotropic *Leishmania* species using image-based phenotypic approach.

The correlation for compounds activity between paired species showed an interesting, but predictable result. As bigger and less focused the compound collection, more divergent is the selection of compounds for different species of *Leishmania*, which also likely increases the chance of selecting species-specific molecules over broad-spectrum ones in single species platforms.

The simultaneous screening of the PBox against four *Leishmania* species along with literature data analysis has resulted in the identification of 12 pan-antileishmanial compounds, which offer potential starting points for medicinal chemistry. Four of these compounds were also active against three *T. cruzi* strains.

The low percentage of reported antileishmanial agents with broad-spectrum activity demonstrates the potential value of including a panel of species in early steps of the drug discovery cascade, but also highlights the challenge of developing pan-antileishmanial agents.

A multi-species assay is undoubtedly a powerful secondary assay. But, as in all experiments, carefully analysis of the results is required, especially when pan-antileishmanial compounds are novel entities and present some level of cytotoxicity to the host cell. In such cases is necessary to exclude the possibility of selecting Pan-Assay Interference Compounds (PAINS). PAINS are recognized by the ability to show activity across a range of assay platforms and against a range of proteins, but their bioactivity is attributated to off-target effects, resulting in false positives. Importantly, the identification of PAINS requests experimental proofs of selectivity, structural PAINS filters solely should not be used (Capuzzi *et al.* 2017).

There was no time to further characterize the compounds with activity against one or two species. In case of confirmation of their specificity, they also represent potential start points to medicinal chemistry. Given to the disease heterogeneity, specie-specific compounds are particularly interesting for tegumentary leishmaniasis, especially if they present intrinsic chemical properties that are desirable to topical administration formulations. So, beyond identification of broad-spectrum compounds, a multi-species assay also assists the identification of species-specific molecules.

To conclude, the multi-species high content assay here established represents an important contribution to *Leishmania spp.* early drug discovery and the molecules identified with broad -spectrum of activity can be further explored as central scaffolds for designing new compounds for the treatment leishmaniasis.

REFERENCES

Adaui, V., Lye, L.-F., Akopyants, N.S., Zimic, M., Llanos-Cuentas, A., Garcia, L., Maes, I., De Doncker, S., Dobson, D.E., Arevalo, J., Dujardin, J.-C., Beverley, S.M., 2016. Association of the Endobiont Double-Stranded RNA Virus LRV1 With Treatment Failure for Human Leishmaniasis Caused by *Leishmania braziliensis* in Peru and Bolivia. *J. Infect. Dis.* 213, 112–21.

Akhoundi, M., Kuhls, K., Cannet, A., Votýpka, J., Marty, P., Delaunay, P., Sereno, D., 2016. A Historical Overview of the Classification, Evolution, and Dispersion of Leishmania Parasites and Sandflies. *PLoS Negl. Trop. Dis.* 10, e0004349.

Alcântara, L.M., 2017. Discovery of new drug candidates for visceral leishmaniasis treatment: from image-based assay development to in vitro compounds screening. PhD thesis, University of Campinas (UNICAMP).

Alcântara, L.M., Ferreira, T.C.S., Gadelha, F.R., Miguel, D.C., 2018. Challenges in drug discovery targeting TriTryp diseases with an emphasis on leishmaniasis. *Int. J. Parasitol. Drugs drug Resist.* 8, 430–439.

Alirol, E., Schrumpf, D., Amici Heradi, J., Riedel, A., de Patoul, C., Quere, M., Chappuis, F., 2013. Nifurtimox-eflornithine combination therapy for second-stage gambiense human African trypanosomiasis: Médecins Sans Frontières experience in the Democratic Republic of the Congo. *Clin. Infect. Dis.* 56, 195–203.

Alvar, J., Yactayo, S., Bern, C., 2006. Leishmaniasis and poverty. *Trends Parasitol.* 22, 552–7.

Aslett, M., Aurrecoechea, C., Berriman, M., Brestelli, J., Brunk, B.P., Carrington, M., Depledge, D.P., Fischer, S., Gajria, B., Gao, X., Gardner, M.J., Gingle, A., Grant, G., Harb, O.S., Heiges, M., Hertz-Fowler, C., Houston, R., Innamorato, F., Iodice, J., Kissinger, J.C., Kraemer, E., Li, W., Logan, F.J., Miller, J.A., Mitra, S., Myler, P.J., Nayak, V., Pennington, C., Phan, I., Pinney, D.F., Ramasamy, G., Rogers, M.B., Roos, D.S., Ross, C., Sivam, D., Smith, D.F., Srinivasamoorthy, G., Stoeckert, C.J., Subramanian, S., Thibodeau, R., Tivey, A., Treatman, C., Velarde, G., Wang, H., 2010. TriTrypDB: a functional genomic resource for the Trypanosomatidae. *Nucleic Acids Res.* 38, D457-62.

Aulner, N., Danckaert, A., Rouault-Hardoin, E., Desrivot, J., Helynck, O., Commere, P.-H., Munier-Lehmann, H., Späth, G.F., Shorte, S.L., Milon, G., Prina, E., 2013. High content analysis of primary macrophages hosting proliferating *Leishmania* amastigotes: application to anti-leishmanial drug discovery. *PLoS Negl. Trop.* Dis. 7, e2154.

Ballell, L., Bates, R.H., Young, R.J., Alvarez-Gomez, D., Alvarez-Ruiz, E., Barroso, V., Blanco, D., Crespo, B., Escribano, J., González, R., Lozano, S., Huss, S., Santos-Villarejo, A., Martín-Plaza, J.J., Mendoza, A., Rebollo-Lopez, M.J., Remuiñan-Blanco, M., Lavandera, J.L., Pérez-Herran, E., Gamo-Benito, F.J., García-Bustos, J.F., Barros, D., Castro, J.P., Cammack, N., 2013. Fueling open-source drug discovery: 177 small-molecule leads against tuberculosis. *ChemMedChem* 8, 313–21.

Bandyopadhyay, A., 2017. Target Product Profile: A Planning Tool for the Drug Development. MOJ *Bioequivalence Bioavailab*. 3, 1–2.

Berges, C., Naujokat, C., Tinapp, S., Wieczorek, H., Höh, A., Sadeghi, M., Opelz, G., Daniel, V., 2005. A cell line model for the differentiation of human dendritic cells. *Biochem. Biophys. Res. Commun*. 333, 896–907.

Berman, J.D., Neva, F.A., 1981. Effect of temperature on multiplication of Leishmania amastigotes within human monocyte-derived macrophages in vitro. *Am. J. Trop. Med. Hyg*. 30, 318–21.

Bern, C., Maguire, J.H., Alvar, J., 2008. Complexities of assessing the disease burden attributable to leishmaniasis. *PLoS Negl. Trop. Dis*. 2, e313.

Berry, S.L., Hameed, H., Thomason, A., Maciej-Hulme, M.L., Saif Abou-Akkada, S., Horrocks, P.,

Price, H.P., 2018. Development of NanoLuc-PEST expressing Leishmania mexicana as a new drug discovery tool for axenic- and intramacrophage-based assays. *PLoS Negl. Trop. Dis.* 12, e0006639.

Bezuneh, A., Mukhtar, M., Abdoun, A., Teferi, T., Takele, Y., Diro, E., Jemaneh, A., Shiferaw, W., Wondimu, H., Bhatia, A., Howard, R.F., Ghalib, H., Ireton, G.C., Hailu, A., Reed, S.G., 2014. Comparison of point-of-care tests for the rapid diagnosis of visceral leishmaniasis in East African patients. *Am. J. Trop. Med. Hyg*. 91, 1109–15.

Blackwell, J.M., Fakiola, M., Ibrahim, M.E., Jamieson, S.E., Jeronimo, S.B., Miller, E.N., Mishra, A., Mohamed, H.S., Peacock, C.S., Raju, M., Sundar, S., Wilson, M.E., 2009. Genetics and visceral leishmaniasis: of mice and man. *Parasite Immunol.* 31, 254–66.

Bland, J.M., Altman, D.G., 1986. Statistical methods for assessing agreement between two methods of clinical measurement. *Lancet (London, England)* 1, 307–10.

Bogdan, C., Donhauser, N., Döring, R., Röllinghoff, M., Diefenbach, A., Rittig, M.G., 2000. Fibroblasts as host cells in latent leishmaniosis. *J. Exp. Med*. 191, 2121–30.

Bot, C., Hall, B.S., Bashir, N., Taylor, M.C., Helsby, N.A., Wilkinson, S.R., 2010. Trypanocidal Activity of Aziridinyl Nitrobenzamide Prodrugs. *Antimicrob. Agents Chemother.* 54, 4246–4252.

Bourreau, E., Ginouves, M., Prévot, G., Hartley, M.-A., Gangneux, J.-P., Robert-Gangneux, F., Dufour, J., Sainte-Marie, D., Bertolotti, A., Pratlong, F., Martin, R., Schütz, F., Couppié, P., Fasel, N., Ronet, C., 2016. Presence of *Leishmania* RNA Virus 1 in *Leishmania guyanensis* Increases the Risk of First-Line Treatment Failure and Symptomatic Relapse. *J. Infect. Dis.* 213, 105–11.

Brahmachari, U.N., 1989. Chemotherapy of antimonial compounds in kala-azar infection. Part IV. Further observations on the therapeutic values of urea stibamine. By U.N. Brahmachari, 1922. *Indian J. Med. Res.* 89, 393–404.

Brettmann, E.A., Shaik, J.S., Zangger, H., Lye, L.-F., Kuhlmann, F.M., Akopyants, N.S., Oschwald, D.M., Owens, K.L., Hickerson, S.M., Ronet, C., Fasel, N., Beverley, S.M., 2016. Tilting the balance between RNA interference and replication eradicates *Leishmania* RNA virus 1 and mitigates the inflammatory response. *Proc. Natl. Acad. Sci. U. S. A.* 113, 11998–12005.

Brito, G., Dourado, M., Guimarães, L.H., Meireles, E., Schriefer, A., de Carvalho, E.M., Machado, P.R.L., 2017. Oral Pentoxifylline Associated with Pentavalent Antimony: A Randomized Trial for Cutaneous Leishmaniasis. *Am. J. Trop. Med. Hyg.* 96, 1155–1159.

Burza, S., Croft, S.L., Boelaert, M., 2018. Leishmaniasis. *Lancet (London, England)* 392, 951–970.

Bush, J.T., Wasunna, M., Alves, F., Alvar, J., Olliaro, P.L., Otieno, M., Sibley, C.H., Strub Wourgaft, N., Guerin, P.J., 2017. Systematic review of clinical trials assessing the therapeutic efficacy of visceral leishmaniasis treatments: A first step to assess the feasibility of establishing an individual patient data sharing platform. *PLoS Negl. Trop. Dis*. 11, e0005781.

Callahan, H.L., Portal, I.F., Bensinger, S.J., Grogl, M., 1996. *Leishmania spp*: temperature sensitivity of promastigotes *in vitro* as a model for tropism *in vivo*. *Exp. Parasitol.* 84, 400–9.

Capuzzi, S.J., Muratov, E.N., Tropsha, A., 2017. Phantom PAINS: Problems with the Utility of Alerts for Pan-Assay INterference CompoundS. *J. Chem. Inf. Model.* 57, 417–427.

Castelli, G., Galante, A., Lo Verde, V., Migliazzo, A., Reale, S., Lupo, T., Piazza, M., Vitale, F., Bruno, F., 2014. Evaluation of two modified culture media for *Leishmania infantum* cultivation versus different culture media. *J. Parasitol.* 100, 228–30.

Castillo, E., Dea-Ayuela, M.A., Bolás-Fernández, F., Rangel, M., González-Rosende, M.E., 2010. The kinetoplastid chemotherapy revisited: current drugs, recent advances and future perspectives. *Curr. Med. Chem.* 17, 4027–51.

Chalghaf, B., Chemkhi, J., Mayala, B., Harrabi, M., Benie, G.B., Michael, E., Ben Salah, A., 2018. Ecological niche modeling predicting the potential distribution of Leishmania vectors in the Mediterranean basin: impact of climate change. *Parasit. Vectors* 11, 461.

Charlton, R.L., Rossi-Bergmann, B., Denny, P.W., Steel, P.G., 2018. Repurposing as a strategy for the

discovery of new anti-leishmanials: the-state-of-the-art. *Parasitology* 145, 219–236.

Childs, G.E., Foster, K.A., McRoberts, M.J., 1978. Insect cell culture media for cultivation of new world *Leishmania*. *Int. J. Parasitol.* 8, 255–8.

Chulay, J.D., Fleckenstein, L., Smith, D.H., 1988. Pharmacokinetics of antimony during treatment of visceral leishmaniasis with sodium stibogluconate or meglumine antimoniate. *Trans. R. Soc. Trop. Med. Hyg.* 82, 69–72.

Chunge, C., Owate, J., Pamba, H., Donno, L., 1990. Treatment of visceral leishmaniasis in Kenya by aminosidine alone or combined with sodium stibogluconate. *Trans R Soc Trop Med Hyg*. 84, 221–5.

Croft, S.L., Engel, J., 2006. Miltefosine--discovery of the antileishmanial activity of phospholipid derivatives. *Trans. R. Soc. Trop. Med. Hyg.* 100 Suppl, S4-8.

Croft, S.L., Hogg, J., Gutteridge, W.E., Hudson, A.T., Randall, A.W., 1992. The activity of hydroxynaphthoquinones against Leishmania donovani. J. Antimicrob. Chemother. 30, 827–32.

Croft, S.L., Seifert, K., Yardley, V., 2006a. Current scenario of drug development for leishmaniasis. *Indian J. Med. Res.* 123, 399–410.

Croft, S.L., Sundar, S., Fairlamb, A.H., 2006b. Drug resistance in leishmaniasis. *Clin. Microbiol. Rev.* 19, 111–26.

Cunha-Júnior, E.F., Andrade-Neto, V.V., Lima, M.L., da Costa-Silva, T.A., Galisteo Junior, A.J., Abengózar, M.A., Barbas, C., Rivas, L., Almeida-Amaral, E.E., Tempone, A.G., Torres-Santos, E.C., 2017. Cyclobenzaprine Raises ROS Levels in *Leishmania infantum* and Reduces Parasite Burden in Infected Mice. *PLoS Negl. Trop. Dis.* 11, e0005281.

da Costa-Silva, T.A., Galisteo, A.J., Lindoso, J.A.L., Barbosa, L.R.S., Tempone, A.G., 2017. Nanoliposomal Buparvaquone Immunomodulates *Leishmania infantum*-Infected Macrophages and Is Highly Effective in a Murine Model. *Antimicrob. Agents Chemother*. 61.

da Luz, R.I., Vermeersch, M., Dujardin, J.-C.J.-C., Cos, P., Maes, L., Inocencio da Luz, R., Vermeersch, M., Dujardin, J.-C.J.-C., Cos, P., Maes, L., 2009. In vitro sensitivity testing of *Leishmania* clinical field isolates: preconditioning of promastigotes enhances infectivity for macrophage host cells. Antimicrob. *Agents Chemother.* 53, 5197–5203.

Dagley, M.J., Saunders, E.C., Simpson, K.J., McConville, M.J., 2015. High-content assay for measuring intracellular growth of *Leishmania* in human macrophages. *Assay Drug Dev. Technol.* 13, 389–401.

DaMata, J.P., Mendes, B.P., Maciel-Lima, K., Menezes, C.A.S., Dutra, W.O., Sousa, L.P., Horta, M.F., 2015. Distinct Macrophage Fates after in vitro Infection with Different Species of Leishmania: Induction of Apoptosis by Leishmania (Leishmania) amazonensis, but Not by *Leishmania (Viannia) guyanensis*. *PLoS One* 10, e0141196.

Datta, R., Imamura, K., Goldman, S.J., Dianoux, A.C., Kufe, D.W., Sherman, M.L., 1992. Functional expression of the macrophage colony-stimulating factor receptor in human THP-1 monocytic leukemia cells. *Blood* 79, 904–12.

De Muylder, G., Ang, K.K.H., Chen, S., Arkin, M.R., Engel, J.C., McKerrow, J.H., 2011. A screen against *Leishmania* intracellular amastigotes: comparison to a promastigote screen and identification of a host cell-specific hit. *PLoS Negl. Trop. Dis*. 5, e1253.

De Rycker, M., Hallyburton, I., Thomas, J., Campbell, L., Wyllie, S., Joshi, D., Cameron, S., Gilbert, I.H., Wyatt, P.G., Frearson, J.A., Fairlamb, A.H., Gray, D.W., 2013. Comparison of a high-throughput high-content intracellular *Leishmania donovani* assay with an axenic amastigote assay. *Antimicrob. Agents Chemother.* 57, 2913–22.

DeKrey, G.K., Lima, H.C., Titus, R.G., 1998. Analysis of the immune responses of mice to infection with *Leishmania braziliensis. Infect. Immun.* 66, 827–9.

Dinesh, N., Kaur, P.K., Swamy, K.K., Singh, S., 2014. Mianserin, an antidepressant kills *Leishmania*

donovani by depleting ergosterol levels. *Exp. Parasitol.* 144, 84–90.

DNDi, 2018a. European Medicines Agency recommends fexinidazole, the first all-oral treatment for sleeping sickness [WWW Document]. *Drugs Neglected Dis. Initiat.* URL https://www.dndi.org/2018/media-centre/press-releases/ema-recommends-fexinidazole-first-all-oral-treatment-sleeping-sickness/ (accessed 1.5.19).

DNDi, 2018b. InfoLeish [WWW Document]. *Drugs Neglected Dis. Initiat.* URL https://www.dndial.org/wp-content/uploads/2018/07/InfoLeish_2018_ENG.pdf (accessed 1.11.19).

DNDi, 2016. Patient Needs-Driven Collaborative R&D Model for Neglected Patients. *Drugs Neglected Dis. Initiat.* URL https://www.dndi.org/wp-content/uploads/2016/08/DNDi_Portfolio-map-2016_web.pdf (accessed 1.5.19)

DNDi, 2015. VL-2098 [WWW Document]. *Drugs Neglected Dis. Initiat*. URL https://www.dndi.org/diseases-projects/portfolio/completed-projects/vl-2098/ (accessed 8.20.18).

Duffy, S., Sykes, M.L., Jones, A.J., Shelper, T.B., Simpson, M., Lang, R., Poulsen, S.-A., Sleebs, B.E., Avery, V.M., 2017. Screening the Medicines for Malaria Venture Pathogen Box across Multiple Pathogens Reclassifies Starting Points for Open-Source Drug Discovery. *Antimicrob. Agents Chemother*. 61.

Eren, R.O., Kopelyanskiy, D., Moreau, D., Chapalay, J.B., Chambon, M., Turcatti, G., Lye, L.-F., Beverley, S.M., Fasel, N., 2018. Development of a semi-automated image-based high-throughput drug screening system. *Front. Biosci.* (Elite Ed). 10, 242–253.

Escobar, P., Matu, S., Marques, C., Croft, S.L., 2002. Sensitivities of *Leishmania* species to hexadecylphosphocholine (miltefosine), ET-18-OCH(3) (edelfosine) and amphotericin B. *Acta Trop.* 81, 151–7.

Ferro, C., López, M., Fuya, P., Lugo, L., Cordovez, J.M., González, C., 2015. Spatial Distribution of Sand Fly Vectors and Eco-Epidemiology of Cutaneous Leishmaniasis Transmission in Colombia. *PLoS One* 10, e0139391.

Ferro, C., Marín, D., Góngora, R., Carrasquilla, M.C., Trujillo, J.E., Rueda, N.K., Marín, J., Valderrama-Ardila, C., Alexander, N., Pérez, M., Munstermann, L.E., Ocampo, C.B., 2011. Phlebotomine vector ecology in the domestic transmission of American cutaneous leishmaniasis in Chaparral, Colombia. *Am. J. Trop. Med. Hyg.* 85, 847–56.

Field, M.C., Horn, D., Fairlamb, A.H., Ferguson, M.A.J., Gray, D.W., Read, K.D., De Rycker, M., Torrie, L.S., Wyatt, P.G., Wyllie, S., Gilbert, I.H., 2017. Anti-trypanosomatid drug discovery: an ongoing challenge and a continuing need. *Nat. Rev. Microbiol.* 15, 217–231.

Freitas-Junior, L.H., Chatelain, E., Kim, H.A., Siqueira-Neto, J.L., 2012. Visceral leishmaniasis treatment: What do we have, what do we need and how to deliver it? Int. J. *Parasitol. Drugs drug Resist.* 2, 11–9.

Furtado, T.A., Cisalpino, E.O., Santos, U.M., 1960. In vitro studies of the effect of amphotericin B on *Leishmania brasiliensis*. *Antibiot. Chemother.* (Northfield, Ill.) 10, 692–3.

Galluzzi, L., Ceccarelli, M., Diotallevi, A., Menotta, M., Magnani, M., 2018. Real-time PCR applications for diagnosis of leishmaniasis. *Parasit. Vectors* 11, 273.

Gamo, F.-J., Sanz, L.M., Vidal, J., de Cozar, C., Alvarez, E., Lavandera, J.-L., Vanderwall, D.E., Green, D.V.S., Kumar, V., Hasan, S., Brown, J.R., Peishoff, C.E., Cardon, L.R., Garcia-Bustos, J.F., 2010. Thousands of chemical starting points for antimalarial lead identification. *Nature* 465, 305–10.

Garg, R., Dube, A., 2006. Animal models for vaccine studies for visceral leishmaniasis. Indian J. Med. Res. 123, 439–54.

Gebauer, M.G., McKinlay, C., Gready, J.E., 2003. Synthesis of quaternised 2-aminopyrimido[4,5-d]pyrimidin-4(3H)-ones and their biological activity with dihydrofolate reductase. *Eur. J. Med. Chem.* 38, 719–728.

Gemma, S., Campiani, G., Butini, S., Kukreja, G., Coccone, S.S., Joshi, B.P., Persico, M., Nacci, V., Fiorini, I., Novellino, E., Fattorusso, E., Taglialatela-Scafati, O., Savini, L., Taramelli, D., Basilico, N., Parapini, S., Morace, G., Yardley, V., Croft, S., Coletta, M., Marini, S., Fattorusso, C., 2008. Clotrimazole scaffold as an innovative pharmacophore towards potent antimalarial agents: design, synthesis, and biological and structure-activity relationship studies. *J. Med. Chem.* 51, 1278–94.

Genin, M., Clement, F., Fattaccioli, A., Raes, M., Michiels, C., 2015. M1 and M2 macrophages derived from THP-1 cells differentially modulate the response of cancer cells to etoposide. *BMC Cancer* 15, 577.

Gomes-Alves, A.G., Maia, A.F., Cruz, T., Castro, H., Tomás, A.M., 2018. Development of an automated image analysis protocol for quantification of intracellular forms of Leishmania spp. *PLoS One* 13, e0201747.

Gómez-Ochoa, P., Castillo, J.A., Gascón, M., Zarate, J.J., Alvarez, F., Couto, C.G., 2009. Use of domperidone in the treatment of canine visceral leishmaniasis: a clinical trial. *Vet. J.* 179, 259–63.

Gonçalves-de-Albuquerque, S. da C., Pessoa-E-Silva, R., Trajano-Silva, L.A.M., de Goes, T.C., de Morais, R.C.S., da C Oliveira, C.N., de Lorena, V.M.B., de Paiva-Cavalcanti, M., 2017. The Equivocal Role of Th17 Cells and Neutrophils on Immunopathogenesis of Leishmaniasis. *Front. Immunol.* 8, 1437.

Goyard, S., Segawa, H., Gordon, J., Showalter, M., Duncan, R., Turco, S.J., Beverley, S.M., 2003. An in vitro system for developmental and genetic studies of Leishmania donovani phosphoglycans. *Mol. Biochem. Parasitol.* 130, 31–42.

Gulati, M., Bajad, S., Singh, S., Ferdous, A.J., Singh, M., 1998. Development of liposomal amphotericin B formulation. *J. Microencapsul.* 15, 137–51.

Gupta, S., Yardley, V., Vishwakarma, P., Shivahare, R., Sharma, B., Launay, D., Martin, D., Puri, S., 2015. Nitroimidazo-oxazole compound DNDI-VL-2098: an orally effective preclinical drug candidate for the treatment of visceral leishmaniasis. *J. Antimicrob. Chemother*. 70, 518–27.

Hartley, M.-A., Drexler, S., Ronet, C., Beverley, S.M., Fasel, N., 2014. The immunological, environmental, and phylogenetic perpetrators of metastatic leishmaniasis. *Trends Parasitol.* 30, 412–22.

Hazarika, A.N., 1949. Treatment of kala-azar with pentamidine isothionate; a study of 55 cases. *Ind. Med. Gaz.* 84, 140–5.

Hefnawy, A., Cantizani, J., Peña, I., Manzano, P., Rijal, S., Dujardin, J.-C., De Muylder, G., Martin, J., 2018. Importance of secondary screening with clinical isolates for anti-leishmania drug discovery. *Sci. Rep.* 8, 11765.

Hurrell, B.P., Regli, I.B., Tacchini-Cottier, F., 2016. Different *Leishmania* Species Drive Distinct Neutrophil Functions. *Trends Parasitol*. 32, 392–401.

Jain, S.K., Sahu, R., Walker, L.A., Tekwani, B.L., 2012. A Parasite Rescue and Transformation Assay for Antileishmanial Screening Against Intracellular *Leishmania donovani* Amastigotes in THP1 Human Acute Monocytic Leukemia Cell Line. *J. Vis. Exp.* 1–14.

Jeronimo, S.M.B., Duggal, P., Ettinger, N.A., Nascimento, E.T., Monteiro, G.R., Cabral, A.P., Pontes, N.N., Lacerda, H.G., Queiroz, P. V, Gomes, C.E.M., Pearson, R.D., Blackwell, J.M., Beaty, T.H., Wilson, M.E., 2007. Genetic predisposition to self-curing infection with the protozoan *Leishmania chagasi*: a genomewide scan. *J. Infect. Dis.* 196, 1261–9.

Jones, N.G., Catta-Preta, C.M.C., Lima, A.P.C.A., Mottram, J.C., 2018. Genetically Validated Drug Targets in Leishmania: Current Knowledge and Future Prospects. *ACS Infect. Dis*. 4, 467–477.

Khare, S., Nagle, A.S., Biggart, A., Lai, Y.H., Liang, F., Davis, L.C., Barnes, S.W., Mathison, C.J.N., Myburgh, E., Gao, M.-Y., Gillespie, J.R., Liu, X., Tan, J.L., Stinson, M., Rivera, I.C., Ballard, J., Yeh, V., Groessl, T., Federe, G., Koh, H.X.Y., Venable, J.D., Bursulaya, B., Shapiro, M., Mishra, P.K., Spraggon, G., Brock, A., Mottram, J.C., Buckner, F.S., Rao, S.P.S., Wen, B.G., Walker, J.R.,

Tuntland, T., Molteni, V., Glynne, R.J., Supek, F., 2016. Proteasome inhibition for treatment of leishmaniasis, Chagas disease and sleeping sickness. *Nature* 537, 229–233.

Koch, L.K., Kochmann, J., Klimpel, S., Cunze, S., 2017. Modeling the climatic suitability of leishmaniasis vector species in Europe. *Sci. Rep.* 7, 13325.

Kuhlmann, F.M., Fleckenstein, J.M., 2017. Antiparasitic *Agents. Infect. Dis.* (Auckl). 1345–1372.e2.

Lansing, T.D., Haskins, J.R., Giuliano, K.A., 2007. High content screening: a powerful approach to systems cell biology and drug discovery. *Humana Press Inc.* Totowa, New Jersey

Laskay, T., van Zandbergen, G., Solbach, W., 2003. Neutrophil granulocytes--Trojan horses for *Leishmania major* and other intracellular microbes? *Trends Microbiol*. 11, 210–4.

Li, W., Upadhyay, A., Fontes, F.L., North, E.J., Wang, Y., Crans, D.C., Grzegorzewicz, A.E., Jones, V., Franzblau, S.G., Lee, R.E., Crick, D.C., Jackson, M., 2014. Novel insights into the mechanism of inhibition of MmpL3, a target of multiple pharmacophores in Mycobacterium tuberculosis. *Antimicrob. Agents Chemother*. 58, 6413–23.

Lima, M.L., Abengózar, M.A., Nácher-Vázquez, M., Martínez-Alcázar, M.P., Barbas, C., Tempone, A.G., López-Gonzálvez, Á., Rivas, L., 2018. Molecular Basis of the Leishmanicidal Activity of the Antidepressant Sertraline as a Drug Repurposing Candidate. *Antimicrob. Agents Chemother*. 62.

Lindoso, J.A.L., Cunha, M.A., Queiroz, I.T., Moreira, C.H.V., 2016. Leishmaniasis-HIV coinfection: current challenges. *HIV. AIDS*. (Auckl). 8, 147–156.

Machado, P.R.L., Lessa, H., Lessa, M., Guimarães, L.H., Bang, H., Ho, J.L., Carvalho, E.M., 2007. Oral pentoxifylline combined with pentavalent antimony: a randomized trial for mucosal leishmaniasis. *Clin. Infect. Dis.* 44, 788–93.

MacLean, R.C., Hall, A.R., Perron, G.G., Buckling, A., 2010. The population genetics of antibiotic resistance: integrating molecular mechanisms and treatment contexts. *Nat. Rev. Genet*. 11, 405–14.

Maes, L., Beyers, J., Mondelaers, A., Van den Kerkhof, M., Eberhardt, E., Caljon, G., Hendrickx, S., 2017. In vitro “time-to-kill” assay to assess the cidal activity dynamics of current reference drugs against *Leishmania donovani* and *Leishmania infantum*. *J. Antimicrob. Chemother.* 72, 428–430.

Marra, F., Chiappetta, M.C., Vincenti, V., 2014. Ear, nose and throat manifestations of mucocutaneous Leishmaniasis: a literature review. *Acta Biomed.* 85, 3–7.

Martinez Garcia, P., Guasch, J., Llaurado, F., 1950. [First cases of infantile kala-azar treated in Spain with diamidines (stilbamidine and pentamidine)]. *Rev. Esp. Pediatr*. 6, 319–46.

Mears, E.R., Modabber, F., Don, R., Johnson, G.E., 2015. A Review: The Current In Vivo Models for the Discovery and Utility of New Anti-leishmanial Drugs Targeting Cutaneous Leishmaniasis. *PLoS Negl. Trop. Dis.* 9, e0003889.

Merlen, T., Sereno, D., Brajon, N., Rostand, F., Lemesre, J.L., 1999. *Leishmania spp*: completely defined medium without serum and macromolecules (CDM/LP) for the continuous in vitro cultivation of infective promastigote forms. *Am. J. Trop. Med. Hyg.* 60, 41–50.

Meunier, F., Prentice, H.G., Ringdén, O., 1991. Liposomal amphotericin B (AmBisome): safety data from a phase II/III clinical trial. *J. Antimicrob. Chemother.* 28 Suppl B, 83–91.

Miettinen, T.P., Björklund, M., 2017. Mitochondrial Function and Cell Size: An Allometric Relationship. *Trends Cell Biol.* 27, 393–402.

Miguel, D.C., Yokoyama-Yasunaka, J.K.U., Andreoli, W.K., Mortara, R.A., Uliana, S.R.B., 2007. Tamoxifen is effective against Leishmania and induces a rapid alkalinization of parasitophorous vacuoles harbouring *Leishmania (Leishmania) amazonensis* amastigotes. *J. Antimicrob. Chemother*. 60, 526–34.

Miguel, D.C., Zauli-Nascimento, R.C., Yokoyama-Yasunaka, J.K.U., Katz, S., Barbiéri, C.L., Uliana, S.R.B., 2009. Tamoxifen as a potential antileishmanial agent: efficacy in the treatment of

Leishmania braziliensis and Leishmania chagasi infections. *J. Antimicrob. Chemother*. 63, 365–8.

Miguel, D.C., Zauli-Nascimento, R.C., Yokoyama-Yasunaka, J.K.U., Pereira, L.I.A., Jerônimo, S.M.B., Ribeiro-Dias, F., Dorta, M.L., Uliana, S.R.B., 2011. Clinical isolates of New World *Leishmania* from cutaneous and visceral leishmaniasis patients are uniformly sensitive to tamoxifen. *Int. J. Antimicrob. Agents* 38, 93–4.

Miró, G., López-Vélez, R., 2018. Clinical management of canine leishmaniosis versus human leishmaniasis due to Leishmania infantum: Putting "One Health" principles into practice. *Vet. Parasitol*. 254, 151–159.

Modabber, F., Buffet, P.A., Torreele, E., Milon, G., Croft, S.L., 2007. Consultative meeting to develop a strategy for treatment of cutaneous leishmaniasis. Institute Pasteur, Paris. 13-15 June, 2006. Kinetoplastid Biol. Dis. 6, 3.

Moradin, N., Descoteaux, A., 2012. Leishmania promastigotes: building a safe niche within macrophages. Front. Cell. Infect. Microbiol. 2, 121. https://doi.org/10.3389/fcimb.2012.00121

Moraes, C.B., Franco, C.H., 2016. Novel drug discovery for Chagas disease. *Expert Opin. Drug Discov.* 0441, 1–9.

Morais-Teixeira, E. de, Damasceno, Q.S., Galuppo, M.K., Romanha, A.J., Rabello, A., 2011. The in vitro leishmanicidal activity of hexadecylphosphocholine (miltefosine) against four medically relevant *Leishmania species* of Brazil. *Mem. Inst. Oswaldo Cruz* 106, 475–478.

Moskalenko, Ni., Pershin, G., 1996. [Comparative study of the chemotherapeutic effect of paromomycin and monomycin in experimental cutaneous leischmaniasis in albino mice]. *Farmakol Toksikol.* 29, 90–4.

Mukherjee, S., Mukherjee, B., Mukhopadhyay, R., Naskar, K., Sundar, S., Dujardin, J.C., Das, A.K., Roy, S., 2012. Imipramine is an orally active drug against both antimony sensitive and resistant Leishmania donovani clinical isolates in experimental infection. *PLoS Negl. Trop. Dis.* 6, e1987.

Murray, D., 2013. Assay validation, performance and quality control. [WWW Document]. URL http://www.biomedbridges.eu/sites/biomedbridges.eu/files/training/9_-_david_murray_-_assay_validation.pdf (accessed 1.11.19).

Musa, A.M., Khalil, E.A., 2015. Trial to Determine Efficacy of Fexinidazole in Visceral Leihmaniasis Patients in Sudan. [WWW Document]. URL https://clinicaltrials.gov/ct2/show/NCT01980199 (accessed 1.11.19)

Naderer, T., Vince, J.E., McConville, M.J., 2004. Surface determinants of *Leishmania* parasites and their role in infectivity in the mammalian host. *Curr. Mol. Med.* 4, 649–65.

Nare, B., Wring, S., Bacchi, C., Beaudet, B., Bowling, T., Brun, R., Chen, D., Ding, C., Freund, Y., Gaukel, E., Hussain, A., Jarnagin, K., Jenks, M., Kaiser, M., Mercer, L., Mejia, E., Noe, A., Orr, M., Parham, R., Plattner, J., Randolph, R., Rattendi, D., Rewerts, C., Sligar, J., Yarlett, N., Don, R., Jacobs, R., 2010. Discovery of novel orally bioavailable oxaborole 6-carboxamides that demonstrate cure in a murine model of late-stage central nervous system african trypanosomiasis. *Antimicrob. Agents Chemother*. 54, 4379–88.

NIH, 2018. CREATE Bio Example: Target Product Profile (TPP) [WWW Document]. *Natl. Inst. Heal.* URL https://www.ninds.nih.gov/funding/apply-funding/application-support-library/create-bio-example-target-product-profile-tpp (accessed 8.20.18).

Novais, F.O., Santiago, R.C., Báfica, A., Khouri, R., Afonso, L., Borges, V.M., Brodskyn, C., Barral-Netto, M., Barral, A., de Oliveira, C.I., 2009. Neutrophils and macrophages cooperate in host resistance against *Leishmania braziliensis* infection. *J. Immunol.* 183, 8088–98.

Olliaro, P., Grogl, M., Boni, M., Carvalho, E.M., Chebli, H., Cisse, M., Diro, E., Fernandes Cota, G., Erber, A.C., Gadisa, E., Handjani, F., Khamesipour, A., Llanos-Cuentas, A., López Carvajal, L., Grout, L., Lmimouni, B.E., Mokni, M., Nahzat, M.S., Ben Salah, A., Ozbel, Y., Pascale, J.M., Rizzo Molina, N., Rode, J., Romero, G., Ruiz-Postigo, J.A., Gore Saravia, N., Soto, J., Uzun, S.,

Mashayekhi, V., Vélez, I.D., Vogt, F., Zerpa, O., Arana, B., 2018. Harmonized clinical trial methodologies for localized cutaneous leishmaniasis and potential for extensive network with capacities for clinical evaluation. *PLoS Negl. Trop. Dis.* 12, e0006141.

PAHO/WHO, 2018. Leishmaniasis: Epidemiological Report of the Americas 2018. [WWW Document]. *Pan American Health Organization/ World Health Organization* URL http://iris.paho.org/xmlui/bitstream/handle/123456789/34856/LeishReport6_eng.pdf?sequence=1&isAllowed=y (accessed 8.20.18).

Palit, P., Ali, N., 2008. Oral therapy with sertraline, a selective serotonin reuptake inhibitor, shows activity against *Leishmania donovani*. *J. Antimicrob. Chemother*. 61, 1120–4.

Palmer, B.D., Sutherland, H.S., Blaser, A., Kmentova, I., Franzblau, S.G., Wan, B., Wang, Y., Ma, Z., Denny, W.A., Thompson, A.M., 2015. Synthesis and structure-activity relationships for extended side chain analogues of the antitubercular drug (6S)-2-nitro-6-{[4-(trifluoromethoxy)benzyl]oxy}-6,7-dihydro-5H-imidazo[2,1-b][1,3]oxazine (PA-824). *J. Med. Chem.* 58, 3036–59.

Pandey, R.K., Sharma, D., Bhatt, T.K., Sundar, S., Prajapati, V.K., 2015. Developing imidazole analogues as potential inhibitor for Leishmania donovani trypanothione reductase: virtual screening, molecular docking, dynamics and ADMET approach. *J. Biomol. Struct. Dyn*. 33, 2541–53.

Patterson, S., Alphey, M.S., Jones, D.C., Shanks, E.J., Street, I.P., Frearson, J.A., Wyatt, P.G., Gilbert, I.H., Fairlamb, A.H., 2011. Dihydroquinazolines as a novel class of Trypanosoma brucei trypanothione reductase inhibitors: discovery, synthesis, and characterization of their binding mode by protein crystallography. *J. Med. Chem*. 54, 6514–30.

Patterson, S., Wyllie, S., Norval, S., Stojanovski, L., Simeons, F.R., Auer, J.L., Osuna-Cabello, M., Read, K.D., Fairlamb, A.H., 2016. The anti-tubercular drug delamanid as a potential oral treatment for visceral leishmaniasis. *eLife* 5.

Peña, I., Pilar Manzano, M., Cantizani, J., Kessler, A., Alonso-Padilla, J., Bardera, A.I., Alvarez, E., Colmenarejo, G., Cotillo, I., Roquero, I., de Dios-Anton, F., Barroso, V., Rodriguez, A., Gray, D.W., Navarro, M., Kumar, V., Sherstnev, A., Drewry, D.H., Brown, J.R., Fiandor, J.M., Julio Martin, J., 2015. New compound sets identified from high throughput phenotypic screening against three kinetoplastid parasites: an open resource. Sci. Rep. 5, 8771. https://doi.org/10.1038/srep08771

Peters, N.C., Egen, J.G., Secundino, N., Debrabant, A., Kimblin, N., Kamhawi, S., Lawyer, P., Fay, M.P., Germain, R.N., Sacks, D., 2008. In vivo imaging reveals an essential role for neutrophils in leishmaniasis transmitted by sand flies. *Science* 321, 970–4.

Piscopo, T. V, Mallia Azzopardi, C., 2007. Leishmaniasis. *Postgrad. Med.* J. 83, 649–57.

Prata, A., 1963. Treatment of kala-azar with amphotericin. *Trans. R. Soc. Trop. Med. Hyg.* 57, 266–8.

Rahman, R., Goyal, V., Haque, R., Jamil, K., Faiz, A., Samad, R., Ellis, S., Balasegaram, M., Boer, M. den, Rijal, S., Strub-Wourgaft, N., Alves, F., Alvar, J., Sharma, B., 2017. Safety and efficacy of short course combination regimens with AmBisome, miltefosine and paromomycin for the treatment of visceral leishmaniasis (VL) in Bangladesh. *PLoS Negl. Trop. Dis.* 11, e0005635.

Real, F., Florentino, P.T.V., Reis, L.C., Ramos-Sanchez, E.M., Veras, P.S.T., Goto, H., Mortara, R.A., 2014. Cell-to-cell transfer of *Leishmania amazonensis* amastigotes is mediated by immunomodulatory LAMP-rich parasitophorous extrusions. *Cell. Microbiol.* 16, 1549–64.

Real, F., Mortara, R.A., 2012. The diverse and dynamic nature of Leishmania parasitophorous vacuoles studied by multidimensional imaging. *PLoS Negl. Trop. Dis.* 6, e1518.

Ridley, D.S., 1980. A histological classification of cutaneous leishmaniasis and its geographical expression. T*rans. R. Soc. Trop. Med. Hyg.* 74, 515–21.

Rittig, M.G., Bogdan, C., 2000. *Leishmania*-host-cell interaction: complexities and alternative views. *Parasitol. Today* 16, 292–7.

Rocha, M.N., Corrêa, C.M., Melo, M.N., Beverley, S.M., Martins-Filho, O.A., Madureira, A.P., Soares, R.P., 2013. An alternative in vitro drug screening test using *Leishmania amazonensis* transfected with red fluorescent protein. Diagn. Microbiol. Infect. Dis. 75, 282–91.

Rodrigues, I.A., Mazotto, A.M., Cardoso, V., Alves, R.L., Amaral, A.C.F., Silva, J.R. de A., Pinheiro, A.S., Vermelho, A.B., 2015. Natural Products: Insights into Leishmaniasis Inflammatory Response. *Mediators Inflamm.* 2015, 835910.

Romero, G.A.S., Boelaert, M., 2010. Control of visceral leishmaniasis in latin america-a systematic review. *PLoS Negl. Trop. Dis*. 4, e584.

Roque, A.L.R., Jansen, A.M., 2014. Wild and synanthropic reservoirs of *Leishmania* species in the Americas. *Int. J. Parasitol. Parasites Wildl*. 3, 251–62.

Rossi, M., Fasel, N., 2018. How to master the host immune system? *Leishmania* parasites have the solutions! *Int. Immunol.* 30, 103–111.

Sabaté, D., Llinás, J., Homedes, J., Sust, M., Ferrer, L., 2014. A single-centre, open-label, controlled, randomized clinical trial to assess the preventive efficacy of a domperidone-based treatment programme against clinical canine leishmaniasis in a high prevalence area. *Prev. Vet. Med.* 115, 56–63.

Sacks, D., Kamhawi, S., 2001. Molecular aspects of parasite-vector and vector-host interactions in leishmaniasis. *Annu. Rev. Microbiol.* 55, 453–83.

Sacks, D.L., Barral, A., Neva, F.A., 1983. Thermosensitivity patterns of Old vs. New World cutaneous strains of *Leishmania* growing within mouse peritoneal macrophages *in vitro*. *Am. J. Trop. Med. Hyg*. 32, 300–4.

Sakthianandeswaren, A., Foote, S.J., Handman, E., 2009. The role of host genetics in leishmaniasis. *Trends Parasitol*. 25, 383–91.

Santarém, N., Cunha, J., Silvestre, R., Silva, C., Moreira, D., Ouellette, M., Cordeiro-DA-Silva, A., 2014. The impact of distinct culture media in *Leishmania infantum* biology and infectivity. *Parasitology* 141, 192–205.

Schwende, H., Fitzke, E., Ambs, P., Dieter, P., 1996. Differences in the state of differentiation of THP-1 cells induced by phorbol ester and 1,25-dihydroxyvitamin D3. J. *Leukoc. Biol*. 59, 555–61.

Scott, P., Novais, F.O., 2016. Cutaneous leishmaniasis: immune responses in protection and pathogenesis. *Nat. Rev. Immunol*. 16, 581–92.

Seifert, K., Escobar, P., Croft, S.L., 2010. In vitro activity of anti-leishmanial drugs against *Leishmania donovani* is host cell dependent. J. *Antimicrob. Chemother.* 65, 508–11.

Sen, R., Ganguly, S., Saha, P., Chatterjee, M., 2010. Efficacy of artemisinin in experimental visceral leishmaniasis. *Int. J. Antimicrob. Agents* 36, 43–9.

Serafim, T.D., Coutinho-Abreu, I. V., Oliveira, F., Meneses, C., Kamhawi, S., Valenzuela, J.G., 2018. Sequential blood meals promote *Leishmania* replication and reverse metacyclogenesis augmenting vector infectivity. *Nat. Microbiol*. 3, 548–555.

Singh, S., Dinesh, N., Kaur, P.K., Shamiulla, B., 2014. Ketanserin, an antidepressant, exerts its antileishmanial action via inhibition of 3-hydroxy-3-methylglutaryl coenzyme A reductase (HMGR) enzyme of *Leishmania donovani. Parasitol. Res.* 113, 2161–8.

Siqueira-Neto, J.L., Moon, S., Jang, J., Yang, G., Lee, C., Moon, H.K., Chatelain, E., Genovesio, A., Cechetto, J., Freitas-Junior, L.H., 2012. An image-based high-content screening assay for compounds targeting intracellular Leishmania donovani amastigotes in human macrophages. *PLoS Negl. Trop. Dis.* 6, e1671.

Siqueira-Neto, J.L., Song, O.-R., Oh, H., Sohn, J.-H., Yang, G., Nam, J., Jang, J., Cechetto, J., Lee, C.B., Moon, S., Genovesio, A., Chatelain, E., Christophe, T., Freitas-Junior, L.H., 2010. Antileishmanial high-throughput drug screening reveals drug candidates with new scaffolds. *PLoS Negl. Trop. Dis*. 4, e675.

Starr, T., Bauler, T.J., Malik-Kale, P., Steele-Mortimer, O., 2018. The phorbol 12-myristate-13-acetate differentiation protocol is critical to the interaction of THP-1 macrophages with Salmonella Typhimurium. *PLoS One* 13, e0193601. 1

Subramanian, A., Sarkar, R.R., 2017. Revealing the mystery of metabolic adaptations using a genome scale model of Leishmania infantum. *Sci. Rep*. 7, 10262.

Sundar, S., Singh, O.P., 2018. Molecular Diagnosis of Visceral Leishmaniasis. Mol. Diagn. Ther. https://doi.org/10.1007/s40291-018-0343-y

Sunyoto, T., Potet, J., Boelaert, M., 2018. Why miltefosine-a life-saving drug for leishmaniasis-is unavailable to people who need it the most. *BMJ Glob. Hea*l. 3, e000709.

Tatipaka, H.B., Gillespie, J.R., Chatterjee, A.K., Norcross, N.R., Hulverson, M.A., Ranade, R.M., Nagendar, P., Creason, S.A., McQueen, J., Duster, N.A., Nagle, A., Supek, F., Molteni, V., Wenzler, T., Brun, R., Glynne, R., Buckner, F.S., Gelb, M.H., 2014. Substituted 2-phenylimidazopyridines: a new class of drug leads for human African trypanosomiasis. *J. Med. Chem.* 57, 828–35.

Tegazzini, D., Cantizani, J., Peña, I., Martín, J., Coterón, J.M., 2017. Unravelling the rate of action of hits in the Leishmania donovani box using standard drugs amphotericin B and miltefosine. *PLoS Negl. Trop. Dis.* 11, e0005629.

Tegazzini, D., Díaz, R., Aguilar, F., Peña, I., Presa, J.L., Yardley, V., Martin, J.J., Coteron, J.M., Croft, S.L., Cantizani, J., 2016. A Replicative In Vitro Assay for Drug Discovery against *Leishmania donovani*. *Antimicrob. Agents Chemother.* 60, 3524–32.

Trask, O.J., Johnston, P.A., 2015. Standardization of high content imaging and informatics. *Assay Drug Dev. Technol*. 13, 341–6.

Travi, B.L., Miró, G., 2018. Use of domperidone in canine visceral leishmaniasis: gaps in veterinary knowledge and epidemiological implications. *Mem. Inst. Oswaldo Cruz* 113, e180301.

Tsuchiya, S., Kobayashi, Y., Goto, Y., Okumura, H., Nakae, S., Konno, T., Tada, K., 1982. Induction of maturation in cultured human monocytic leukemia cells by a phorbol diester. *Cancer Res.* 42, 1530–6.

Tsuchiya, S., Yamabe, M., Yamaguchi, Y., Kobayashi, Y., Konno, T., Tada, K., 1980. Establishment and characterization of a human acute monocytic leukemia cell line (THP-1). Int. J. cancer 26, 171–6.

Uliana, S.R.B., Trinconi, C.T., Coelho, A.C., 2018. Chemotherapy of leishmaniasis: present challenges. *Parasitology* 145, 464–480.

Underhill, D.M., 2003. Macrophage recognition of zymosan particles. *J. Endotoxin Res*. 9, 176–80.

Vianna, G., 1912. Tratamento da leishmaniose tegumentar por injeções intravenosas de tártaro emético. An. do 7º Congr. Bras. Med. e Cirurg 426–428.

Voak, A.A., Gobalakrishnapillai, V., Seifert, K., Balczo, E., Hu, L., Hall, B.S., Wilkinson, S.R., 2013. An essential type I nitroreductase from Leishmania major can be used to activate leishmanicidal prodrugs. *J. Biol. Chem*. 288, 28466–76.

Voak, A.A., Seifert, K., Helsby, N.A., Wilkinson, S.R., 2014. Evaluating Aziridinyl Nitrobenzamide Compounds as Leishmanicidal Prodrugs. *Antimicrob. Agents Chemother.* 58, 370–377.

Voak, A.A., Standing, J.F., Sepúlveda, N., Harris, A., Croft, S.L., Seifert, K., 2018. Pharmacodynamics and cellular accumulation of amphotericin B and miltefosine in Leishmania donovani-infected primary macrophages. *J. Antimicrob. Chemother*. 73, 1314–1323.

Wang, M.Z., Zhu, X., Srivastava, A., Liu, Q., Sweat, J.M., Pandharkar, T., Stephens, C.E., Riccio, E., Parman, T., Munde, M., Mandal, S., Madhubala, R., Tidwell, R.R., Wilson, W.D., Boykin, D.W., Hall, J.E., Kyle, D.E., Werbovetz, K.A., 2010. Novel arylimidamides for treatment of visceral leishmaniasis. *Antimicrob. Agents Chemother.* 54, 2507–16.

WHO, 2018. Leishmaniasis [WWW Document]. *World Heal. Organ*. URL

www.who.int/leishmaniasis/en/ (accessed 8.20.18).

WHO, 2017. Report of the Tenth Meeting of the WHO Strategic and Technical Advisory Group for Neglected Tropical Diseases. WWW Document]. *World Heal. Organ*. URL http://www.who.int/neglected_diseases/NTD_STAG_report_2017.pdf (accessed 8.20.18).

WHO, 2012. Research priorities for Chagas disease, human African trypanosomiasis and leishmaniasis. World Health Organ. Tech. Rep. Ser. v–xii, 1-100.

Wyatt, P.G., Gilbert, I.H., Read, K.D., Fairlamb, A.H., 2011. Target validation: linking target and chemical properties to desired product profile. *Curr. Top. Med. Chem.* 11, 1275–83.

Wyllie, S., Thomas, M., Patterson, S., Crouch, S., De Rycker, M., Lowe, R., Gresham, S., Urbaniak, M.D., Otto, T.D., Stojanovski, L., Simeons, F.R.C., Manthri, S., MacLean, L.M., Zuccotto, F., Homeyer, N., Pflaumer, H., Boesche, M., Sastry, L., Connolly, P., Albrecht, S., Berriman, M., Drewes, G., Gray, D.W., Ghidelli-Disse, S., Dixon, S., Fiandor, J.M., Wyatt, P.G., Ferguson, M.A.J., Fairlamb, A.H., Miles, T.J., Read, K.D., Gilbert, I.H., 2018. Cyclin-dependent kinase 12 is a drug target for visceral leishmaniasis. *Nature* 560, 192–197.

Yardley, V., Croft, S.L., 2000. A comparison of the activities of three amphotericin B lipid formulations against experimental visceral and cutaneous leishmaniasis. *Int. J. Antimicrob. Agents* 13, 243–248.

Younis, Y., Douelle, F., Feng, T.-S., González Cabrera, D., Le Manach, C., Nchinda, A.T., Duffy, S., White, K.L., Shackleford, D.M., Morizzi, J., Mannila, J., Katneni, K., Bhamidipati, R., Zabiulla, K.M., Joseph, J.T., Bashyam, S., Waterson, D., Witty, M.J., Hardick, D., Wittlin, S., Avery, V., Charman, S.A., Chibale, K., 2012. 3,5-Diaryl-2-aminopyridines as a novel class of orally active antimalarials demonstrating single dose cure in mice and clinical candidate potential. *J. Med. Chem.* 55, 3479–87.

Zanella, F., Lorens, J.B., Link, W., 2010. High content screening: seeing is believing. *Trends Biotechnol.* 28, 237–45.

Zauli-Nascimento, R.C., Miguel, D.C., Yokoyama-Yasunaka, J.K.U., Pereira, L.I.A., Pelli de Oliveira, M.A., Ribeiro-Dias, F., Dorta, M.L., Uliana, S.R.B., 2010. *In vitro* sensitivity of L*eishmania (Viannia) braziliensis* and *Leishmania (Leishmania) amazonensis* Brazilian isolates to meglumine antimoniate and amphotericin B. *Trop. Med. Int. Health* 15, 68–76.

Zeng, C., Wang, W., Yu, X., Yang, L., Chen, S., Li, Y., 2015. Pathways related to PMA-differentiated THP1 human monocytic leukemia cells revealed by RNA-Seq. *Sci. China. Life Sci.* 58, 1282–7.

Zhang, Chung, Oldenburg, 1999. A Simple Statistical Parameter for Use in Evaluation and Validation of High Throughput Screening Assays. *J. Biomol. Screen.* 4, 67–73.

Zhang, W.-W., Lypaczewski, P., Matlashewski, G., 2017. Optimized CRISPR-Cas9 Genome Editing for Leishmania and Its Use To Target a Multigene Family, Induce Chromosomal Translocation, and Study DNA Break Repair Mechanisms. *mSphere* 2.

Zilberstein, D., Dwyer, D.M., 1984. Antidepressants cause lethal disruption of membrane function in the human protozoan parasite *Leishmania. Science* 226, 977–9.

Zulfiqar, B., Jones, A.J., Sykes, M.L., Shelper, T.B., Davis, R.A., Avery, V.M., 2017a. Screening a Natural Product-Based Library against Kinetoplastid Parasites. *Molecules* 22.

Zulfiqar, B., Shelper, T.B., Avery, V.M., 2017b. Leishmaniasis drug discovery: recent progress and challenges in assay development. *Drug Discov. Today* 22, 1516–1531.

APPENDIX 1

Data reported in (Alcântara 2017).

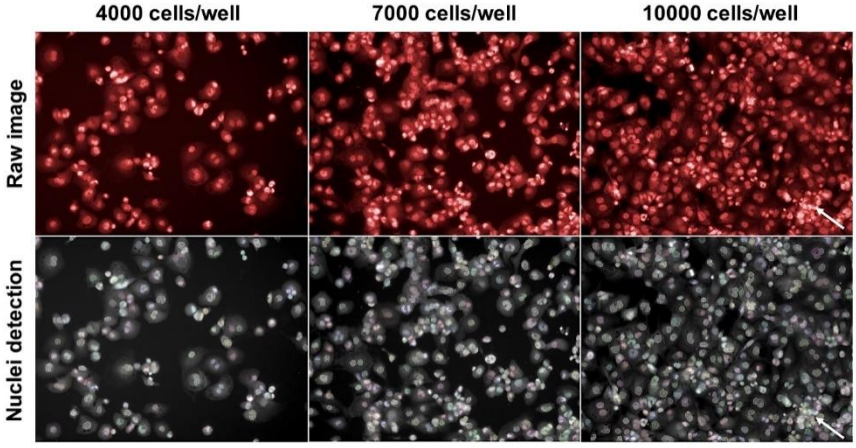

Standardization the best THP-1 cell density for 384-well plates. THP-1 cells were differentiated with 50 ng/mL PMA and plated at 3 different densities: 4,000 (left images), 7,000 (middle images) and 10,000 (right images) cells/well. After 48 hours of PMA treatment, plates were fixed with 4% PMA and stained with 5 µM Draq 5. Images were acquired by Operetta High Content System (Perkim Elmer) and were analysed by Harmony software. Arrows indicates cells clusters caused by higher densities of the culture. Magnification: 20x.

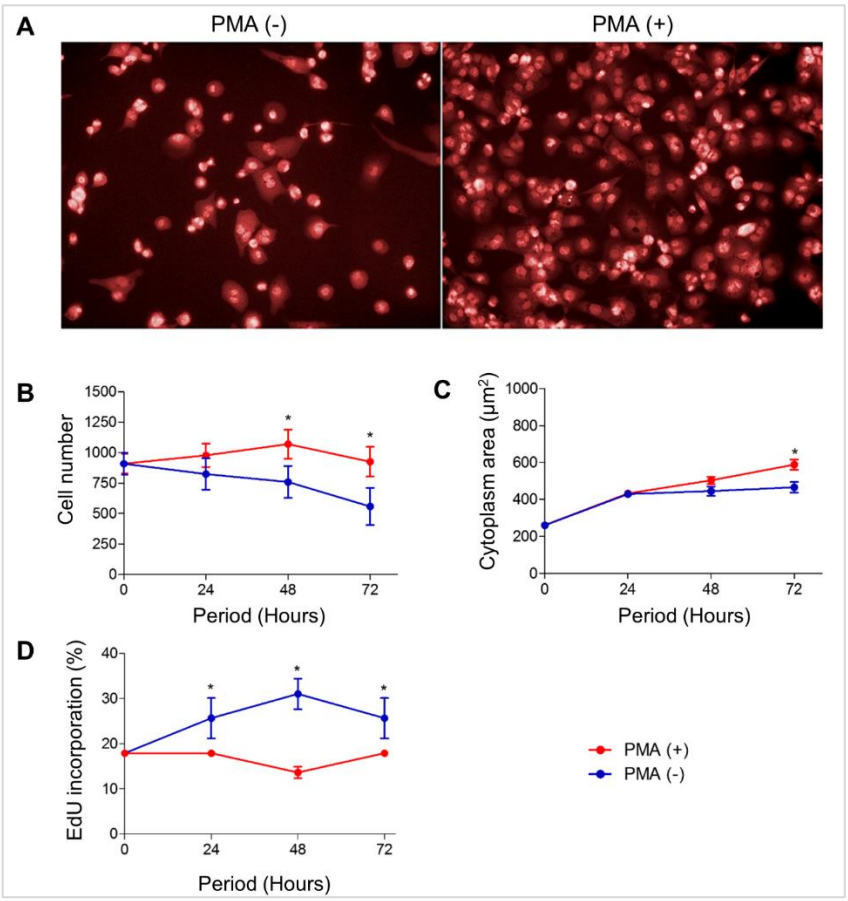

Effect of PMA removal after cells differentiation. (a) Posteriorly to 48 hours, cells were maintained with (right/ PMA (+)) or without (left/ PMA (-)) PMA reagent. Images were acquired 72 h after. Magnification: 20x.(b), (c), (d) and (e) Differences between PMA (+) and PMA (-) cultures in the number of cells, the cytoplasm area, the cytoplasm ratio width to length and ratio of cellular multiplication, respectively. Asterisks (*) indicate ($p<0.0001$).

APPENDIX 2

Representative images of the 12 pan-antileishmanial compounds efficacy. A representative image for each specie is shown, starting with negative controls (infected cells treated with 0.5 % DMSO) and positive controls (10µM amphotericin B). For the tested compounds, the normalized activity (upper right) and cell ratio (bottom right) are also shown. The images were acquired by the IN Cell Analyzer 2200 system.

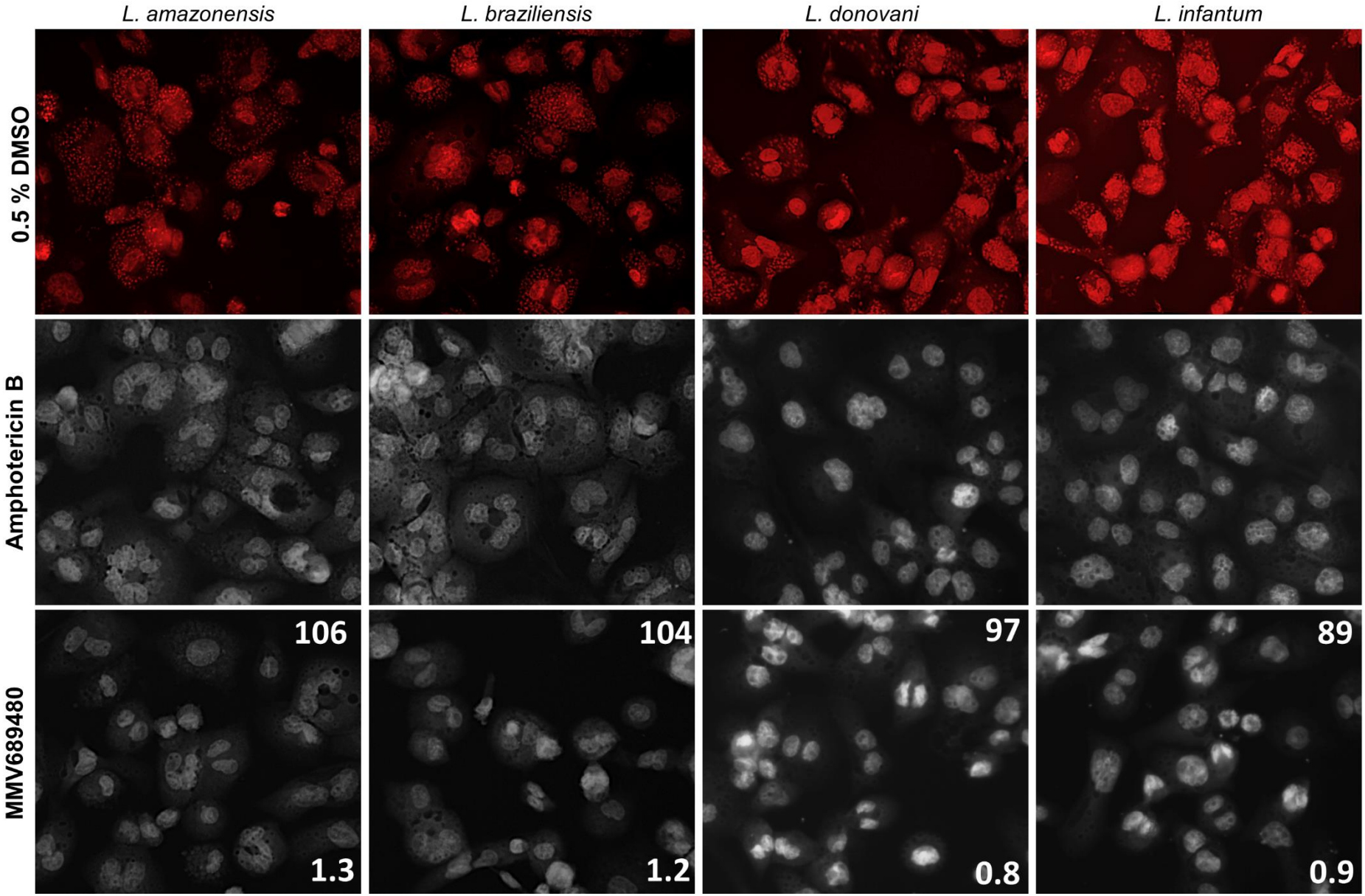
L. amazonensis
L. braziliensis
L. donovani
L. infantum
0.5 % DMSO
Amphotericin B
MMV689480
106
1.3
104
1.2
97
0.8
89
0.9

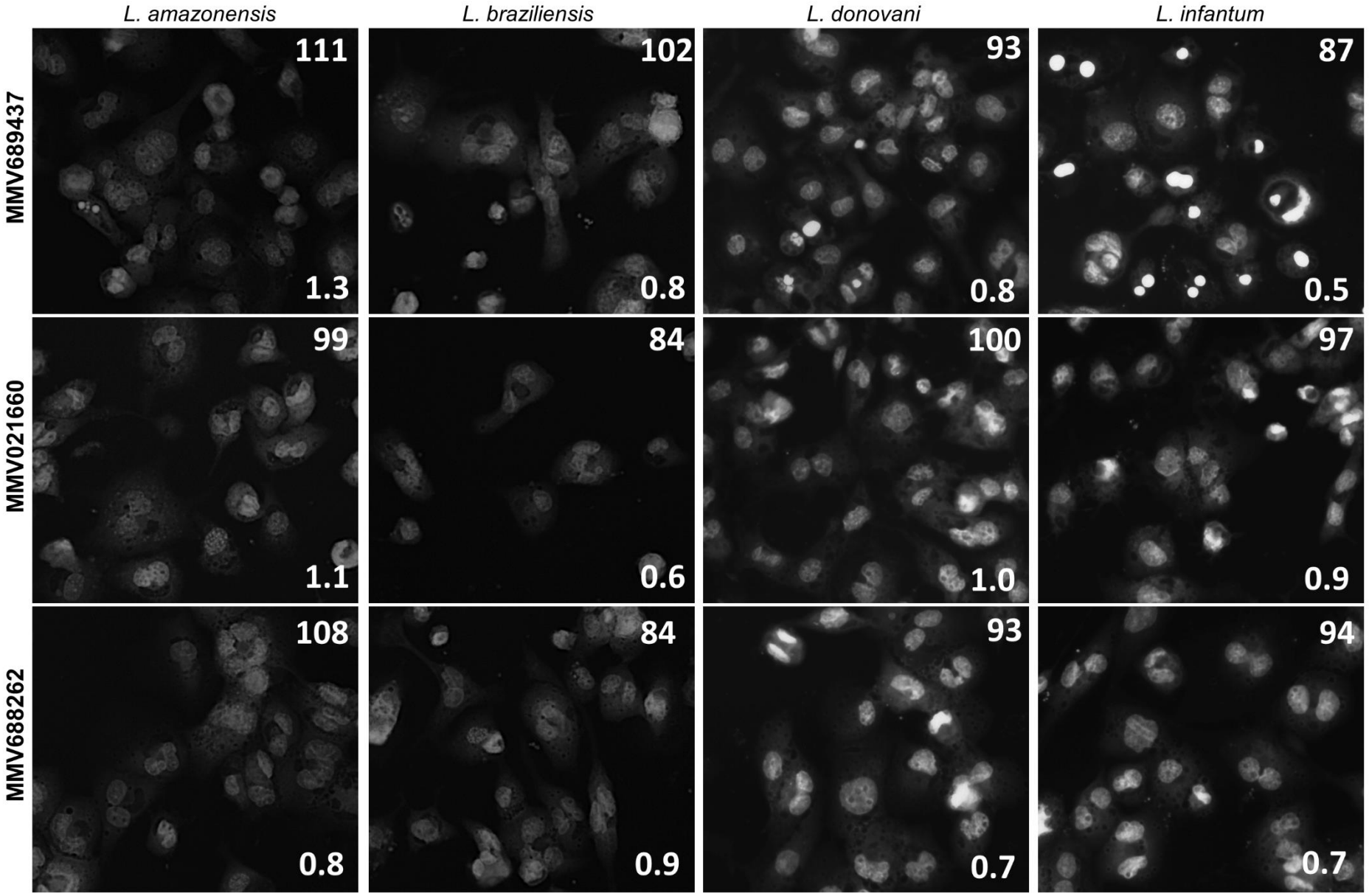
L. amazonensis
L. braziliensis
L. donovani
L. infantum
MMV689437
MMV021660
MMV688262
111
1.3
102
0.8
93
0.8
87
0.5
99
1.1
84
0.6
100
1.0
97
0.9
108
0.8
84
0.9
93
0.7
94
0.7

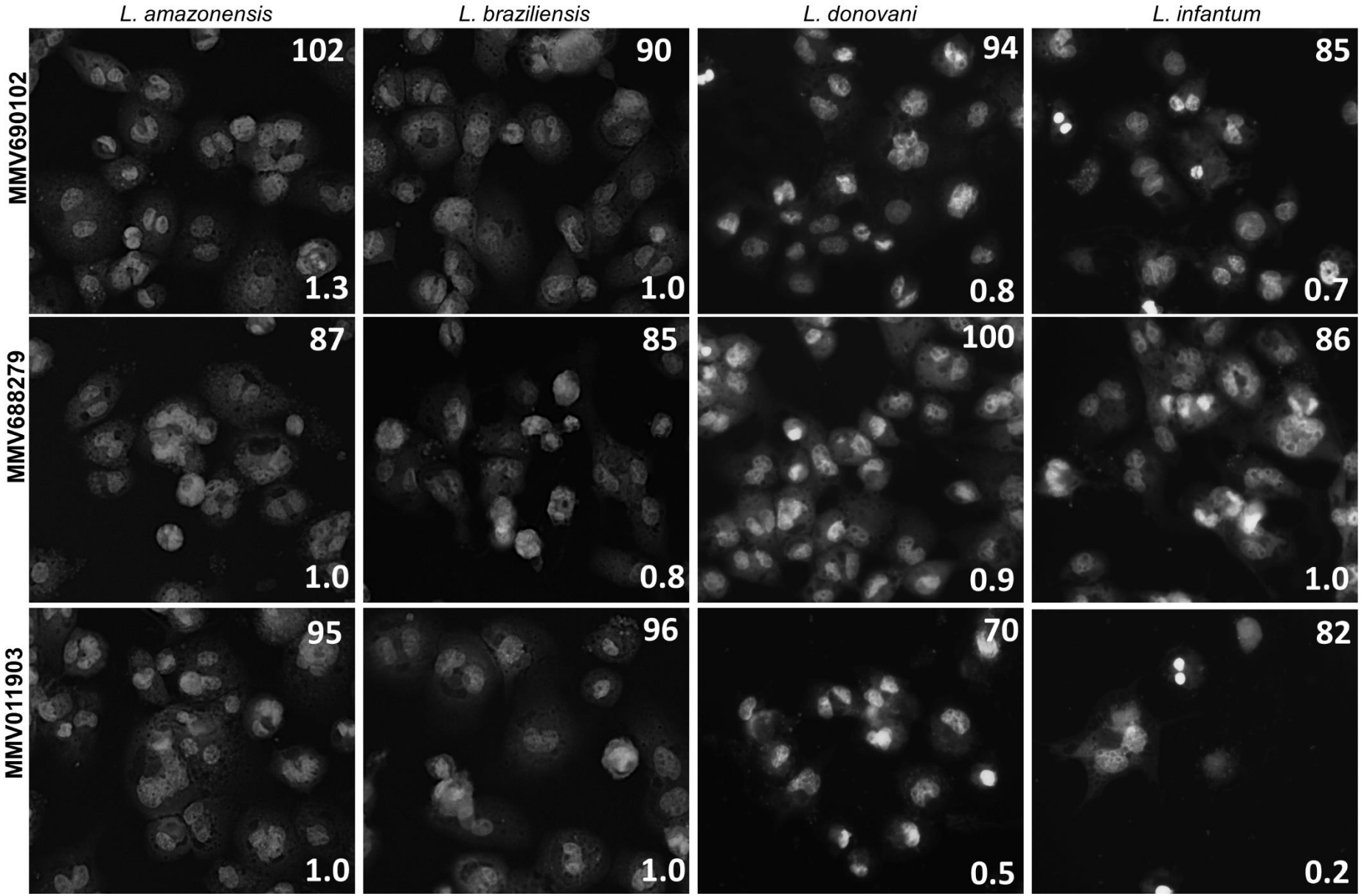
L. amazonensis
L. braziliensis
L. donovani
L. infantum
MMV690102
MMV688279
MMV011903
102
1.3
90
1.0
94
0.8
85
0.7
87
1.0
85
0.8
100
0.9
86
1.0
95
1.0
96
1.0
70
0.5
82
0.2

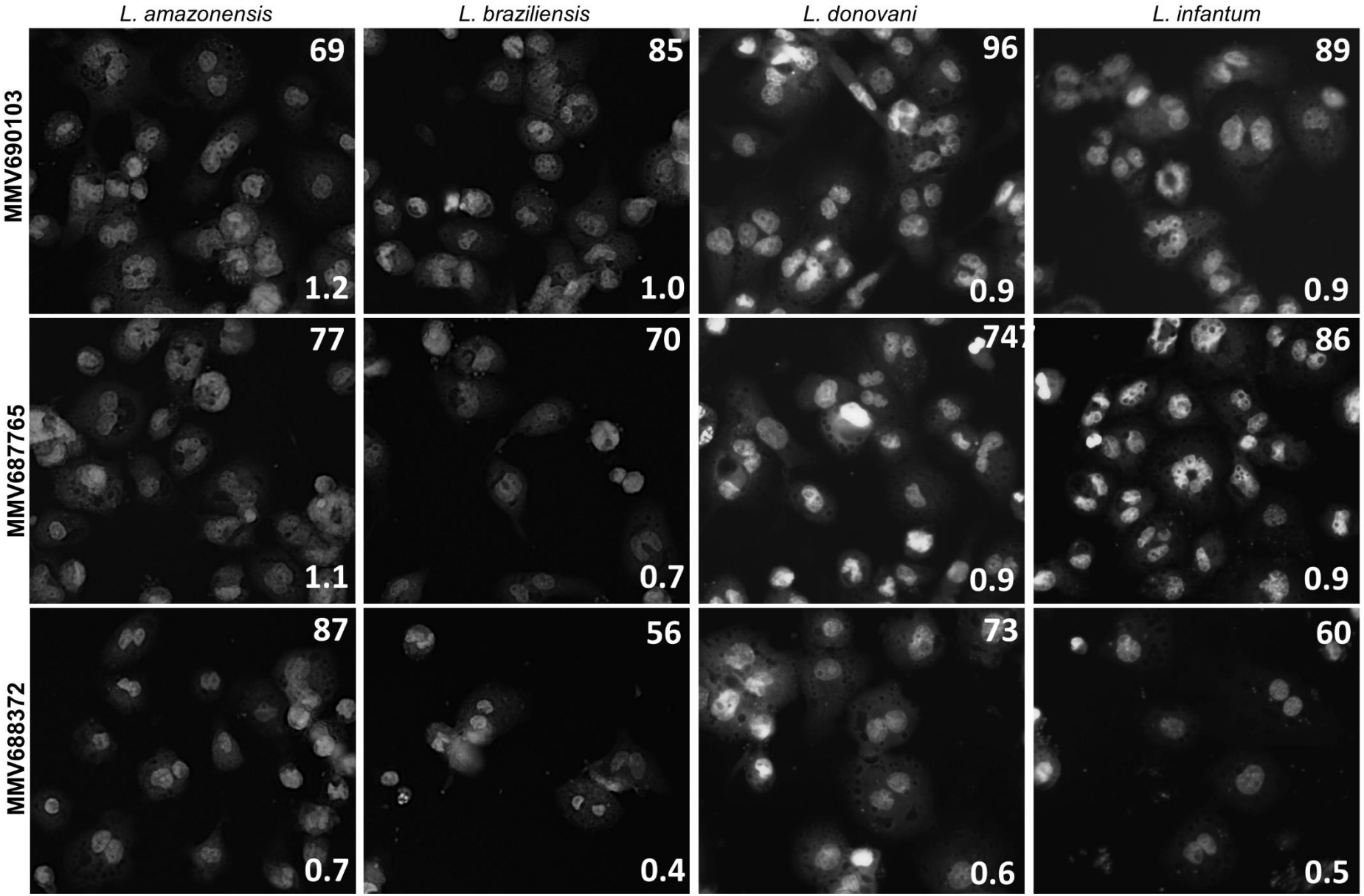
L. amazonensis
L. braziliensis
L. donovani
L. infantum
MMV690103
MMV687765
MMV688372
69
1.2
85
1.0
96
0.9
89
0.9
77
1.1
70
0.7
74
0.9
86
0.9
87
0.7
56
0.4
73
0.6
60
0.5

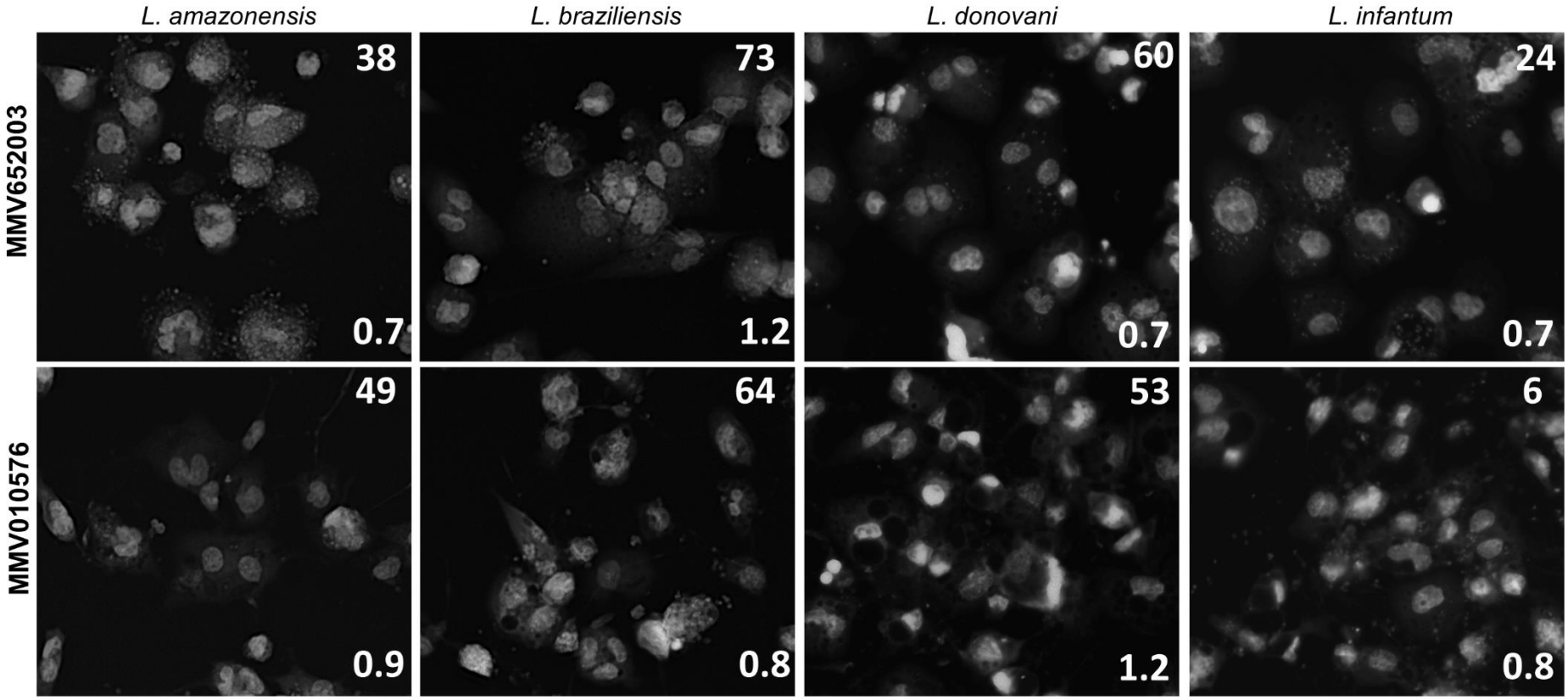
L. amazonensis
L. braziliensis
L. donovani
L. infantum
MMV652003
MMV010576
38
0.7
73
1.2
60
0.7
24
0.7
49
0.9
64
0.8
53
1.2
6
0.8

ANNEX I

UNICAMP

CEUA/Unicamp

Comissão de Ética no Uso de Animais
CEUA/Unicamp

CERTIFICADO

Certificamos que o projeto de pesquisa intitulado **O PAPEL DAS PROTEÍNAS LIGANTES DE ÁCIDOS GRAXOS NA INFECÇÃO DE MACRÓFAGOS POR LEISHMANIA: UM ALVO POTENCIAL PARA NOVAS DROGAS CONTRA LEISHMANIOSE** (protocolo CEUA/UNICAMP nº **4047-1**), de responsabilidade do **Prof. Dr. Danilo Ciccone Miguel** e das pós-graduandas **Karen Caroline Minori Vieira** e **Vivian Midori Maruyama** teve incluído também como executor a pós-graduanda **Thalita Camelo da Silva Ferreira**.

Trata-se apenas de inclusão de executor não havendo alteração alguma em relação ao número de animais envolvidos no projeto, bem como em relação aos procedimentos experimentais previstos.

Este documento é válido apenas se apresentado junto com o certificado emitido originalmente pela CEUA/UNICAMP em 26/10/2015.

Campinas, 22 de setembro de 2016.

Profa. Dra. Liana M. C. Verinaud
Presidente

Fátima Alonso
Secretária Executiva

CEUA/UNICAMP
Caixa Postal 6109
13083-970 Campinas, SP – Brasil

Telefone: (19) 3521-6359
E-mail: comisib@unicamp.br
http://www.ib.unicamp.br/ceea/

ANNEX II

UNICAMP

CEUA/UNICAMP

CERTIFICADO

Certificamos que o projeto intitulado **"O PAPEL DAS PROTEÍNAS LIGANTES DE ÁCIDOS GRAXOS NA INFECÇÃO DE MACRÓFAGOS POR LEISHMANIA: UM ALVO POTENCIAL PARA NOVAS DROGAS CONTRA LEISHMANIOSE"**, protocolo nº **4047-1**, sob a responsabilidade de **Prof. Dr. Danilo Ciccone Miguel / Karen Caroline Minori Vieira / Vivian Midori Maruyama**, que envolve a produção, manutenção e/ou utilização de animais pertencentes ao filo *Chordata*, subfilo *Vertebrata* (exceto o homem) para fins de pesquisa científica ou ensino, encontra-se de acordo com os preceitos da **LEI Nº 11.794, DE 8 DE OUTUBRO DE 2008**, que estabelece procedimentos para o uso científico de animais e do **DECRETO Nº 6.899, DE 15 DE JULHO DE 2009**, e com as normas editadas pelo **Conselho Nacional de Controle da Experimentação Animal - CONCEA**, e foi aprovado pela **Comissão de Ética no Uso de Animais** da **Universidade Estadual de Campinas - CEUA/UNICAMP,** em **26 de outubro de 2015**.

Vigência do projeto: 11/2015-07/2019
Espécie/Linhagem: Camundongo isogênico / Balb/c
No. de animais: 220
Idade/Peso: 04 semanas / 23g
Sexo: fêmeas
Origem: CEMIB/UNICAMP

A aprovação pela CEUA/UNICAMP não dispensa autorização prévia junto ao **IBAMA**, **SISBIO** ou **CIBio**.

Campinas, 26 de outubro de 2015.

Profa. Dra. Liana Maria Cardoso Verinaud
Presidente

Fátima Alonso
Secretária Executiva

ANNEX III

COORDENADORIA DE PÓS-GRADUAÇÃO
INSTITUTO DE BIOLOGIA
Universidade Estadual de Campinas
Caixa Postal 6109. 13083-970, Campinas, SP, Brasil
Fone (19) 3521-6378. email: cpgib@unicamp.br

DECLARAÇÃO

Em observância ao **§5º do Artigo 1º da Informação CCPG-UNICAMP/001/15**, referente a Bioética e Biossegurança, declaro que o conteúdo de minha Tese de Doutorado, intitulada "***Relevance of multi-species phenotypic assays in Leishmania early drug discovery***", desenvolvida no Programa de Pós-Graduação em Biociências e Tecnologia de Produtos Bioativos do Instituto de Biologia da Unicamp, não versa sobre pesquisa envolvendo seres humanos, animais ou temas afetos a Biossegurança.

Assinatura: Thalita Camêlo da S. Ferreira
Nome do(a) aluno(a): Thalita Camêlo da Silva Ferreira

Assinatura: _____
Nome do(a) orientador(a): Lúcio Holanda Gondim de Freitas Júnior

Data: 17 de Abril de 2019

ANNEX IV

Declaração

As cópias de artigos de minha autoria ou de minha co-autoria, já publicados ou submetidos para publicação em revistas científicas ou anais de congressos sujeitos a arbitragem, que constam da minha Dissertação/Tese de Mestrado/Doutorado, intitulada **Relevance of multi-species phenotypic assays in Leishmania early drug discovery**, não infringem os dispositivos da Lei n.° 9.610/98, nem o direito autoral de qualquer editora.

Campinas, 17 de Abril de 2019

Assinatura : Thalita Camêlo da S. Ferreira
Nome do(a) autor(a): **Thalita Camêlo da Silva Ferreira**
RG n.° DF 2.830.283

Assinatura : _____
Nome do(a) orientador(a): **Lucio Holanda Gondim de Freitas Júnior**
RG n.° SP 57.656.051-0